5-2023

Multiomic Explorations of Fruit Texture and Postharvest Quality in Blackberry and Muscadine Grape

Thomas Mason Chizk
University of Arkansas, Fayetteville

Multiomic Explorations of Fruit Texture and Postharvest Quality in Blackberry and Muscadine Grape

A dissertation submitted in partial fulfillment
of the requirements for the degree of
Doctor of Philosophy in Horticulture

by

Thomas Mason Chizk
Oklahoma State University
Bachelor of Science in Plant and Soil Science, 2015
North Carolina State University
Master of Science in Crop and Soil Science, 2018

May 2023
University of Arkansas

This dissertation is approved for recommendation to the Graduate Council.

_____
Margaret Worthington, Ph.D.
Committee Chair

_____
Renee Threlfall, Ph.D.
Committee Member

_____
Ya-Jane Wang, Ph.D.
Committee Member

_____
Jacquelyn Lee, Ph.D.
Committee Member

_____
Larry Purcell, Ph.D.
Committee Member

ABSTRACT

For most fresh-market fruit crops, texture is an important trait that strongly affects both shipping potential and consumer opinion. Efficient, scalable phenotyping methods are required by breeding programs to effectively select for improvements to fruit texture quality. In muscadine, we have developed a recommendation for characterizing complex muscadine grape texture profiles by comparing the results of breeders' ratings, descriptive sensory panel results, and an array of instrumental protocols. Regression models were constructed to predict awareness of skins, crispness, hardness, and visual separation explaining 85%, 91%, 82%, and 83% of variance respectively. Genotypes that scored most highly in breeders' ratings of overall texture had soft skins and firm flesh, suggesting that both qualities are important targets for texture improvement in muscadine. We have also developed an R shiny based web-application, called ShinyFruit, for image-based analysis of fruit morphology and color quality. ShinyFruit was tested against manual methods of size and red drupelet reversion (RDR) estimation in a diverse population of blackberry cultivars and breeding selections. ShinyFruit results shared a strong positive correlation with manual measurements for blackberry length ($r = 0.96$) and significant, albeit weaker, correlations with manual RDR estimation methods ($r = 0.62$ - 0.70). Further validation of ShinyFruit's potential was provided when it was used to generate phenotypic datasets across a genome wide association study (GWAS) panel of 300 diverse blackberry genotypes. This GWAS panel is the first reported in autotetraploid blackberry, and numerous quantitative trait loci (QTL) for blackberry texture and RDR were identified, spanning chromosomes Ra01, Ra02, Ra03, and Ra06. All QTL associated with RDR were located on Ra02 and most of these 212 single nucleotide polymorphisms (SNPs) were in high linkage disequilibrium. Three variants on homologs of polygalcturonase (PG), pectin methylesterase (PME), and β-glucosidase explained 27% of variance in fruit firmness and were located on

chromosomes Ra06, Ra01, and Ra02 respectively. Both fruit firmness and RDR appear to be complex, moderately heritable traits, which may be most effectively incorporated into a genomic selection model. Expression-level evidence suggests that an inhibitor of PME may be associated with the fruit firmness QTL identified on Ra01. The expression of this PME inhibitor was negatively correlated with PME activity through fruit development in the 'crispy' fruited A-2453T. Expansin-like proteins were also expressed more highly in A-2453T compared to the soft-fruited 'Black Gem^{TM}', suggesting that this protein family could play a unique role in the 'crispy' texture phenotype. By combining newly developed phenotyping methods with informative genomic and transcriptomic datasets, we provide a strong foundation for continued research. Future improvement of texture in blackberry should prioritize training genomic selection models which could be trained on our accumulated datasets and supported by ShinyFruit phenotyping.

ACKNOWLEDGEMENTS

I am grateful to the countless colleagues and mentors I have encountered during all my academic and professional endeavors that have guided me to this accomplishment. The pages of this manuscript could be filled with all of those I have been fortunate enough to interact with on my journey, but there are several that must be credited above all. The patience of my beloved wife has known no bounds, as over the past few years. Without her, I would not have had the ability to pursue my passion and complete this dissertation. I also owe acknowledgement to my academic advisor, Dr. Margaret Worthington, for believing in my potential and allowing me to be a part of her lab. I owe gratitude to Dr. Jacquelyn Lee and all the employees of the UA fruit research station in Clarksville, AR. Without these hard-working individuals, we never could have achieved the scale and quality of work that was accomplished.

I am deeply indebted to my fellow graduate students for the many hours spent assisting with data collection and supporting work. Carmen Johns deserves special recognition for never hesitating to put in extra hours when the need arose. Last, but certainly not least, I am grateful to my remaining committee members, who have all made themselves available for advising and support. I hope to one day get the opportunity to return the favor to a new generation of scientists and professionals.

DEDICATION

To Silas,

My life gained new meaning when yours begun. Your world will be different from mine. Every day now, I think of that world, where you will do things bigger than I could ever imagine.

TABLE OF CONTENTS

LITERATURE REVIEW

A Brief Overview of Fruit Texture

Food texture has been broadly defined by the International Organization for Standardization as "all the mechanical, geometrical, surface and body attributes of a product perceptible by means of kinesthetic and somesthetic receptors, and (where appropriate) visual and auditory receptors from first bite to final swallowing" (ISO 5492:2008). For the purposes of this study food texture will be primarily discussed in terms that relate to fleshy, non-climacteric fruits, as following discussions will shift towards a more specific investigation of blackberry (*Rubus* subgenus *Rubus* Watson) and muscadine (*Vitis rotundifolia* Michx.) texture qualities. Even so, fruit texture remains a highly complex trait, as evidenced by the number of physiological and biochemical components that are known to be associated with textural attributes. Such components tend to include cell turgor, pectin composition, cellulose content, mineral content, physiological maturity, and features specific to the unique botanical structure or structures of which the fruit itself is composed (Brecht et al., 2007; Brummel and Harpster, 2001; Toivonen and Brummel, 2008). The complexity of fruit texture is further demonstrated by the number of techniques that are used to quantify the trait. Using objective instrumental techniques, fruit texture has been explored through various quantitative, well-defined rheological components such as firmness, crispness, elasticity, hardness, gumminess, chewiness, and many others. Most of these factors have been readily derived from a force by deformation curve, generated from a universal testing machine (UTM) (Rolle et al., 2012; Vincent, 1998; Vishwakarma et al., 2016). This approach is relatively inexpensive after the initial cost of the instrument and is easily standardized and repeatable, but not always easy to interpret in relation to consumer preference. In contrast, fruit texture has also been characterized through the

implementation of more subjective consumer or descriptive sensory panels, which are, by nature, easily related to consumer opinion. Sensory panels often result in data that are correlated with instrumentally measured attributes, but the nature and magnitude of these correlations may vary between crops (Cliff, 2018; Felts et al., 2018; Mann et al., 2005). Though both of these techniques are widely implemented, many crop species lack proper comparisons between instrumental and sensory evaluation methods. An expanded understanding of these relationships may accelerate the development of cost-effective standardized methods of screening for improved consumer opinion.

For most horticultural fruit crops, improved fruit texture is a subject of intense interest to the fresh fruit market as it often thought to serve two main functions: enhanced postharvest quality and consumer opinion. In a 2009 study, it was estimated that nearly 10.9 billion pounds of fresh fruit was lost to food waste in the United States, accounting for about 30% of annual fruit production (Buzby et al., 2011). Of those losses, about 4.2 billion pounds were at the retail and processing level, indicating that about 12% of all fruit produced did not make it to the end consumer before becoming unmarketable. While improvements to fruit texture will not solve this problem entirely, they are likely to reduce waste at the retail and consumer levels by extending shelf life. In addition to food waste, crops like muscadine are thought to have texture profiles that present a barrier to marketability evidenced by a lack of consumer acceptance (Brown et al., 2016). In such cases, improvement of texture quality, with respect to consumer opinion, would likely promote growth of the existing fresh fruit market. The perceived importance of fruit texture was further emphasized by a 2012 survey of rosaceous fruit breeders (Gallardo et al., 2012) which concluded that fruit texture was consistently ranked in the top three most important traits across all species surveyed. Breeders also consistently reported that the needs of both

producers and marketers were most influential in determining the importance of fruit texture to their breeding programs (Gallardo et al., 2019), suggesting that the appeal to improved fruit texture is far-reaching.

Many of the natural texture and storage characteristics of a crop are determined by factors that are inherent to the species and the tissue being harvested. These crop-specific limitations often include cellular properties, such as size, arrangement, adhesion, and cell wall thickness (Toivonen and Brummel, 2008). Toivonen and Brummel (2008) also note the critical importance of softening pattern (melting or fracturable flesh) and the role of ethylene (climacteric or nonclimacteric) in determining the rate of textural degradation for a crop species. Although these factors mentioned are often genetically determined, they tend to be fairly uniform across a species, with softening in peach being a notable exception (Peace et al., 2005). Muscadine and blackberry both can be widely categorized as nonclimacteric, melting flesh fruit crops, meaning that they soften greatly as they ripen, but they do not experience a sharp autocatalytic increase in ethylene production and stimulated respiration with ripening (Brecht et al., 2007; Toivonen and Brummel, 2008). Because of this qualification, it can be suggested that ethylene does not play as large of a role in softening as with climacteric fruits, such as tomato, peach, or banana. Regardless, the possible presence of genetic variation for expression of factors affecting cell integrity and loss of turgor remains.

Within the confines of predetermined ripening patterns, most economically important fruit crops are known to have a degree of heritable variation in fruit texture and softening as well. This is often attributed to differential expression of enzymes that modify cell wall components, like polygalacuronase (PG). In apple (*Malus* x *domestica* Borkh.), genetically modified individuals with reduced PG expression were shown to produce apples that soften at a slower

rate than apples with normal PG expression (Atkinson et al., 2012). Similarly, down regulation of PG in transgenic strawberry (*Fragaria* x *ananassa* Duchesne 'Chandler') resulted in lower levels of pectin solubilization and increased covalent bonding of pectins to cell walls, which are both associated with softening (Quesada et al., 2009). In peach (*Prunus persica* [L.] Batsch) only two tightly linked PG genes are responsible for determining the phenotypic expression of stone adhesion and melting flesh (Gu et al., 2016; Peace et al., 2005). Despite the frequent importance of single genes in controlling certain cell wall degrading enzymes, as demonstrated through both natural observations and transgenic studies, breeding populations often display a striking range of natural phenotypic texture qualities that appear to be much more quantitative in nature. In blackberry, a sample of eight genotypes from the UA breeding program representing a range of texture qualities revealed that the firmest blackberry genotype (A-2453T) was more than twice as firm as the softest berry ('Black Magic') according to UTM instrumental texture analysis (McCoy et al., 2016). A similar report in muscadine, surveying 27 muscadine genotypes from the University of Georgia breeding program revealed a similar range of natural variation for flesh maximum force, skin break force, and several other traits, with firmest accessions often being two to three times firmer than the softest accessions (Conner, 2013). The magnitude of phenotypic variation reported suggests that the genetic base of these crops is more than adequate to provide breeders with the opportunity to improve texture qualities with respect to storability and consumer opinion, provided that the heritability of these textural attributes are sufficient to support meaningful genetic gain.

Texture and Fresh Muscadines

Of all the American grape species, muscadine (*Vitis rotundifolia* Michx.), is the most distantly related to the more familiar European common grapevine (*Vitis vinifera* L.), diverging approximately 18 million years ago (Wan et al., 2013). This may be no surprise to those who enjoy muscadines, as the fruit bears a number of striking differences from the European grape. The exocarp tissue, which slips easily (often referred to as a 'slipskin') from the mesocarp, tends to be much thicker than that of a common table grape. The muscadine mesocarp is often gummy and more difficult to macerate, strongly clinging to 2 to 6 large seeds (Conner, 2013; Olien, 1990). This contrasts with crisp table grapes like 'Red Globe' or 'Thompson Seedless', which have firm pulp that is easily chewed, and thin, almost unnoticeable skins. Despite having a few challenging textural attributes, fresh muscadine boasts a strong following in the native range of the southeastern United States. It has been speculated that, if these texture qualities could be improved through traditional plant breeding methods to produce a muscadine texture resembling a crisp table grape, then this localized fresh muscadine market might expand to an even wider base of consumers. These speculations are supported by the findings of Brown et al. (2016), who demonstrated that consumer panelists from the University of Florida who were familiar with muscadines were heavily influenced by flesh and skin qualities when asked how much they liked various muscadine cultivars and breeding selections. They also showed that even panelists who were familiar with muscadines tended to prefer thinner skins, highlighting this attribute as an important target for future breeding improvements.

In addition to bolstering consumer opinion, variation in muscadine texture may also be associated with postharvest quality and storability. Barchenger et al. (2015) showed that the force required to penetrate the skin of a muscadine reduced over time in cold storage, but that the

rate of this reduction varied significantly between genotypes. Similarly, Conner (2012) noted that the muscadine cultivar 'Supreme' maintained its firmness considerably compared to other genotypes over four weeks in storage. Others have also pointed out that the presence of wet stem scars may be an important cause of an immediate decline in firmness, which also leads to acceleration of molding, decay, and loss of quality in cold storage (Ballinger and Nesbitt, 1982; Conner, 2012), although in this case the decay could easily be the result of wounding rather than a direct consequence of texture quality. Collectively, literature describing the role of muscadine texture quality in determining storability is scarce, but there is reason to believe that some relationship between the two exists and additional work may be required to understand its importance.

History of Muscadine Breeding

Although the Native American consumption of muscadine grape certainly predates even the early French colonists of 1565, who reportedly made wine from wild landraces (Winsor, 1889), the recorded history of the crop is quite young compared to that of *Vitis vinifera,* in which cultivation dates back approximately 6000 years (Einset and Pratt, 1975). The earliest efforts to improve the fruit quality of muscadine are traced back to the mid-nineteenth century (Reimer and Detjen, 1914), prior to the rediscovery of the Mendelian laws of inheritance. These efforts consisted of the collection, planting, and subsequent evaluation of open-pollinated seed. In the evaluation of these early seedlings, J. Van Buren stated that "Many, doubtless will be inferior to the parents, while some will be equal and others superior in size and flavor", demonstrating a basic understanding of the need for large population sizes to select from (Reimer and Detjen, 1914). The first publicly supported breeding program began in 1908 at Willard, North Carolina as a cooperation between the USDA and North Carolina State University, and it was followed by

the initiation of several others in the southeastern U.S. (Goldy, 1992). The goals of these early programs often considered improvements in color, uniform-ripening, dry stem scar, fruit cluster size, shattering, and perfect, self-fertile flowering. Since the early days of muscadine breeding, several noteworthy strides have been made in these areas, including the self-fertility of 'Hope', the improved pigment of 'Noble', and the high yield and ideal processing characteristics of 'Carlos' (Goldy, 1992). However, many of these original breeding goals persist as important objectives to the present day (Goldy, 1992). Similarly, 'Scuppernong', which was the first documented muscadine cultivar also remains one of the most widely recognized cultivars (Olien, 1990). Through the past century of breeding efforts, muscadine improvement has occurred at a slow, yet gradual pace.

Breeding and Screening for Improved Texture in Muscadine

Muscadine and other species belonging to subgenus *Muscadinia* Planch. contain an additional pair of chromosomes (2n = 40) compared to *V. vinifera* and other 'bunch grapes' in the subgenus *Euvitis* Planch (2n = 38) (Wan et al., 2013). This difference in chromosome number has proven to be a considerable obstacle to breeders who would seek to combine the fruit quality of *Euvitis* with the disease resistance and environmental adaptation of *Muscadinia* through hybridization. Despite this difficulty, some breeders have had limited success, often accompanied by sterility in the progeny, when using muscadine as the male parent (Goldy, 1992; Olien, 1990). Alternatively, substantial variation in texture has been reported among muscadine germplasm, with flesh textures ranging from soft and melting to tough and stringy (Conner and Worthington, 2023). The muscadine breeding program at the University of Georgia, has managed to achieve measurable gains in the texture quality of fresh muscadines through crossing and selection of diverse muscadine germplasm, as reflected by the newly released home garden

variety, ‘RubyCrisp’, which has tender, palatable skins and firm, crisp flesh (Conner, 2019). Some of the newer selections bred for table use from the University of Georgia program were shown to have skin break force approaching those of *V. vinifera* table varieties, further demonstrating that the genetic base of *Muscadinia* alone is sufficient to support improvement of tenderness of skins (Conner, 2013). Therefore, Conner (2013) and Barchenger et al. (2015) have recommended routine screening of new breeding selections for texture attributes as a cost-effective method of predicting consumer acceptance and storability.

Many breeders have determined that laboratory instruments like the Stable Micro Systems TA.XT Texture Analyzer (Texture Technologies Corporation, Hamilton, MA) are an effective alternative or complement to panel-based texture analyses and breeders’ field ratings (Conner, 2013; Rolle et al., 2012). *V. vinifera* researchers have already tested and reported uses for a range of probes with diverse shapes and functions (Rolle et al., 2012). For instance, flat, cylindrical compression probes have been used to estimate traits like hardness, cohesiveness, springiness, and chewiness (Cefola et al., 2011; Martinez-Romero et al., 2003; Rolle et al., 2011). The needle-like 2mm cylinder probe has been used to measure elasticity, rupture force, and skin thickness (Rolle et al., 2011; Vargas et al., 2001). Other experiments in *V. vinifera* have explored uses for spring clamps (Deng et al., 2005), conical probes (Letaief et al., 2008), and rounded probes (Maury et al., 2009). Instrumental texture research in muscadine is much less mature. At the time of writing, all published work in muscadine has relied solely on the 2 mm and 5 mm cylinder probes (Barchenger et al., 2015, Brown et al., 2016, Conner 2013, Felts et al., 2018). Conner (2013) used both probes to evaluate texture in 26 muscadine genotypes using four different measurement protocols. Conner (2013) used the 2 mm cylinder probe to measure berry deformation at first peak and berry maximum force. The 5 mm cylinder probe was used to

measure flesh maximum force and skin break force. Using these four protocols, Conner (2013) suggested that berry penetration work estimated with the 2 mm probe and flesh maximum force estimated with the 5 mm probe would be most useful in routine texture screening. Still, many texture analysis protocols and attachments remain untested in the muscadine literature. The Kramer Shear Cell (KSC), for instance, has been recommended as a supplement or replacement to the 2 mm probe penetration tests (Harker et al., 1997). This instrument consists of five parallel blades positioned over a metal box with five grates at the bottom. Bulk fruit samples are placed in the box and macerated by the blades to simulate one or more cycles of chewing.

Postharvest Qualities of Fresh Blackberries

Fresh-market blackberries are a commodity of growing economic importance in the United States, but the seasonal availability of fresh blackberries is heavily dependent on shipping channels, due to a reliance on centralized domestic production and imports. In 2018, blackberries were the fourth most important berry crop following strawberry, blueberry (*Vaccinium angustifolium* Aiton), and raspberry (*Rubus idaeus* L.) respectively (California Strawberry Commission, 2019). Domestic production in the US is mainly concentrated on the Pacific coast and the Southeast, and was valued at about 650 million dollars in 2018 (California Strawberry Commission, 2019). Oregon currently leads the nation in blackberry production, at over 58 million lbs. in 2016 (USDA-NASS, 2016), signaling an increase of 28% compared to 2014. This figure, however, mostly consists of processing types as opposed to fresh-market types, which are thought to prevail in California and the southeastern states. Blackberries are considered one of the most challenging fruits to ship, as they often suffer from a short shelf life due to factors including moisture loss, high respiration rate, mold susceptibility, ethylene production, juice leakage, discoloration, and berry softening (Perkins-Veazie, 2017; Segantini et

al., 2017). As a crop, the postharvest quality of blackberry is disadvantaged by fragile, thin skins and the notable lack of cuticle or protective rind, which allows moisture to escape more easily. However, certain postharvest characters can vary drastically depending on both cultivar and cultural practices such as soil nutrition, harvest maturity, storage temperature, light exposure, shipping practices, and packaging (Edgeley et al., 2019a; Perkins-Veazie et al., 1996; Perkins Veazie, 2017). Therefore, a holistic understanding of the effects of commonly implemented cultural practices on postharvest quality and how they may interact with the observed phenotypes of advanced breeding selections should guide the breeding of shipping-quality blackberries.

Fruit Appearance and Red Drupelet Reversion

Fruit appearance is one of the most important characters used in the assessment of postharvest quality because it is ultimately the factor upon which the consumer will make a purchasing decision (Clark and Finn, 2011). As such, blackberries are considered most attractive when they are glossy, fully black, and absent of leakage or decay (Perkins-Veazie and Clark, 2005). A severe reduction in marketability can occur when color is compromised through a postharvest disorder known as red drupelet reversion (RDR), red drupelet disorder, or simply reddening. This disorder occurs when berries that are harvested fully black ‘revert’ to a red color after a period of shipping and storage (Clark and Finn, 2011). In an online survey of demographically diverse blackberry consumers, individuals strongly preferred images of blackberries with minimal RDR (Threlfall et al., 2020). These results were also validated in a subsequent in-person consumer sensory panel (Threlfall et al., 2021). In addition to deterring would-be consumers, severe cases of RDR can also result in more immediate and apparent economic losses. According to USDA-AMS guidelines, entire lots of blackberries can be rejected if RDR damage affects at least 10% of the berry lot by volume or only 5% by volume if

the damage is categorized as severe (USDA-AMS, 2018). Much like other postharvest conditions, RDR is affected by genetic factors (Lawrence and Melgar, 2018; Salgado and Clark, 2016) and cultural practices such as temperature and handling at harvest (Edgley et al., 2019c), shipping vibration patterns (Pérez-Pérez et al., 2018), and nitrogen fertilizer application rates (Edgley et al., 2019b).

In recent work, Edgley and colleagues showed that RDR likely occurs in response to mechanical damage leading to cell disruption, separation, and loss of integrity in the upper mesocarp (2019a). These findings are consistent with the work of Pérez-Pérez and others who concluded that shipping practices with vibration patterns exceeding 10 Hz leads to a loss of cell integrity and subsequent RDR (2018). In theory, damage of this kind might lead to decompartmentalization of the anthocyanin pigments (primarily cyanidin 3-glucoside) and their subsequent degradation through enzymatic oxidative activity or change in color due to a higher pH environment. Color loss due to enzymatic degradation of anthocyanins has been widely reported in other crops and is often facilitated by polyphenol oxidases (PPO) or peroxidases (Pifferi and Cultrera, 1974; Taranto et al., 2017; Tomas-Barberan and Espin, 2001). Anthocyanins are also considered to be good pH indicators, as the wavelengths they absorb are closely tied to the pH of their environment (Torskangerpoll and Anderson, 2005). This theory is also consistent with the findings of Kim et al. (2019) who determined that anthocyanins were generally lower in red drupelets compared to black drupelets in reverted berries. Kim and others also observed that the concentration of lysophosphatidylcholine, a cell membrane component, was much higher in red drupelets, suggesting a possible loss of membrane integrity (2019). Lastly, Pérez-Pérez et al. (2018) also observed that, relative to non-reverted drupelets, the monomeric anthocyanin content of reverted drupelets was low and the polymeric anthocyanin

content was high. From this evidence, it may be suggested that the decompartmenatlization of anthocyanins from a low pH vacuole to a more neutral environment could encourage polymerization of mono-glucosidic anthocyanins leading to color change, as recently demonstrated in purple sweet potato (*Ipomoea batatas* L.) (Jiang et al., 2019).

Phenotyping RDR

Currently, the quantification and screening of RDR is almost exclusively conducted through manual techniques that involve either counting of reverted drupelets (Edgley et al., 2019a; Lawrence and Melgar, 2018; Segantini et al., 2017) or subjective classification of RDR severity into different grades (USDA-AMS, 2018). The latter is relatively quick, cheap, and effective in determining if a lot of blackberries is suitable to be sold according to provided standards. However, manual counting of reverted drupelets to quantify the degree of reversion between different treatments or genotypes can be prohibitively laborious and time-consuming, especially when reporting RDR in terms of average percent RDR on individual berries. For this reason, some investigators have reported RDR estimates on the basis of as few as five berries per experimental unit (Segantini et al., 2017). This small sample size is almost certain to lead to an inflation of error variance and a loss of overall accuracy, since the postharvest RDR characteristics of berries harvested from a single plot can vary tremendously from berry to berry. In addition to a possible loss of accuracy, this logistic barrier reduces the scalability of experiments that require screening of this disorder. For instance, screening of entire breeding populations or conducting large-scale mapping studies would be entirely impractical using manual counting techniques.

Although current phenotyping procedures are labor-intensive, the idea behind diagnosing and scoring RDR according to USDA standards is simple and relies on the assessment of two

factors: color intensity and number of affected drupelets (USDA-AMS, 2018). In this way, scoring of RDR is not entirely different from a wide range of other color-dependent assessments such as nutrient deficiency, drought-tolerance, flood-tolerance, ground coverage, and the presence of pigment-altering diseases. In other crops, high-throughput phenotyping methods that rely on digital image processing have been widely adopted to facilitate scalability and ease of data collection among these traits. ImageJ, an open-source java-based program, has been proven to be especially helpful in this role, as it provides researchers with the ability to develop batch-processing macro scripts that quantify image pixel counts based on user-defined thresholds based on HSB, RGB, or LAB color spaces (Ferreira and Rasband, 2012). ImageJ macro-processing has been successfully been implemented in phenotyping protocols for multiple crops including soybean, wheat, papaya, and others (Chizk et al., 2018; Cortes et al., 2017; Maloney et al., 2014) on a range of traits.

Blackberry Texture and UA 'Crispy' Selections

Just as visual attractiveness plays a crucial role in determining if the blackberry clamshell will pass from the retailer to the picky consumer, fruit texture is crucial in determining if the clamshell will successfully pass from the producer to the retailer without incurring a fatal loss of marketability due to leakage, mold, or softening. In the United States, the year-round availability of fresh-market blackberries is heavily dependent on imports from Mexico during the winter months. From 2019 to 2022, US fresh-market blackberry imports have sharply risen by about 52% (USDA-ERS, 2023) to meet growing demand from consumers. Considering this heavy dependency on shipping, improved fruit texture has become a central focus of many breeding programs including the University of Arkansas System Division of Agriculture (UA) fruit breeding program (Clark and Finn, 2011). Though once considered an intractable trait, texture

advancements in recent decades have exceeded former expectations, as evidenced by the excellent shipping potential of cultivars like ‘Navaho’ and ‘Chester Thornless’ (Clark, 2005). More recently, the UA program has identified a uniquely valuable ‘crispy’ phenotype in fruit texture among the full-sib selections, A-2453T and A-2454T, which were selected in 2008 (Salgado and Clark, 2016). Compared to other UA breeding selection and cultivars, A-2453T and A-2454T are distinctly firmer and more resistant to softening and RDR. These distinctions were initially observed subjectively through field observations and postharvest analyses but have since been verified through objective UTM texture analyzer instrumental techniques (McCoy et al., 2016; Salgado and Clark, 2016). The enhanced texture quality of A-2453T has also been associated with low incidence of RDR (Salgado and Clark, 2016; Segantini et al., 2017). Salgado and Clark observed that the firmer crispy genotypes only experienced RDR in 13% of berries, when non-crispy genotypes exposed to identical storage conditions experienced 41% reversion (2016).

The novel texture qualities of the UA crispy germplasm hold great promise for the continued improvement of blackberry shelf life and shipping potential, yet the underlying mechanism for this distinctive trait is not yet well understood. Salgado and Clark observed that A-2453T had notably smaller intercellular space and better cell adhesion compared to non-crispy genotypes (2016). This observation is likely due to differences in the integrity of the middle lamella, which is primarily composed of pectin and serves an important structural function by holding cells together (Toivonen and Brummel, 2008). Toivonen and Brummel (2008) also noted that pectin is observed to a lesser extent, along with cellulose, hemicellulose, and proteins, in the primary cell wall structure, where it contributes to structural integrity. Interestingly, cell separation and loss of cell wall integrity are also two of the previously discussed symptoms of

RDR (Edgley, 2019a; Kim, 2019; Pérez-Pérez, 2018), which could provide a partial explanation for the RDR resistance observed among crispy genotypes.

There is a large body of evidence among other crops implicating polygalacturonase (PG) as the key enzyme responsible for degradation of middle lamellar pectic polymers leading to cell separation and subsequent softening, particularly with respect to deesterified pectic polymers (Berger and Reid, 1979; Crookes and Grierson, 1983; Peace et al., 2005; Toivonen and Brummel, 2008). All forms of PG enzymes have the capability to depolymerize pectin, but the *endo* form is particularly detrimental to fruit texture, because it can cleave α-1,4 glycosidic linkages of pectins nonspecifically at deesterified regions rather than just at the non-reducing ends, as is the case with *exo*-PG enzymes (Watkins, 2017). The depolymerizing activity of *endo*-PG is thought to be enhanced by the enzymatic activity of pectin methylesterase (PME), which catalyzes the removal of methyl groups, thereby lowering the degree of esterification (Watkins, 2017). The solubilization of pectin, which often accompanies PG activity (Brummell and Harpster, 2001), has been widely observed as an indicator of enzymatic activity and degradation of the cell wall- middle lamella complex (Van Buren, 1991). In general, the three documented solubility states of pectin include protopectins, chelator-soluble pectins, and water-soluble pectins. The latter two forms are associated with the middle lamella, while protopectins are thought to be embedded in the primary cell wall structure (Selvendran, 1985). A loss of protopectin and an increase in water-soluble pectin content is associated with PG activity and can, therefore, be interpreted as an indicator of enzymatic depolymerization (Van Buren, 1991).

Genetics of Postharvest Quality

Several gene-silencing transgenic studies in other crops have provided additional insight to the potential magnitude of *endo*-PG's role in fruit softening. In strawberry, antisense silencing

of the *FaPG1* gene coding for polygalacturonase resulted in reduced softening which corresponded with a reduction in pectin solubilization (Mercado et al., 2009). Similarly, Atkinson and colleagues observed that down-regulation of *PG1* in apple resulted in reduced softening accompanied by improved cell cohesion, which is indicative of a structurally intact middle lamella (2012). In tomato, down-regulation of PG alone was not enough the prevent softening of fruit, but it did result in improved storage and transport characteristics, indicating that the integrity of cellular structures was likely preserved in some way (Schuch et al., 1991). Beyond transgenic studies, genetic variation for PG expression is known to exist naturally among other species. Peach (*Prunus persica* [L.] Batsch) is a particularly striking example, as it contains natural allelic variants of two tightly linked *endo*-PG genes, *PpendoPGF* and *PpendoPGM* (Gu et al., 2016; Peace et al., 2005). Gu and colleagues (2016) reported that *PpendoPGM* controls melting flesh, while *PpendoPGF* displays pleiotropic effects for both melting flesh and stone adhesion, and that collectively they are the most important determinants of stone adhesion and melting flesh expression.

Despite the recurring theme of *endo*-PG genes in literature relating to fruit texture, other enzymes and cell wall proteins are expected to play important roles in postharvest quality as well, including pectin methylesterases (PME), cellulases, expansins, β-galactosidases, pectate lyases (PL), and xyloglucan endotransglycosylases to name a few (Brummell and Harpster, 2001; Youssef et al., 2013). Transgenic down-regulation of β-galactoside 4 in tomato has resulted reduced softening with maturation (Smith et al., 2002), while similar suppression of PME has not resulted in any apparent reduction of softening (Brummel and Harpster, 2001). Pectate lyase plays an apparent role in strawberry texture, as transgenic suppression of this enzyme has reportedly reduced softening compared to wild-types, while similar suppression of

β-1,4-glucanase (a type of cellulase) resulted in no change in softening (Youssef et al., 2013). Lastly, simultaneous suppression of expansin (a cell wall protein) and PG genes in tomato has been reported to reduce susceptibility to *Botrytis cinerea* (Cantu et al., 2008), which is a fungal pathogen that can lead to severe loss of marketability. All these examples emphasize the simplicity of genetic control over the expression and activity of key individual proteins, while also highlighting the complexity of the ripening process in relation to cell wall modification. Therefore, further investigation into the genetic cause of crispness in blackberry warrants consideration of a number of potential candidate genes, with *endo*-PG likely being the most important.

History of Blackberry Breeding

In the southern US, the earliest efforts to develop improved blackberry cultivars began at Texas A and M University in 1909, resulting in the notable release of 'Brazos' (Clark, 2016). Over fifty years later, the blackberry breeding program at the University of Arkansas began under the direction of James N. Moore, with objectives including improved fruit size, fruit quality, cane architecture, harvest season extension, thornlessness, and productivity (Clark, 1999). Moore used USDA-ARS materials derived from 'Merton Thornless' along with diverse parents like 'Brazos' and 'Darrow' to build the foundation of this new breeding program (Clark, 2016). A cross between 'Brazos' and 'Darrow' resulted in the release of the thorny cultivar, 'Cherokee', in 1974, which was valued for its improved texture characteristics at the time. In 1989, the release of 'Navaho' represented a landmark achievement, as a thornless cultivar with impressive shipping potential, and signaled a shift in focus toward the importance of breeding for improved postharvest storage potential (Clark, 2016; Perkins-Veazie et al., 1999). Following this release, protocols to subjectively evaluate postharvest storage potential were swiftly

developed and implemented in the screening of advanced selections, leading to the identification of the previously discussed crispy selections (Clark, 2016). Today, the importance of fruit texture and postharvest storage potential remains central to the UA program, but recent technological advancements have encouraged the exploration of new screening protocols accompanied by high-throughput techniques and marker-assisted selection.

Genome-Wide Association in Blackberry

Advancements in fields of computer science and biotechnology combined with the increasing availability of powerful statistical programming tools have both contributed to the growing importance and viability of genome-wide association studies (GWAS) in investigating marker-phenotype associations, which can ultimately be implemented in highly efficient marker assisted selection (MAS) or genomic selection (GS) schemes. In addition to its growing accessibility, GWAS carries several distinct advantages over more traditional linkage mapping approaches including higher mapping resolution, consistency of marker effects across a diverse discovery population, and no requirement of the costly, time-consuming step of population development (Myles et al., 2009). The recent development of the R package, GWASpoly, has made association mapping even more accessible to autopolyploid researchers by providing an open-source tool capable of testing allele dosage with the Q + K mixed model (Rosyara et al., 2016). While this software has been successfully utilized in the analysis of multiple potato populations (Berdugo-Cely et al., 2017; Rosyara et al., 2016), it has not yet been used for GWAS in autopolyploid blackberry. Finally, the generation of high-quality reference genomes in *Rubus* species have provided novel tools that enable the alignment of sequencing data and the identification of candidate genes. The *R. occidentalis* genome was the first annotated *Rubus* genome to be sequenced (VanBuren et al., 2016; VanBuren et al., 2018) followed by the *R.*

idaeus genome (Davik et al., 2022). Even more recently, the *R. argutus* diploid blackberry genome was assembled and annotated (Brůna et al., 2022). Together, the availability of the newly developed GWASpoly package and reliable reference genomes promote association mapping as a promising strategy for investigating the genetic basis of phenotypic variation for fruit texture in UA blackberry germplasm.

Literature Cited

Atkinson RG, Sutherland PW, Johnston SL, Gunaseelan K, Hallett IC, Mitra D, Brummell DA, Schröder R, Johnston JW, Schaffer RJ. 2012. Down-regulation of POLYGALACTURONASE1 alters firmness, tensile strength and water loss in apple (*Malus x domestica*) fruit. BMC Plant Biol. 12:129.

Ballinger WE, Nesbitt WB. 1982. Postharvest decay of muscadine grapes ('Carlos') in relation to storage temperature, time, and stem condition. Amer. J. of Enol. 33:173-175.

Barchenger DW, Clark JR, Threlfall RT, Howard LR, Brownmiller CR. 2015. Evaluation of physicochemical and storability attributes of muscadine grapes (*Vitis rotundifolia* Michx.). HortScience 50:104-111.

Berdugo-Cely J, Valbuena RI, Sánchez-Betancourt E, Barrero LS, Yockteng R. 2017. Genetic diversity and association mapping in the Colombian Central Collection of *Solanum tuberosum* L. Andigenum group using SNP markers. PloS One 12:0173039.

Berger RK, Reid PD. 1979. Role of polygalacturonase in bean leaf abscission. Plant Physiol. 63:1133-1137.

Blumenkrantz N, Asboe-Hansen G. 1973. New method for quantitative determination of uronic acids. Anal. Biochem. 54:484-489.

Brecht JK, Ritenour MA, Haard NF, Chism GW. 2017. Postharvest Physiology of Edible Plant Tissues. p.976-1046. In: S. Damodaran and K.L. Parkin (eds.). Fennema's Food Chemistry. CRC Press, Boca Raton, Florida.

Brown K, Sims C, Odabasi A, Bartoshuk L, Conner P, Gray D. 2016. Consumer acceptability of fresh-market muscadine grapes. J. Food Sci. 81:S2808-S2816.

Brummel DA, Labavitch JM. 1997. Effect of antisense suppression of endopolygalacturonase activity on polyuronide molecular weight in ripening tomato fruit and in fruit homogenates. Plant Physiol. 115:717-725.

Brummell DA, Harpster MH. 2001. Cell wall metabolism in fruit softening and quality and its manipulation in transgenic plants. Plant Mol. Biol. 47:311-340.

Brůna, T., Aryal, R., Dudchenko, O., Sargent, D. J., Mead, D., Buti, M., et al. (2022). A chromosome-length genome assembly and annotation of blackberry (*Rubus argutus*, cv. 'Hillquist'). G3 Genes|Genomes|Genetics. doi: 10.1093/g3journal/jkac289.

Buzby JC, Hyman J, Stewart H, Wells HF. 2011. The value of retail-and consumer-level fruit and vegetable losses in the United States. J. Consumer Affairs 45:492-515.

California Strawberry Commission. 2019. U.S. Retail Category Trends. Calif. Strawb. Comm. November, 2019. <http://www.calstrawberry.com/en-us/market-data/retail-category-trends>

Cantu D, Vicente AR, Greve LC, Dewey FM, Bennett AB, Labavitch JM, Powell ALT. 2008. The intersection between cell wall disassembly, ripening, and fruit susceptibility to *Botrytis cinerea*. Proc. Natl. Acad. Sci. 105:859-864.

Chizk TM, 2018. The effects of row-spacing and seed-size on canopy traits and yield among 25 late-planted soybean cultivars and breeding lines. M.S. Thesis. North Carolina State Univ.

Clark JR. 1999. The blackberry breeding program at the University of Arkansas: thirty-plus years of progress and development for the future. Acta Hort. 505:73-78.

Clark JR. 2005. Intractable traits in eastern US blackberries. HortScience 40:1954-1955.

Clark JR, Stafne ET, Hall HK, Finn CE. 2007. Blackberry breeding and genetics. Plant Breeding Rev. 29:19-146.

Clark JR, Finn CE. 2011. Blackberry breeding and genetics. Fruit, Veg., and Cereal Sci. and Biotechnol. 5:27-43.

Clark JR, Perkins-Veazie P. 2011. 'APF-45' primocane-fruiting blackberry. HortScience 46:670-673.

Clark JR. 2016. Breeding southern US blackberries, idea to industry. Acta Hort. 1133:3-12

Cliff MA, Bejaei M. 2018. Inter-correlation of apple firmness determinations and development of cross-validated regression models for prediction of sensory attributes from instrumental and compositional analyses. Food Res. Intl. 106:752-762.

Conner PJ. 2012. Evaluation of muscadine genotypes for storage ability. HortScience 47:S386

Conner PJ. 2013. Instrumental textural analysis of muscadine grape germplasm. HortScience 48:1130-1134.

Conner PJ. 2019. 'Rubycrisp' a new home-garden muscadine grape with hermaphroditic flowers and large red berries. HortScience 54:S189.

Cortes DFM, Catarina RS, Barros GBDA, Arêdes FAS, Silveira SFD, Ferreguetti GA, Ramos HCC, Viana AP, Pereira MG. 2017. Model-assisted phenotyping by digital images in papaya breeding program. Scientia Agricola 74:294-302.

Crookes PR, Grierson D. 1983. Ultrastructure of tomato fruit ripening and the role of polygalacturonase isoenzymes in cell wall degradation. Plant Physiol. 72:1088-1093.

Davik J, Dag R, Erik L, Matteo B, Simeon R, Muath A, Erez LA, Olga D, and Daniel JS. 2022. A chromosome-level genome sequence assembly of the red raspberry (*Rubus idaeus* L.). Plos one 17(3):e0265096.

Dische Z. 1962. Color reactions of hexoses. Vol. 1. p. 488-490. In: R.L. Whistler and M.L. Wolfrom (eds.) Methods in carbohydrate chemistry. Academic Press, New York.

Edgley M, Close DC, Measham PF, Nichols DS. 2019a. Physiochemistry of blackberries (*Rubus* L. subgenus *Rubus* Watson) affected by red drupelet reversion. Postharvest Biol. Technol. 153:183-190.

Edgley M, Close DC, Measham PF. 2019b. Nitrogen application rate and harvest date affect red drupelet reversion and postharvest quality in 'Ouachita' blackberries. Scientia Hort. 108543.

Edgley M, Close DC, Measham PF. 2019c. Effects of climatic conditions during harvest and handling on the postharvest expression of red drupelet reversion in blackberries. Scientia Hort. 253:399-404.

Einset J, Pratt C. 1975. Grapes. p.130-153. In: J. Janick and J.N. Moore (eds.). Advances in Fruit Breeding. Purdue Univ. Press. West Lafayette, Indiana.

Endelman JB, Jannink J. 2012. Shrinkage estimation of the realized relationship matrix. G3: Genes, Genomes, Genet. 2:1405-1413.

Felts M, Threlfall RT, Clark JR, Worthington ML. 2018. Physiochemical and descriptive sensory analysis of Arkansas muscadine grapes. HortScience 53:1570-1578.

Ferreira T, Rasband W. 2012. ImageJ user guide. ImageJ/Fiji, 1:155-161.

Gallardo RK, Nguyen D, McCracken V, Yue C, Luby J, McFerson JR. 2012. An investigation of trait prioritization in rosaceous fruit breeding programs. HortScience 47:771-776.

Garrison E, Marth G. 2012. Haplotype-based variant detection from short-read sequencing. arXiv preprint arXiv:1207.3907. <https://arxiv.org/abs/1207.3907>

Goldy. 1992. Breeding muscadine grape. Hort. Rev. 14:357-401.

Gu C, Wang L, Wang W, Zhou H, Ma B, Zheng H, Fang T, Ogutu C, Vimolmangkang S, Han Y. 2016. Copy number variation of a gene cluster encoding endopolygalacturonase mediates flesh texture and stone adhesion in peach. J. Exp. Bot. 67:1993-2005.

IOS (International Organization for Standardization). 2009. Sensory Analysis–Vocabulary. ISO 5492:2009.

Jiang T, Mao Y, Sui L, Yang N, Li S, Zhu Z, Wang C, Yin S, He J, He Y. 2019. Degredation of anthocyanins and polymeric color formation during heat treatment of purple sweet potato extract at different pH. Food Chem. 274:460-470.

Jombart T, Devillard S, Balloux F. 2010. Discriminant analysis of principal components: a new method for the analysis of genetically structured populations. BMC Genet. 11:94.

Kim D, Pertea G, Trapnell C, Pimentel H, Kelley R, Salzberg SL. 2013. TopHat2: accurate alignment of transcriptomes in the presence of insertions, deletions and gene fusions. Genome Biol. 14:R36.

Kim MJ, Lee MY, Shon JC, Kwon YS, Liu KH, Lee CH, Ku KM. 2019. Untargeted and targeted metabolomics analyses of blackberries–Understanding postharvest red drupelet disorder. Food Chem. 300:125169.

Lawrence B, Melgar JC. 2018. Harvest, handling, and storage recommendations for improving postharvest quality of blackberry cultivars. HortTechnology 28:578-583.

Leggett RM, Ramirez-Gonzalez RH, Clavijo B, Waite D, Davey RP. 2013. Sequencing quality assessment tools to enable data-driven informatics for high throughput genomics. Frontiers Genet. 4:288.

Le Moigne M, Maury C., Bertrand D, Jourjon F. 2008. Sensory and instrumental characterisation of Cabernet Franc grapes according to ripening stages and growing location. Food Quality and Preference 19:220-231.

Li H, Durbin R. 2009. Fast and accurate short read alignment with Burrows-Wheeler transform. Bioinformatics 25:1754-1760.

Love MI, Huber W, Anders S. 2014. Moderated estimation of fold change and dispersion for RNA-seq data with DESeq2. Genome Biol. 15:550.

Maloney PV, Petersen S, Navarro RA, Marshall D, McKendry AL, Costa JM, Murphy JP. 2014. Digital image analysis method for estimation of *Fusarium*-damaged kernels in wheat. Crop Sci. 54:2077-2083.

Mann H, Bedford D, Luby J, Vickers Z, Tong C. 2005. Relationship of instrumental and sensory texture measurements of fresh and stored apples to cell number and size. HortScience 40:1815-1820.

McCoy JE, Clark JR, Salgado AA, Jecmen A. 2016. Evaluation of harvest time/temperature and storage temperature on postharvest incidence of red drupelet reversion development and

firmness of blackberry (*Rubus* L. subgenus *Rubus* Watson). Discovery The Student Journal of Dale Bumpers College of Agricultural, Food and Life Sciences 17:59-65.

Myles S, Peiffer J, Brown PJ, Ersoz ES, Zhang Z, Costich DE, Buckler ES. 2009. Association mapping: critical considerations shift from genotyping to experimental design. The Plant Cell 21:2194-2202.

Olien WC. 1990. The muscadine grape: botany, viticulture, history, and current industry. HortScience 25:732-739.

Peace CP, Crisosto CH, Gradziel TM. 2005. Endopolygalacturonase: a candidate gene for freestone and melting flesh in peach. Mol. Breeding 16:21-31.

Pérez-Pérez GA, Fabela-Gallegos MJ, Vázquez-Barrios ME, Rivera-Pastrana DM, Palma-Tirado L, Mercado-Silva E, Escalona V. 2016. Effect of the transport vibration on the generation of the color reversion in blackberry fruit. In VIII Intl. Postharvest Symp.: Enhancing Supply Chain and Consumer Benefits-Ethical and Technol. Issues 1194:1329-1336.

Perkins-Veazie P, Collins JK, Clark JR. 1996. Cultivar and maturity affect postharvest quality of fruit from erect blackberries. HortScience 31:258-261.

Perkins-Veazie P, Collins JK, Clark JR. 1999. Shelf-life and quality of 'Navaho' and 'Shawnee' blackberry fruit stored under retail storage conditions. J. Food Quality 22:535-544.

Perkins Veazie P, Clark J. 2005. Blackberry research in Arkansas and Oklahoma. In Proc. of the North Amer. Bramble Growers Assn. Annu. Mtg. 9.

Perkins-Veazie, P. 2017. Postharvest storage and transport of blackberries. Blackberries and their hybrids. Crop Production Sci. Hort. 26:266.

Pifferi PG, Cultrera, R. 1974. Enzymatic degradation of anthocyanins: the role of sweet cherry polyphenol oxidase. J. Food Sci. 39:786-791.

Porebski S, Bailey LG, Baum BR. 1997. Modification of a CTAB DNA extraction protocol for plants containing high polysaccharide and polyphenol components. Plant Mol. Biol. Reporter 15:8-15.

Quesada MA, Blanco-Portales R, Posé S, García-Gago JA, Jiménez-Bermúdez S, Muñoz-Serrano A, Caballero JL, Pliego-Alfaro F, Mercado JA, Muñoz-Blanco J. 2009. Antisense down-regulation of the FaPG1 gene reveals an unexpected central role for polygalacturonase in strawberry fruit softening. Plant Physiol. 150:1022-1032.

Reimer FC, Detjen LR. 1914. Breeding *rotundifolia* grapes: a study of transmission of character No. 8-13. North Carolina Agricultural Experiment Station.

Rolle L, Siret R, Segade SR, Maury C, Gerbi V, Jourjon F. 2012. Instrumental texture analysis parameters as markers of table-grape and winegrape quality: A review. Amer. J. of Enol. and Viticult. 63:11-28.

Rosyara UR, De Jong WS, Douches DS, Endelman JB. 2016. Software for genome-wide association studies in autopolyploids and its application to potato. The Plant Genome 9.

Salgado AA, Clark JR. 2016. “Crispy” blackberry genotypes: a breeding innovation of the university of arkansas blackberry breeding program. HortScience 51:468-471.

Sato A. 1997. Varietal diffeences in the berry texture of grape berries measured by penetration tests. Vitis 36:7-10.

Schuch W, Kanczler J, Robertson D, Hobson G, Tucker G, Grierson D, Bright S, Bird C. 1991. Fruit quality characteristics of transgenic tomato fruit with altered polygalacturonase activity. HortScience 26:1517-1520.

Segantini DM, Threlfall R, Clark JR, Brownmiller CR, Howard LR, Lawless LJ. 2017. Changes in fresh-market and sensory attributes of blackberry genotypes after postharvest storage. J. Berry Res. 7:129-145.

Selvendran RR. 1985. Developments in the chemistry and biochemistry of pectic and hemicellulosic polymers. J Cell Sci. 51-88.

Simpson CG, Cullen DW, Hackett CA, Smith K, Hallett PD, McNicol J, Woodhead M, Graham J. 2017. Mapping and expression of genes associated with raspberry fruit ripening and softening. Theoretical Appl. Genet. 130:557-572.

Smith DL, Abbott JA, Gross KC. 2002. Down-regulation of tomato β-galactosidase 4 results in decreased fruit softening. Plant Physiol. 129:1755-1762.

Taranto F, Pasqualone A, Mangini G, Tripodi P, Miazzi M, Pavan S, Montemurro C. 2017. Polyphenol oxidases in crops: biochemical, physiological and genetic aspects. Intl. J. Mol. Sci. 18:377.

Threlfall RT, Clark JR, Dunteman AN, and Worthington ML. 2021. Identifying marketable attributes of fresh-market blackberries through consumer sensory evaluations. HortScience. 56(1):30–35. doi: 10.21273/HORTSCI15483-20.

Threlfall RT, Dunteman AN, Clark JR, Worthington ML. 2020. Using an online survey to determine consumer perceptions of fresh-market blackberries. Acta Hortic. 1277:469–476. doi: 10.17660/ActaHortic.2020.1277.67.

Toivonen PM, Brummell DA. 2008. Biochemical bases of appearance and texture changes in fresh-cut fruit and vegetables. Postharvest Biol. and Technol. 48:1-14.

Tomás-Barberán FA, Espín JC. 2001. Phenolic compounds and related enzymes as determinants of quality in fruits and vegetables. J. of the Sci. of Food and Agr. 81:853-876.

Torskangerpoll K. Andersen ØM. 2005. Colour stability of anthocyanins in aqueous solutions at various pH values. Food Chem. 89:427-440.

Uitdewilligen, JG, Wolters AMA, Bjorn B, Borm TJ, Visser RG, van Eck HJ. 2013. A next-generation sequencing method for genotyping-by-sequencing of highly heterozygous autotetraploid potato. PloS One 8:62355.

United States Department of Agriculture, National Agricultural Statistics Service. 2016. Quick Stats. November 2019. <https://quickstats.nass.usda.gov/>

United States Department of Agriculture, Economic Research Service. 2023. Fruit and Tree Nut Data. November 2019. <https://www.ers.usda.gov/data-products/fruit-and-tree-nut-data/data-by-commodity/>

United States Department of Agriculture, Agricultural Marketing Service. 2019. Shipping Point Inspection Instructions and Market Inspection Instructions Patch 34. November 2019. <https://www.ams.usda.gov/sites/default/files/media/PATCH034Berries081718.pdf.>

VanBuren R, Wai CM, Colle M, Wang J, Sullivan S, Bushakra JM, Liachko I, Vining KJ, Dossett M, Finn CE, Jibran R, Chagné D, Childs K, Edger PP, Mockler TC, Bassil NV. 2018. A near complete, chromosome-scale assembly of the black raspberry (*Rubus occidentalis*) genome. GigaScience 7:1-9.

Van Buren JP. 1991. Function of pectin in plant tissue structure and firmness. p.1-22. In: R.H. Walter (ed.). The chemistry and technology of pectin. Academic Press Inc. San Diego, California.

Vincent JF. 1998. The quantification of crispness. J. of the Sci. of Food and Agr. 78:162-168.

Vishwakarma RK, Chavan RS, Shivhare US, Basu S. 2016. Textural and rheological properties of fruit and vegetables. p.11-53. In: R.M.S. Cruz, I. Khmelinskii, and M.C. Vieira (eds.). Methods in food analysis. CRC Press, Boca Raton, Florida.

Wan Y, Schwaninger HR, Baldo AM, Labate JA, Zhong GY, Simon CJ. 2013. A phylogenetic analysis of the grape genus (*Vitis* L.) reveals broad reticulation and concurrent diversification during neogene and quaternary climate change. BMC Evolutionary Biol. 13:141.

Winsor J. (ed.), 1889. English explorations and settlements in North America. Vol. 3 of 8, p.1497-1689. In: Narrative and Critical History of America. The Riverside Press, Cambridge, Massachusetts.

Youssef SM, Amaya I. López-Aranda JM, Sesmero R, Valpuesta V, Casadoro G, Blanco-Portales R, Pliego-Alfaro F, Quesada MA, Mercado JA. 2013. Effect of simultaneous down-regulation of pectate lyase and endo-β-1, 4-glucanase genes on strawberry fruit softening. Mol. Breeding 31:313-322.

Zhang Z, Ersoz E, Lai C, Todhunter RJ, Tiwari HK, Gore MA, Bradbury PJ, Yu J, Arnett DK, Ordovas JM, Buckler ES. 2010. Mixed linear model approach adapted for genome-wide association studies. Nature Genet. 42:

CHAPTER I

SHINYFRUIT: INTERACTIVE FRUIT PHENOTYPING SOFTWARE AND ITS APPLICATION IN BLACKBERRY

Abstract

Horticultural plant breeding programs often demand large volumes of phenotypic data to capture visual variation in quality of harvested products. Increasing the throughput potential of phenomic pipelines enables breeders to consider data-hungry molecular breeding strategies such as genome-wide association studies and genomic selection. We present an R-based web application called ShinyFruit for image-based phenotyping of size, shape, and color-related qualities in fruits and vegetables. Here, we have demonstrated one potential application for ShinyFruit by comparing its estimates of fruit length, width, and red drupelet reversion (RDR) with analogous manual phenotyping techniques in a population of blackberry cultivars and breeding selections from the University of Arkansas System Division of Agriculture Fruit Breeding Program. ShinyFruit results shared a strong positive correlation with manual measurements for blackberry length (r = 0.96) and significant, albeit weaker, correlations with manual RDR estimation methods (r = 0.62 - 0.70). Neither phenotyping method detected genotypic differences in blackberry fruit width, suggesting that this trait is unlikely to be heritable in the population observed. It is likely that implementing a treatment to promote RDR expression in future studies might strengthen the documented correlation between phenotyping methods by maximizing genotypic variance. Even so, our analysis has suggested that ShinyFruit provides a viable, open-source solution to efficient phenotyping of size and color in blackberry fruit. The ability for users to adjust analysis settings should also extend its utility to a wide range of fruits and vegetables.

Introduction

The value of a horticultural product is almost always influenced by its appearance, which can be decomposed into color, size, shape, and other morphological components. These characteristics are often important indices of maturity, harvest efficiency, structural integrity, disease, insect damage, and flavor. Even when flavor differences are not present, individuals perceive differences in flavor intensities between differently colored but otherwise identical, food products (Shankar, 2009; Bayarri et al., 2001). The United States Department of Agriculture (USDA) Agricultural Marketing Service (AMS) has implemented visual grading and inspection guidelines for nearly all fresh-market fruit and vegetable crops. Inspectors assess color and shape using subjective visual techniques, which can become costly and time-consuming for researchers when a high degree of accuracy is desired. With modern photography and computing, it is now possible to construct low-cost objective phenotyping pipelines that are high throughput and based exclusively in open-source software. ImageJ software is a general user interface (GUI) enabled tool that has been widely used to construct such phenotyping pipelines (Maloney et al., 2014; Cortes et al., 2017; Chizk, 2018). Unfortunately, using ImageJ for customized batch image processing requires an understanding of the ImageJ macro programming language, which is a java-based language that is somewhat restrictive in scope to the utilities present in the tool.

We present an alternative R-based approach (R Core Team, 2020) called ShinyFruit, which is a software package that offers an interactive GUI designed to simultaneously perform color, size, and shape analyses on large sets of fruit images. ShinyFruit users currently can detect fruit in .jpg images by setting color threshold values in red-green-blue (RGB), hue-saturation-brightness (HSB), and L*a*b* color spaces. Following fruit detection, the user can indicate a

size reference and select from a list of traits to include in the .csv output file. We demonstrate one implementation of this tool in blackberry (*Rubus* subgenus *Rubus*) by comparing automated phenotypic measurements with those from traditional manual techniques. Traits measured include fruit length, fruit width, and red drupelet reversion (RDR), which is a disorder that occurs when fruit that are harvested fully black 'revert' to a red color after a period of shipping and storage (Clark et al., 2011).

With a growing fresh-market blackberry industry, RDR has become an issue of increasing concern among producers and distributors due to negative public perception. In an online survey of demographically diverse blackberry consumers, individuals strongly preferred images of blackberries with minimal RDR (Threlfall et al., 2020). These results were also validated in a subsequent in-person consumer sensory panel (Threlfall et al., 2021). In addition to deterring would-be consumers, severe cases of RDR can also result more immediate and apparent economic losses. According to USDA-AMS guidelines, entire lots of blackberries can be rejected if RDR damage affects at least 10% of the berry lot by volume or only 5% by volume if the damage is categorized as severe (USDA-AMS, 2018). Much like other postharvest conditions, RDR is affected by genetic factors (Salgado and Clark, 2016; Lawrence and Melgar, 2018) and cultural practices such as temperature and handling at harvest (Edgley et al., 2019a; Armour et al., 2021), shipping vibration patterns (Pérez-Pérez et al., 2018), and nitrogen fertilizer application rates (Edgley et al., 2019b). On the cellular level, RDR has been well characterized (Edgley et al., 2019c; Kim et al., 2019) and is likely the result of mechanical cell disruption, separation, and loss of integrity in the upper mesocarp leading to the decompartmentalization and subsequent oxidative degradation of anthocyanin pigments. However, published methods for detection are somewhat inconsistent and are exclusively

performed using subjective visual assessment. For instance, Clark and Perkins-Veazie (2011) evaluated RDR by categorizing entire berries as reverted or non-reverted based on a minimum threshold of three reverted drupelets, and Segantini et al. (2017) quantified RDR on individual berries by dividing the total number of reverted drupelets by total drupelets on each berry. Edgley et al. (2019a) devised a similar approach that also accounted for partially reverted drupelets. Developing a standardized, efficient, and objective technique would benefit breeders by providing the necessary framework for a scalable, simplified RDR screening protocol, improving their ability to select shipping tolerant genotypes.

Beyond color quality, morphological berry traits are often important to breeders as well. Large fruit size has been a key objective of the University of Arkansas (UA) System Division of Agriculture Fruit Breeding Program since its inception in 1964 (Clark, 1999). In fresh-market blackberry production, where fruit is harvested by hand, large fruit presents an obvious benefit to harvest efficiency. Surveyed consumers also tend to prefer blackberries that are large and oblong rather than small and round (Threlfall et al., 2020; Threlfall et al., 2021). Drastic gains in size have been achieved by modern cultivars like ‘Natchez’ (8.0 – 10.2 g/berry) (Clark and Moore, 2008), which can reach twice the size of the earliest UA releases (4.8 – 6.0 g/berry) (Moore et al., 1974). These large-fruited cultivars have approached maximum desirable size for packaging, but adequate size remains an important qualification for any new release. Like RDR, fruit size may easily be incorporated in an automated imaging pipeline, replacing the traditional use of scales or calipers. With flexible, user-determined input settings, the utility of an image analysis pipeline may be extended to data collection in a wider array of morphological characteristics in blackberry or even other fruits and vegetables, allowing breeders to have more versatility in selection methods. In the present study, we seek to compare the ShinyFruit software package,

which has been designed with these specific objectives in mind, to more traditional phenotyping techniques in a blackberry population of diverse sizes and shipping qualities.

Materials and Methods

Plant Material and Harvest. Floricane blackberry fruit from fourteen UA breeding selections and cultivars representing a diverse range of textures and susceptibility to RDR were harvested from 6 m plots located at UA System Fruit Research Station (FRS) in Clarksville, Arkansas in 2019, 2020, and 2021. The FRS site is located at 35º31'5"N and long. 93º24'12"W, in USDA hardiness zone 7b (USDA, 2021), on Linker fine sandy loam. All plots evaluated were treated with standard production practices including and early spring application of ammonium nitrate (56 $kg.ha^{-1}$ N) and a biweekly fertigation application of 20N-4.4P-17K from flowering to harvest. Liquid lime sulfur fungicide (94 $L.ha^{-1}$) was applied during bud break, five weeks before first harvest, and three weeks before first harvest to minimize anthracnose (*Elsinoë veneta*), botrytis fruit rot (*Botrytis cinerea*), and cane and leaf rust (*Kuehneola uredines*). Multiple pesticides containing active ingredients zeta-cypermethrin, bifenthrin, and malathion were applied weekly from flowering until floricane harvest in June to control spotted wing drosophila (*Drosophila suzukii*). A bifenthrin-containing insecticide was also applied annually in October to control raspberry crown borer (*Pennisetia marginata*). All plants were trained to a four-wire, horizontal T-trellis with low and high wires at 0.5 m and 1.0 m height. Plants were tipped to 1.1 m height in mid-May and lateral branches were pruned in August. Plots were grown in black plastic mulch to reduce weed pressure.

The 14 genotypes evaluated included A-2444T, A-2453T, A-2454T, A-2491T, 'Black Gem™', 'Black Magic™', 'Sweet-Ark® Caddo', 'Natchez', 'Osage', 'Ouachita', 'Sweet-Ark®

Ponca', 'Prime-Ark® Horizon', 'Prime-Ark® Freedom' and 'Prime-Ark® Traveler'. Blackberries were harvested at the shiny black stage in 500 mL clamshells on two separate harvest dates each year, with at least one week of separation between harvest dates. All fruit was harvested after 10:00 AM, when temperatures were usually over 27 °C, to encourage occurrence of red drupelet reversion (RDR) (Edgley et al., 2019a; Armour et al., 2021). Clamshells were filled just below the lid and placed directly into a portable cooler chilled by ice packs until they could be transported. In 2020 and 2021, harvested fruit samples were placed on a custom-built steel table for 30 minutes, with a vibrating surface that produced 2 mm of displacement and a frequency of 10 Hz. This treatment was intended to simulate shipping conditions that lead to RDR by replicating the findings of Perez-Perez et al. (2018). Samples were stored in an on-site refrigerator for a period of seven days at 5 °C and 90% relative humidity. Clamshells were removed from the refrigerator and allowed to reach room temperature before photographs were taken.

Image Capture. Photographs were collected seven days after harvest to allow RDR to occur during cold storage. Clamshells of fruit were photographed in a photo box (LimoStudio 16" x 16" Table Top Photo Photography Studio Lighting Light Tent Kit in a Box, AGG349; Las Vegas, Nevada, USA) constructed on a countertop with a Canon EOS Rebel T3 (Tokyo, Japan) camera mounted directly above a green cutting board on which the fruit was staged. The camera was equipped with a Canon EFS 18-55mm lens (Tokyo, Japan) and images were captured in close-up mode with International Organization for Standardization (ISO) values ranging from 250-3200. Fruit from a single clamshell were divided into two portions to be photographed separately due to the size of the staging area. Number of berries photographed in each sample varied depending on berry size, with 10-15 berries included in larger genotypes and 20-25

included in smaller genotypes. In 2019, a standard US quarter dollar was included in each image as a size reference. In 2020 and 2021, an X-Rite ColorChecker Classic Mini (Grand Rapids, Michigan, USA) was included in each image and used as a size reference.

Fruit Size. Length and width of five berries from each sample clamshell were measured using Pittsburgh digital calipers (Harbor Freight Tools, Camarillo, CA). Length of a fruit was defined as the distance between the abscission scar and the terminal drupelet. Berry width was defined as the maximum distance between drupelets on the equatorial plane. Fruit lengths and widths were only measured in 2020 and 2021.

Subjective Evaluation of Red Drupelet Reversion. After all images were captured, each clamshell was subjectively evaluated on a 'by-berry' and 'by-drupelet' basis. In both methods, the Royal Horticultural Society Greyed-Purple 185-A color value (L*a*b = 34.4, 42.0, 12.7) was used as a reference threshold. Drupelets matching that value or brighter were counted as reverted. For the 'by-berry' method, the number of berries in each clamshell were recorded. Then, each fruit was individually inspected for reverted drupelets, with fruit having three or more red drupelets scored as reverted while fruit with two or fewer red drupelets were scored as not reverted following Clark and Perkins-Veazie (2011). For the 'by-drupelet' method, five berries from each clamshell were selected at random. Each fruit was mounted on a toothpick through the abscission scar to aid in viewing. Red drupelets, including fully red and any deviated from standard black toward red, were counted and marked with a paint pen. After red drupelet count, the remaining drupelets were counted in the same manner for a total drupelet count per fruit. Percent reverted drupelets were calculated for each of the five berries per clamshell following Segantini et al. (2017).

ShinyFruit. Source code for version 0.1.0 of the ShinyFruit software (Chizk, 2022) is maintained and publicly available on GitHub (https://github.com/mchizk1/ShinyFruit) under an MIT license.

ShinyFruit's image-processing utilities were built using the R packages magick (Ooms, 2021) and imager (Barthelme, 2022), which both offer efficient C++-based methods for image manipulation. The GUI was built using the shiny (Chang et al., 2022) package for web application development. Upon reading user-provided sample images in .jpg format, ShinyFruit automatically processes images in several ways to prepare for analysis and maximize efficiency. All images are downsized such that the maximum dimension does not exceed 1500 pixels. This reduces time required for batch-image processing at the potential expense of fine resolution. Contrast in images is increased by normalizing pixel values to span the full RGB range. Finally, differences in color intensity are sharpened and the images are enhanced to reduce noisy or inconsistent pixel color values. Following read-in, the user may proceed through the image analysis pipeline detailed in Figure 1.1. Despeckling, which is implemented in the background removal and color feature detection steps, is achieved by successive shrinking and swelling of detected pixel groups. In this way, small, isolated groups of pixels (dust, juice, debris, etc.) are avoided during feature detection. Running the batch image analysis potentially generates two types of outputs including processed images and a comma separated value (csv) formatted text file containing requested data and implemented user settings for repeatability.

For each year of this study, a single representative image of blackberry fruit containing observable levels of RDR was read into the ShinyFruit program to remove background pixels, calibrate size references, and determine the appropriate color cutoff thresholds in the L*a*b* color space (Table 1.1). Figure 1.2 provides an example of the ShinyFruit GUI at the color thresholding stage of image analysis. Size and color settings specific to each year of image data were uniformly applied to batch-process all images. In 2019, the diameter of a US quarter dollar included in each image was used as the known size reference. In 2020 and 2021, the ruler edge

of the X-Rite ColorChecker Classic Mini was used as the known size reference. The location surrounding these size references was designated to be uniformly cropped out during image processing. Pixels with an a* value of greater than 7.51, 16.15, and 8.58 were counted as reverted in 2019, 2020, and 2021 respectively. No cutoff thresholds were needed for L* or b* values to identify red regions. Resulting images were output for visual post-analysis quality checking.

Experimental Design and Statistics. All analyses were performed using R version 4.1.2 (R Core Team, 2022). An analysis of variance (ANOVA) was performed using type III sums of squares and following a randomized complete block design. Harvest date was used as the blocking effect, while genotype and year were treated as fixed and random effects respectively. Estimated marginal means were calculated using the emmeans package (Lenth, 2022), and Tukey's honestly significant differences (HSD) were calculated using $P < 0.05$ for all dependent variables for which significant genotypic differences were detected. Pearson's correlations were calculated for genotypic means across years and pairwise linear regression were fitted with the ggplot2 (Wickham, 2016) and ggpubr (Kassambara, 2020) packages to compare automated and manual data collection methods.

Results

ShinyFruit, manual counting 'by-berry', and manual counting 'by-drupelet' all detected genotypic differences for fruit length, but none of these methods detected genotypic differences in fruit width. Genotype by year interactions for fruit length and fruit width were only significant in the ShinyFruit analysis (Table 1.2). Prime-Ark® Freedom and Natchez were both shorter in 2020 than in 2021 and this difference was most apparent in the ShinyFruit dataset (Appendix A).

Across years, ‘Natchez’ produced the longest fruit regardless of method, but the caliper-based method only distinguished ‘Natchez’ significantly from ‘Osage’ and A-2453T (Table 1.2). The latter two genotypes consistently produced the shortest fruit, regardless of method. Genotypic differences between mean fruit lengths were more pronounced in the ShinyFruit analysis. According to the ShinyFruit results, ‘Natchez’ and ‘Prime-Ark® Horizon’ had significantly longer fruit than all other genotypes except for ‘Prime-Ark® Freedom’. Similarly, A-2453T fruit was significantly shorter than all other genotypes except for ‘Osage’ and ‘Sweet-Ark® Ponca’. ShinyFruit and caliper-based methods for measuring fruit length were very tightly correlated (Table 1.3, Figure 1.3c, $r = 0.962$).

As with fruit length, ShinyFruit, manual counting ‘by-berry’, and manual counting ‘by-drupelet’ were all capable of distinguishing differences between genotypes across all three years for RDR (Table 1.2). ‘Black Magic™’ had significantly more reversion than most other genotypes tested (Table 1.2), regardless of phenotyping method. The ShinyFruit analysis distinguished ‘Black Magic™’ from all other genotypes except for ‘Sweet-Ark® Caddo’, with RDR levels at least three times higher than the remaining genotypes. The two manual RDR counting methods were much more highly correlated with one another (Table 1.3, $r = 0.940$) than with ShinyFruit RDR estimates, but both were still significantly correlated with ShinyFruit results. Drupelet-based RDR estimation was more tightly correlated with the ShinyFruit method (Table 1.3, Figure 1.3b, $r = 0.696$), although fruit-based RDR estimation was significantly correlated with ShinyFruit as well (Table 1.3, Figure 1.3a, $r = 0.621$). The manual ‘by-drupelet’ and ‘by-berry’ RDR methods both grouped ‘Black Magic™’, ‘Black Gem™’, ‘Prime-Ark® Freedom’, and A-2444T together in the highest reversion group. The ShinyFruit RDR method also grouped ‘Black Magic™’ among the highest RDR genotypes, but underestimated ‘Black

Gem™', 'Prime-Ark® Freedom', and A-2444T. 'Sweet-Ark® Caddo' only grouped among the highest RDR genotypes using the ShinyFruit estimation method.

Discussion

Manual measures of RDR using the 'by-drupelet' and 'by-berry' method were generally low compared to previous studies that have implemented similar methods. Segantini et al. (2017) and Felts (2020) observed RDR ranges of 0.7-6.1% and 2.43-8.06%, respectively, using the 'by-drupelet' method to evaluate germplasm closely related to the materials included in this study. In contrast, our 'by-drupelet' RDR observations only ranged from 0.06-4.63%. Similarly, Armour et al. (2021) observed a range of 1.42-79.83% using the by-berry RDR estimation method in closely related germplasm, while our own observations ranged from 0.50-34.97%. Each of these studies considered only partially overlapping samples of UA germplasm, which could partially account for differences in observed RDR ranges. However, this comparison suggests that our vibration treatment following Pérez-Pérez et al. (2018) was likely insufficient in promoting higher levels of RDR expression across the population. There were several notable similarities between our observed genotypic rankings for RDR expression levels and those reported by others. Unsurprisingly, we observed that 'Black Magic™' consistently grouped with the highest RDR genotypes using manual techniques. These findings are consistent with Armour et al. (2021), who reported that 'Black Magic™' had the softest fruited and highest RDR among the seven genotypes evaluated in that study. 'Natchez' has also expressed a moderate to high level of RDR in previous studies (Armour et al., 2021; Felts et al., 2020), although 'Natchez' was only in the highest RDR statistical group using the 'by-berry' RDR method in this study (Table 1.2). This discrepancy could suggest a bias present in the by-berry method, which may overestimate

RDR in large-fruited genotypes like ‘Natchez’ with many drupelets (Table 1.2). This bias was not confirmed by any statistically significant correlation between fruit length and ‘by-berry’ RDR estimation, but of all the RDR methods, the ‘by-berry’ method was most correlated with fruit length (Table 1.3). As noted in previous studies of RDR, A-2453T, ‘Osage’, and ‘Prime-Ark® Traveler’ all consistently grouped with the least reverted genotypes (Armour et al., 2021; Felts et al., 2020). Among these low-RDR genotypes, A-2453T and ‘Prime-Ark® Traveler’ are both noteworthy for their firm texture (Armour et al., 2021) and shipping potential (Clark and Salgado, 2016; Salgado and Clark, 2016).

ShinyFruit rankings of RDR intensity were similar to manual methods in most respects, with a few exceptions in the intermediate ranges. According to ShinyFruit, ‘Sweet-Ark® Caddo’ grouped with ‘Black Magic™’ in the highest RDR group, while both manual techniques grouped A-2444T, ‘Black Gem™’, and ‘Prime-Ark® Freedom’ with ‘Black Magic™’ as the genotypes with highest RDR. ShinyFruit RDR estimates were more highly correlated with the manual ‘by-drupelet’ ($r = 0.70$) method than the ‘by-berry’ method ($r = 0.62$). This was consistent with expectations, since the ‘by-berry’ method is expected to be biased by fruit size and the other two methods are not. Even so, the manual ‘by-berry’ and ‘by-drupelet’ methods were much more correlated with one another ($r = 0.94$) than either was with ShinyFruit (Figure 1.3). This may partly be explained by the fact that both manual estimates considered all drupelets on each berry, and each drupelet was categorically considered to be either reverted or non-reverted. Unlike the manual techniques, ShinyFruit estimates only considered the upper surface area of berry samples that were visible in each image. Furthermore, instead of categorizing each drupelet as reverted or non-reverted, ShinyFruit categorizes individual pixels based on color thresholds. Thus, ShinyFruit can provide RDR estimates that accurately account for partial reversion of drupelets.

Similarly, by using two separate reversion thresholds, one could measure reversion with varying degrees of color intensity as suggested by Edgley et al. (2019c). Future implementations of ShinyFruit should be able to compensate for the problem of RDR half-estimation, from only measuring one side of the fruit, by doubling the amount of fruit imaged. Through manual inspection of ShinyFruit output images, it is also clear that the digital image analysis pipeline also detected certain non-RDR discolorations of features such as desiccated, ruptured, or anthracnose-infected drupelets. RDR on berries with excessive glossiness may have also been underestimated with ShinyFruit, since the reflection of light can mask the color of the drupelets underneath. Future work may investigate this hypothesis through a correlation of ShinyFruit RDR estimation and glossiness. If such a relationship exists, future pipelines may consider glossiness as a covariate for ShinyFruit RDR estimation.

ShinyFruit measurements of fruit length and RDR were tightly correlated with those from manual data collection techniques. This resemblance is especially clear for fruit length measurements, which were within 1 mm of caliper-based measurements in all genotypes except for A-2453T and ‘Black Magic™’ (Table 1.2). Occasional and slight differences between fruit length measurements could arise from a slight difference in the way ShinyFruit estimates length compared to calipers. ShinyFruit considers the length between the uppermost detected berry pixel from the lowest berry pixel. Thus, berry orientation is key in producing accurate results. Calipers measure the length between the peduncle attachment point and the terminal drupelet. In addition, ShinyFruit relies on user-provided size standardization from a single sample image, and it assumes that the fixed camera height is kept consistent between other images analyzed in the same batch. Violation of this assumption could result in inaccuracies. Despite very tight correlations between length phenotyping methods ($r = 0.96$, Table 1.3), Genotype by year

interactions were also present in ShinyFruit-based fruit length estimations, but not in caliper-based measurements (Table 1.2). This could stem from slight differences in camera settings, ambient lighting, or ShinyFruit parameters between years, which may affect genotypic length measurements differently based on interfering qualities such as glossiness or turgidity. It seems more likely, based on a comparison of means *P* values within years (Appendix A), that this interaction could indicate a 'real' effect which is only detectable in larger sample sizes (up to 25 per image). 'Prime-Ark® Freedom' provides a clear example of this interaction. Both ShinyFruit and caliper methods indicate that mean fruit lengths of 'Prime-Ark® Freedom' were at least 5 mm longer in 2021 than in 2020, but only ShinyFruit statistically distinguished this genotype from the shortest genotypes in 2021. ShinyFruit may provide an improvement in accuracy, even compared to direct caliper measurement of fruit length, because of its enhanced throughput. In the present study, only five randomly sampled berries were measured with calipers, while entire clamshells were easily analyzed using ShinyFruit. The ability to measure greater numbers of berries reduces experimental error and improves the ability of the researcher to make strong inferences between genotypes or treatment groups.

Based on the evidence presented, ShinyFruit appears to be capable of sufficiently estimating RDR and fruit size in blackberry, but this is only one of many potential applications for this tool. Efficient strategies for estimation of size could be applied to numerous horticultural products by imitating ImageJ-based strategies (Cortes et al., 2017b; Manolikaki et al., 2022), but the detection of color-based features could provide an even greater number of implementations. In blackberry alone, protocols could be developed to mimic existing phenotyping methods for glossiness (Segantini et al., 2017) or white drupelet disorder (Stafne et al., 2017). More generally, ShinyFruit could be used to quantify and characterize descriptive color value

distributions for specific cultivars by using the optional ‘Color Profile’ feature. This feature reports the nearest matched RHS color descriptor to maximum, minimum, and median RGB color values in detected features. Such information may be of value in providing a standardized color description for new releases with unique color characteristics. Diseased or necrotic regions of fruit or leaves could easily be quantified by ShinyFruit following the approach used by Stewart et al. (2014) or Maloney et al. (2014) in wheat. ShinyFruit is an open-source response to proprietary image analysis tools, like Assess, and it is much simpler to use than ImageJ. Future updates to ShinyFruit will focus on developing image segmentation algorithms for counting aggregated features, such as blackberry drupelets or grapes on a cluster.

Conclusion

The ShinyFruit R package provides a flexible GUI-enabled tool for estimating size and color attributes in a variety of horticultural products. In blackberry, we have observed tight correlations with manual measurements of fruit length ($r = 0.96$) and moderate correlations with manual measurements of RDR using the ‘by-drupelet’ ($r = 0.70$) and ‘by-berry’ ($r = 0.62$) methods. ShinyFruit RDR values aligned with manual measurements on high RDR and low RDR genotypes, but intermediate rankings between methods shifted slightly. Unlike the ‘by-berry’ method, ShinyFruit RDR phenotyping is unbiased by fruit size, but additional fruit should be harvested to account for ShinyFruit’s implicit half-measurement problem. The inclusion of a vibration shipping treatment in 2020 and 2021 did not appear to elevate RDR expression levels in the observed population. Strategies should be developed in future studies to implement ShinyFruit phenotyping in fruit morphology and color-based trait measurement across a wide range of species and horticultural products.

References Cited

Armour ME, Worthington M, Clark JR, Threlfall RT, Howard L. 2021. Effect of harvest time and fruit firmness on red drupelet reversion in blackberry. HortScience. 56(8):889–896. doi: 10.21273/HORTSCI15853-21.

Barthelme S. 2022. imager: image processing library based on 'CImg'. https://CRAN.R-project.org/package=imager. [accessed 15 Feb 2023]

Bayarri S, Calvo C, Costell E, and Durán L. 2001. Influence of color on perception of sweetness and fruit flavor of fruit drinks. Food Science and Technology International. 7(5):399–404. doi: 10.1106/JJWN-FFRQ-JBMC-LQ5R.

Chang W, Cheng J, Allaire J, Sievert C, Schloerke B, Xie Y, Allen J, McPherson J, Dipert A, Borges B. 2022. shiny: web application framework for R. https://CRAN.R-project.org/package=shiny. [accessed 15 Feb 2023]

Chizk TM. 2018. An evaluation of canopy traits in soybean: heritability within an RIL population and implications of seed size sieving and narrow row-spacing practices in 25 diverse, late-planted cultivars and breeding lines (MS Thesis). North Carolina State University, Raleigh, North Carolina, USA.

Chizk, TM. 2022. ShinyFruit: batch image analysis GUI for small fruits. https://github.com/mchizk1/ShinyFruit. [accessed 15 Feb 2023]

Clark JR. 1999. The blackberry breeding program at the University of Arkansas: thirty-plus years of progress and developments for the future. Acta Hortic. 505:73–78. doi: 10.17660/ActaHortic.1999.505.8.

Clark JR, Finn C. 2011. Blackberry breeding and genetics. Fruit, Vegetable, and Cereal Science and Biotechnology. 5(1):27–43.

Clark JR, Moore JN. 2008. “Natchez” thornless blackberry. HortScience. 43(6):1897-1899.

Clark JR, Perkins-Veazie P. 2011. “APF-45” primocane-fruiting blackberry. HortScience. 46(4):670-673.

Clark JR, Salgado A. 2016. ‘Prime-ark® traveler’ primocane-fruiting thornless blackberry for the commercial shipping market. HortScience. 51(10):1287–1293. doi: 10.21273/HORTSCI10753-16.

Cortes DFM, Catarina RS, Barros GB, Arêdes FAS, da Silveira SF, Ferreguetti GA, Ramos HCC, Viana, AP. 2017. Model-assisted phenotyping by digital images in papaya breeding program. Sci Agric. 74(4):294–302. doi: 10.1590/1678-992X-2016-0134.

Edgley M, Close DC, Measham PF. 2019a. Effects of climatic conditions during harvest and handling on the postharvest expression of red drupelet reversion in blackberries. Sci Hortic. 253:399–404. doi: 10.1016/j.scienta.2019.04.052.

Edgley M, Close DC, Measham PF. 2019b. Nitrogen application rate and harvest date affect red drupelet reversion and postharvest quality in ‘Ouachita’ blackberries. Sci Hortic. 256:1-7. doi: 10.1016/j.scienta.2019.108543.

Edgley M, Close DC, Measham PF, and Nichols DS. 2019c. Physiochemistry of blackberries (*Rubus* L. subgenus *Rubus* Watson) affected by red drupelet reversion. Postharvest Biol Technol 153:183–190. doi: 10.1016/j.postharvbio.2019.04.012.

Kassambara A. 2020. ggpubr: ggplot2 Based Publication Ready Plots. Available at: https://rpkgs.datanovia.com/ggpubr/.

Kim MJ, Lee MY, Shon JC, Kwon, YS, Liu KH, Lee CH, Ku KM. 2019. Untargeted and targeted metabolomics analyses of blackberries – Understanding postharvest red drupelet disorder. Food Chem. 300:1-8. doi: 10.1016/j.foodchem.2019.125169.

Lawrence B, Melgar JC. 2018. Harvest, handling, and storage recommendations for improving postharvest quality of blackberry cultivars. Horttechnology 28(5):578–583. doi: 10.21273/HORTTECH04062-18.

Lenth R. 2022. emmeans: Estimated Marginal Means, aka Least-Squares Means. Available at: https://github.com/rvlenth/emmeans.

Maloney P, Petersen S, Navarro RA, Marshall D, McKendry AL, Costa JM, Murphy JP. 2014. Digital image analysis method for estimation of Fusarium-damaged kernels in wheat. Crop Sci. 54(5):2077–2083. doi: 10.2135/cropsci2013.07.0432.

Manolikaki I, Sergentani C, Tul S, Koubouris G. 2022. Introducing three-dimensional scanning for phenotyping of olive fruits based on an extensive germplasm survey. Plants. 11(11):1501. doi: 10.3390/plants11111501.

Moore JN, Brown E, Sistrunk WA. 1974. 'Comanche' blackberry1. HortScience. 9(3):245–246. doi: 10.21273/HORTSCI.9.3.245.

Ooms J. 2021. magick: advanced graphics and image-processing in R. https://CRAN.R-project.org/package=magick [accessed 15 Feb 2023]

Pérez-Pérez GA, Fabela-Gallegos MJ, Vázquez-Barrios ME, Rivera-Pastrana DM, Palma-Tirado L, Mercado-Silva E, Escalona V. 2018. Effect of the transport vibration on the generation of the color reversion in blackberry fruit. Acta Hortic. 1194:1329–1336. doi: 10.17660/ActaHortic.2018.1194.187.

R Core Team. 2022. R: a language and environment for statistical computing. Available at: https://www.R-project.org/. [accessed 15 Feb 2023]

Salgado AA, Clark JR. 2016. "'Crispy'" blackberry genotypes: a breeding innovation of the University of Arkansas blackberry breeding program. HortScience. 51(5):468-471.

Segantini DM, Threlfall R, Clark JR, Brownmiller CR, Howard LR, Lawless LJR. 2017. Changes in fresh-market and sensory attributes of blackberry genotypes after postharvest storage. J Berry Res. 7(2):129–145. doi: 10.3233/JBR-170153.

Shankar M, Levitan C, Prescott J, Spence C. 2009. The influence of color and label information on flavor perception. Chemosensory Perception. 2(2):53-58.

Stafne ET, Rezazadeh A, Miller-Butler M, Smith BJ. 2017. Environment affects white drupelet disorder expression on three blackberry cultivars in south Mississippi. Horttechnology. 27(6):840–845. doi: 10.21273/HORTTECH03880-17.

Stewart EL, McDonald BA. 2014. Measuring quantitative virulence in the wheat pathogen *Zymoseptoria tritici* using high-throughput automated image analysis. 104(9):985-992.

Threlfall RT, Clark JR, Dunteman AN, and Worthington ML. 2021. Identifying marketable attributes of fresh-market blackberries through consumer sensory evaluations. HortScience. 56(1):30–35. doi: 10.21273/HORTSCI15483-20.

Threlfall RT, Dunteman AN, Clark JR, Worthington ML. 2020. Using an online survey to determine consumer perceptions of fresh-market blackberries. Acta Hortic. 1277:469–476. doi: 10.17660/ActaHortic.2020.1277.67.

USDA-AMS. 2018. Patch #034. https://www.ams.usda.gov/sites/default/files/media/PATCH034Berries081718.pdf. [accessed 15 Feb 2023].

USDA-ARS. 2021. USDA plant hardiness zone map. https://planthardiness.ars.usda.gov/. [accessed 15 Feb 2023].

Wickham H. 2016. ggplot2: elegant graphics for data analysis. Springer-Verlag New York Available at: https://ggplot2.tidyverse.org.

Tables and Figures

Table 1.1. ShinyFruit settings used for image processing and detection of blackberry red drupelet reversion (RDR) in 2019-2021.

Step	Year	L[i]	a	b
Background removal	2019	FR[ii]	>-10.00	FR
	2020	FR	>-12.00	FR
	2021	FR	>-8.50	FR
RDR detection	2019	FR	>7.51	FR
	2020	FR	>16.15	FR
	2021	FR	>8.58	FR

[i]Lab colorspace threshold values

[ii]The full range of values were accepted for the associated colorspace channel

Table 2. Least square means and Tukey's HSD mean separation groupings for manually and automatically measured blackberry fruit characteristics in 2019, 2020, and 2021[i].

	Red drupelet reversion						Fruit length				Fruit width	
Genotype	ShinyFruit		By drupelet		By berry		ShinyFruit		Calipers		ShinyFruit	Calipers
	----------%----------						----------mm----------					
A-2444T	0.66	a[v]	2.31	ab	13.80	ab	30.84	b	29.18	ab	24.05	23.98
A-2453T	0.14	a	0.07	a	0.50	a	22.35	a	23.89	a	19.90	21.66
A-2454T	0.18	a	0.06	a	2.37	a	27.97	b	27.91	ab	23.48	23.90
A-2491T	0.16	a	0.18	a	1.19	a	30.57	b	32.27	b	21.16	21.58
Black Gem	0.64	a	2.87	ab	26.23	ab	28.47	b	29.29	ab	21.92	23.24
Black Magic	3.18	b	4.62	b	34.97	b	29.21	b	28.00	ab	22.67	22.05
SA[i] Caddo	1.66	ab	0.60	a	7.18	a	30.60	b	31.69	b	22.37	22.82
Natchez	0.82	a	1.45	a	21.57	ab	36.58	c	36.98	b	23.74	23.56
Osage	0.69	a	0.44	a	2.10	a	25.49	ab	24.57	a	22.50	22.59
Ouachita	0.35	a	1.12	a	8.23	a	28.13	b	28.09	ab	23.92	23.74
PA[ii] Freedom	0.21	a	2.05	ab	21.77	ab	31.36	bc	32.11	b	24.31	25.04
PA Horizon	0.80	a	1.05	a	6.81	a	35.45	c	35.44	b	21.77	22.71
PA Traveler	0.51	a	0.76	a	6.68	a	29.73	b	31.04	b	21.00	21.87
SA Ponca	0.33	a	0.82	a	4.49	a	25.75	ab	26.52	ab	21.06	20.73
P_G[iii]	0.002		0.002		0.001		0.014		0.001		0.504	0.427
P_{GY}[iv]	0.767		0.374		0.666		0.021		0.825		0.044	0.769

[i]Fruit length and width were only measured in 2020 and 2021
[ii]SA = Sweet-Ark®
[iii]PA = Prime-Ark®
[iv]*P* values for genotypes
[v]*P* values for genotype by year interactions
[vi]Letters indicate significant differences between genotypes ($P < 0.05$) using Tukey's Honestly Significant Difference

Table 3. Pearson correlation of genotypic mean fruit characteristics between automated and manually measured blackberry fruit characteristics

		Red drupelet reversion		Fruit length	
		By drupelet	By berry	ShinyFruit	Calipers
Red drupelet reversion	ShinyFruit	0.696 **	0.621 *	0.179 NS	0.058 NS
	By drupelet		0.940 **	0.225 NS	0.085 NS
	By berry			0.361 NS	0.265 NS
Fruit length	ShinyFruit				0.962 **
	Calipers				

NS, *, and ** Nonsignificant or significant at $P < 0.05$ or 0.01, respectively.

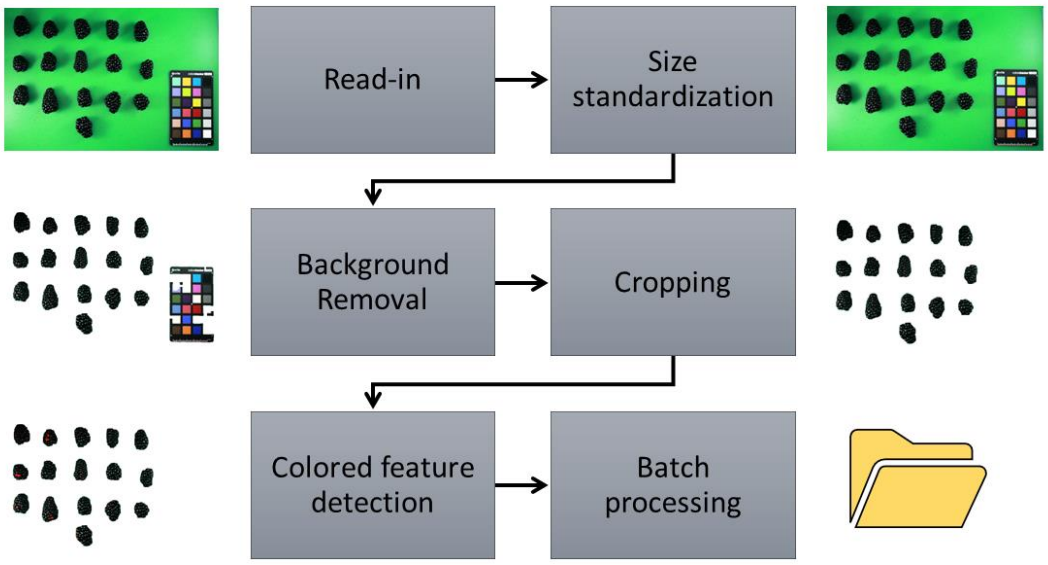

Figure 1. ShinyFruit image processing pipeline for colored feature detection using the example of red drupelet reversion (RDR) in blackberry fruit.

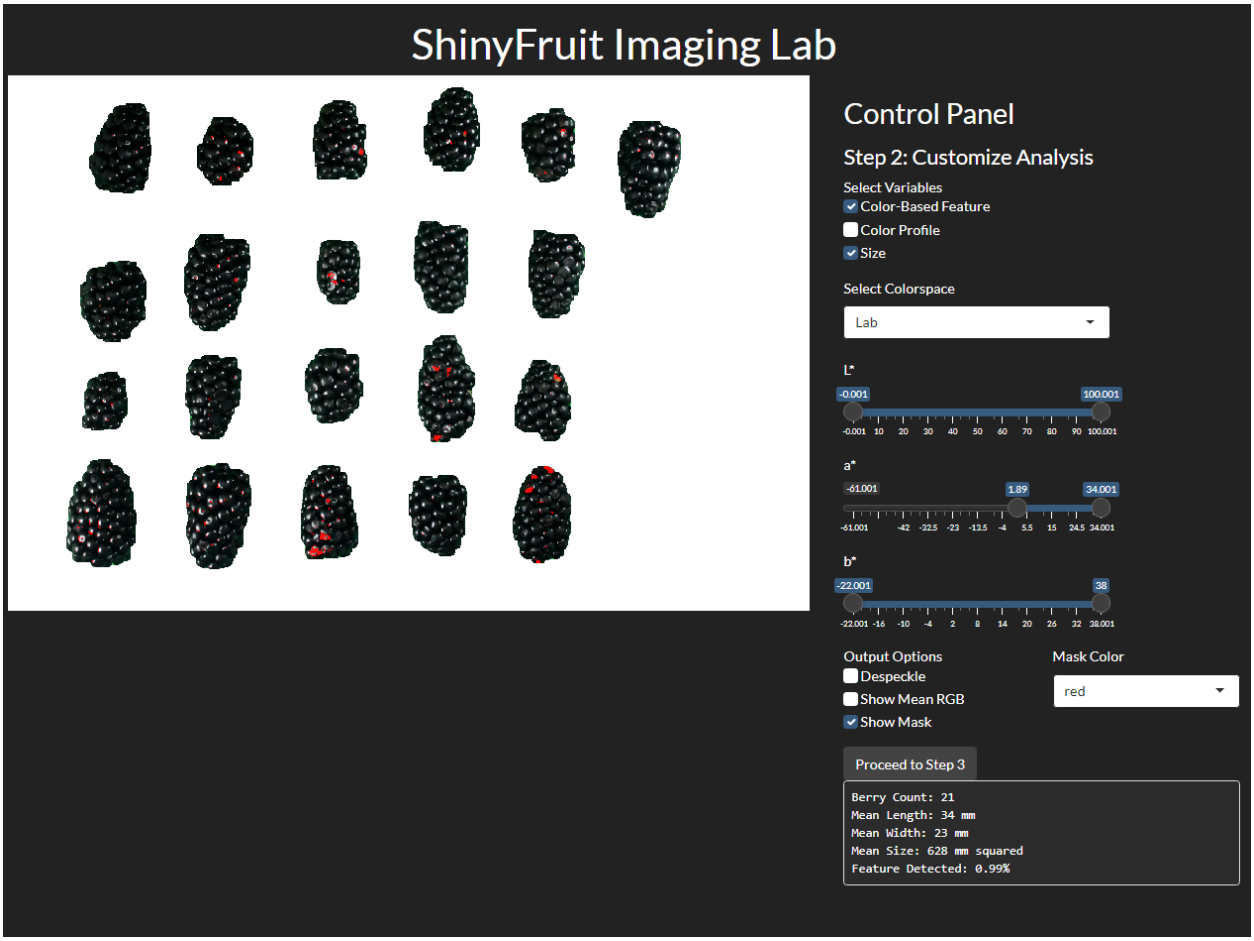

Figure 2. ShinyFruit general user interface (GUI) example during the colored feature detection step.

Figure 3. (A) Manual ‘by-berry’ red drupelet reversion (RDR) estimation of blackberry fruit regressed against ShinyFruit RDR estimation. (B) Manual ‘by-drupelet’ RDR estimation of blackberry fruit regressed against ShinyFruit RDR estimation. (C) Caliper measurements of blackberry fruit length regressed against ShinyFruit estimation of blackberry fruit length.

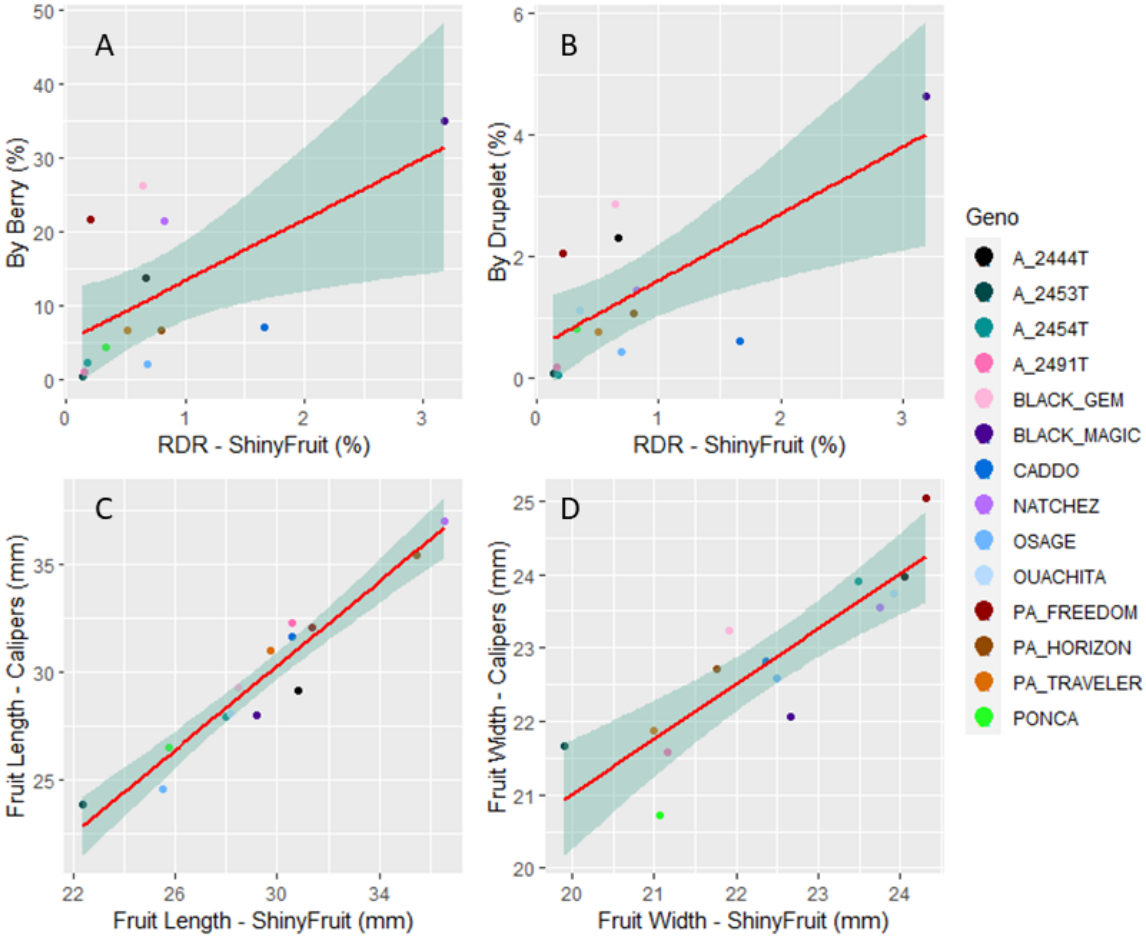

CHAPTER II

GENOME WIDE ASSOCIATION IDENTIFIES KEY LOCI CONTROLLING BLACKBERRY POSTHARVEST QUALITY

Abstract

Blackberry (*Rubus* subgenus *Rubus*) is a soft-fruited specialty crop that often suffers economic losses due to degradation in the shipping process. During transportation, fresh-market blackberries commonly leak, decay, deform, or become discolored through a disorder known as red drupelet reversion (RDR). Over the past 50 years, breeding programs have achieved significant gains in fruit firmness and postharvest quality through traditional selection methods, but the underlying genetic variation associated with these gains is not well understood. We report a genome-wide association of fruit firmness and RDR measured in 300 tetraploid fresh-market blackberry genotypes from 2019-2021 with 65,995 SNPs concentrated in genic regions of the *R. argutus* reference genome. Fruit firmness and RDR had entry-mean broad sense heritabilities of 68% and 34%, respectively. Three variants on homologs of polygalcturonase (PG), pectin methylesterase (PME), and β-glucosidase explained 27% of variance in fruit firmness and were located on chromosomes Ra06, Ra01, and Ra02 respectively. Another PG homolog variant on chromosome Ra02 explained 8% of variance in RDR, but it was in strong linkage disequilibrium with 212 other RDR-associated SNPs across a 23 Mb region. A large cluster of six PME and PME inhibitor homologs was located near the fruit firmness quantitative trait locus (QTL) identified on Ra01. RDR and fruit firmness were only weakly correlated (r = -0.28) in this study, but they shared overlapping QTL regions on Ra02. Our work demonstrates the complex nature of postharvest quality traits in blackberry, which are likely controlled by many small-effect variants. This study is the first large-scale effort to map the genetic control of quantitative traits

in blackberry and provides a strong framework for future GWAS. Phenotypic and genotypic datasets may be used to train genomic selection models that target the improvement of postharvest quality.

Introduction

In the United States, fresh-market blackberries are growing in popularity, and year-round availability is heavily dependent on imports from Mexico during the winter months. From 2019 to 2022, US fresh-market blackberry imports have sharply risen by about 52% (USDA-ERS, 2023) to meet growing demand from consumers. Soft-fruited blackberries that are shipped over long distances suffer from numerous postharvest issues, including leakage, mold, berry softening, deformation, weight loss, and discoloration through red drupelet reversion (RDR). RDR is a postharvest disorder that causes individual drupelets on fully ripe blackberries to 'revert' from shiny black to a red, underripe appearance. This disorder presents a particularly important risk to producers because the USDA-AMS has established a grading standard that recommends the rejection of blackberry lots if 10% of the berries are affected by RDR or 5% are categorized as severe (USDA-AMS, 2018). These standards align with the opinions of consumers, who strongly prefer blackberries with minimal RDR (Threlfall et al., 2020).

Many cultural factors impact the incidence and severity of RDR, including mechanical damage during harvest and shipping, climate conditions, time of harvest, and excessive nitrogen fertilization (Pérez-Pérez et al., 2018; Edgley et al., 2019b, 2019c). At the chemical level, RDR is characterized by the delocalization of anthocyanins from vacuoles, leading to degradation and color change (Edgley et al., 2019d; Kim et al., 2019). RDR has been disproportionately associated with soft-fruited cultivars (Salgado and Clark, 2016; Armour et al., 2021), suggesting that RDR may be a visual indicator of poor fruit texture observable under certain postharvest conditions. Several studies have documented the broad range of phenotypic diversity for fruit texture and RDR present across University of Arkansas (UA) System Division of Agriculture Fruit Breeding Program blackberry germplasm (Salgado and Clark, 2016; Threlfall et al., 2016;

Segantini et al., 2018; Armour et al., 2021). Fruit texture was once considered an intractable trait, but cultivars released in recent decades have achieved excellent gains in shipping potential. Landmark cultivars like ‘Navaho’ and ‘Chester Thornless’ (Clark, 2005) were some of the first to have true shipping potential, thus expanding the potential for a global blackberry industry. Major improvements in texture quality have coincided with growth in blackberry popularity and an increasing emphasis on improved fruit texture for fresh-market breeding programs (Clark and Finn, 2011; Finn and Clark, 2011). Several UA blackberry breeding selections possess a distinctly firm-textured phenotype described as ‘crispy’. These cultivars are resistant to RDR compared to non-crispy genotypes (Salgado and Clark, 2016). Great strides in the improvement of blackberry shipping potential over decades of selection demonstrate the heritability of firm texture and RDR resistance among the UA population, but the genetic control of these traits remains unexplored.

Advances in computer science and biotechnology and the increasing availability of powerful statistical programming tools have enabled genome-wide association studies (GWAS) to investigate marker-phenotype associations in autopolyploid plant species (Bourke et al., 2018). The initial objective of such studies is to identify the physical genomic positions of large-effect quantitative trait loci (QTL) influencing traits of interest in breeding populations. A natural downstream objective of these studies is the identification of causal variants or loci which are in a state of high linkage disequilibrium (LD) with causal variants. Such variants may then be implemented in marker assisted selection (MAS) strategies to cull seedling populations and select optimal parental combinations. In the context of perennial crops, like blackberry, where fruit is often not observed until the second year of growth, MAS may greatly improve the rate of genetic gain in breeding programs (Foster et al., 2019). Identification of loci influencing fruit

quality in blackberry may provide breeders with a path to select genotypes of superior texture in less than half the time of traditional phenotyping methods.

The blackberry germplasm in the UA Fruit Breeding Program consists predominately of autotetraploid materials. Thus, it is important to consider an association model that accounts for polyploid allele dosage. Driven partly by declining costs and technological advances, a growing community of polyploid researchers have produced open-source tools in recent years that will enable more robust GWAS pipelines. The R package, updog, provides researchers with the ability to flexibly genotype polyploids using messy next generation sequencing (NGS) data (Gerard et al., 2018). The GWASpoly package has made association mapping of autopolyploids more accessible by providing functions capable of testing multiple hypothetical dominance models (Rosyara et al., 2016). GWASpoly also allows users to build models that consider both random marker effects and fixed population structure (Q + K model). In tetraploid blueberry, polyploid GWAS models detected greater numbers of QTLs than diploid models (Ferrão et al., 2018). Lastly, the ldsep package contains utilities for pairwise estimation of linkage disequilibrium (LD) in polyploids (Gerard, 2021) which may provide an important contextual understanding for newly identified QTLs and their potential associations with nearby genes.

Functional understanding of the blackberry genome is in its infancy, but the recent assembly and annotation of a diploid blackberry reference genome (Brůna et al., 2022) has established a strong foundation for association mapping. The assembled genome, *Rubus argutus* cv. ‘Hillquist’ (298 MB), is an important donor of the primocane-fruiting trait to the UA germplasm. A novel algorithm integrating genomic, transcriptomic and cross-species protein evidence was used to predict a total of 38,503 protein-coding genes, of which 72% were functionally annotated. With available NGS strategies, previously described software packages,

and an annotated reference genome, conditions are ideal to perform a GWAS that investigates complex quantitative traits in blackberry, like fruit texture and postharvest quality.

Materials and Methods

Plant Materials and Harvest. The GWAS panel consisted of 300 UA blackberry breeding selections and publicly available fresh-market blackberry cultivars. These cultivars and selections were maintained in 6 m plots at the UA Fruit Research Station (FRS) in Clarksville, AR. The FRS site is located at 35º31’5”N and long. 93º24’12”W, in USDA hardiness zone 7b (USDA, 2021), on Linker fine sandy loam. All plots were maintained with varying degrees of routine cultural inputs such as training/tipping primocanes to a hedgerow training system, annual dormant pruning, irrigation, chemical weed, disease, and pest control. The panel was evaluated in 2019, 2020, and 2021 for firmness and red drupelet reversion. For each genotype, blackberries were harvested at the shiny black stage into 500 mL clamshells on two separate harvest dates per year, with at least one week of separation between harvest dates. All fruit was harvested in the months of June and July between 10:00 a.m. and 5:00 p.m. to encourage RDR occurrence as reported by Edgley et al. (2019a) and Armour et al. (2021). After rain events, a minimum period of 24 hours was allowed to pass before harvest was allowed to resume. Fruit containing defects, such as ruptured or discolored drupelets, were discarded before placing in storage. Clamshells were filled just below the lid and placed directly into a portable cooler chilled by ice packs until they could be transported. In 2020 and 2021, harvested fruit samples were placed on a custom-built steel table for thirty minutes, with a vibrating surface that produced 2 mm of displacement and a frequency of 10 Hz. This treatment was intended to simulate shipping conditions that lead to RDR by replicating the findings of Perez-Perez et al. (2018). Samples were stored in an on-site refrigerator for a period of exactly seven days at 5 °C and 90% relative humidity. Prior to

obtaining images, clamshells were removed from refrigeration and allowed to reach room temperature.

Red Drupelet Reversion and Image Analysis. After seven days of cold storage, fruit was removed from cold storage and returned to room temperature. Fruit was arranged in a single layer, with spacing between fruit, on a green plastic cutting board and photographed in photo box (LimoStudio 16" x 16" Table Top Photo Photography Studio Lighting Light Tent Kit in a Box, AGG349; Las Vegas, Nevada, USA) using a Canon EOS Rebel T3 (Tokyo, Japan) mounted directly above the staging board. In 2019, a standard US quarter dollar was included in each image as a size reference. In 2020 and 2021, an X-Rite ColorChecker Classic Mini (Grand Rapids, Michigan, USA) was included in each image and used as a size reference. Digital images were analyzed using the ShinyFruit app (Chizk et al., 2023), which is maintained on GitHub (https://github.com/mchizk1/ShinyFruit).

Fruit Firmness. Following image analysis, ten randomly selected berries per clamshell were assessed for firmness using a Stable Micro Systems TA.XT.Plus Texture Analyzer (Texture Technologies Corporation, Hamilton, MA). A fruit compression test was performed by placing individual berries horizontally on a flat surface using a cylindrical plane probe of 7.6 cm diameter at a rate of 2 $mm.s^{-1}$ with a trigger force of 0.02 N. The probe travelled 5 mm after first contact, and the peak force (N) was recorded as berry firmness.

BLUP and Heritability Analysis. Best linear unbiased predictions (BLUPs) of fruit firmness and RDR were calculated for each genotype across years and harvest replicates with the help of the

lme4 (Bates et al., 2015) in R (R Core Team, 2022). Because of imbalanced replication inherent to the large phenotypic dataset, harmonic means for year (*y*) and replicate (*r*) were used in entry-mean heritability analyses. Genotypic variance (σ^2_g), genotype by year variance (σ^2_{gy}), and residual variance (σ^2) components were estimated with the lme4 model and used to calculate broad sense heritability as follows:

$$H_{per-plot} = \frac{\sigma_g^2}{\sigma_g^2 + \sigma_{gy}^2 + \sigma^2}$$

$$H_{entry-mean} = \frac{\sigma_g^2}{\sigma_g^2 + {\sigma_{gy}^2}/{y} + {\sigma^2}/{yr}}$$

All custom R scripts used to produce BLUPs, harmonic means, variance estimates, and heritabilities are available through a GitHub repository for repeatability (https://github.com/mchizk1/UA_Fruit_Breeding).

Genotyping with Capture-Seq. Young leaf tissue was collected from each of 300 genotypes in the GWAS panel and DNA was extracted using a modified cetyltrimethylammonium bromide (CTAB) extraction protocol following Porebski et al. (1997). Quantification of DNA was performed using the Qubit dsDNA assay kit (Invitrogen, Carlsbad, CA) and samples were standardized to 40 ng/µl. Capture-Seq genotyping was performed at RAPiD Genomics (Gainesville, FL) with 35,054 custom biotinylated 120-mer probes distributed across the *R. argutus* genome. The majority of the probes were designed to target genic regions, including a number of genes implicated in cell wall metabolism in other fruits such as polygalacturonase (PG), pectinmethylesterase (PME), pectin lyase, and expansin. DNA libraries were sequenced with Illumina HiSeq to achieve about 150x coverage per SNP on average.

SNP Calling and Quality Filtering. Raw sequencing data was cleaned, trimmed, and aligned to the *R. argutus* genome (Brůna et al., 2022) using MOSAIK (Lee et al., 2014). Initial diploid variant calling was performed using Freebayes (Garrison and Marth, 2012). The VCF file was filtered using VCFtools (Danecek et al., 2011) to produce a file with biallelic markers with minor allele frequency ≥ 0.01 and read depths ranging between three and 750 per sample. The filtered diploid VCF file was recalled estimating tetraploid allele dosage using the multidog function in updog (Gerard et al., 2018) and SNPs with greater than 5% estimated error rate were discarded.

Population Structure. A Q matrix was generated in STRUCTURE (Pritchard et al., 2000) using the population admixture model and proposed K values ranging from two to eight with a burnin period of 10,000 and 20,000 Markov chain Monte Carlo replications. An appropriate K value was selected based on the ΔK statistic reported by Evanno et al. (2005).

Genome-Wide Association. Association analyses were conducted using the GWASpoly package (Rosyara et al., 2016) in R. Both fruit firmness and RDR BLUPs were associated with the filtered set of tetraploid SNPs under the 'Q+K' model. The K matrix was constructed internally using the leave-one-chromosome-out (LOCO) method and the STRUCTURE-generated Q matrix was included to account for fixed admixed population clusters across individuals. Additive, simplex dominance (1-dom), and general models of gene action were considered. Minor allele frequency and maximum genotypic thresholds were set to 0.05 and 0.95, respectively. Marker scores were tested internally using a α=0.05 significance threshold and the 'M.eff' method. Using this method, *LOD* significance thresholds of 5.45, 5.45, 4.38, and 5.38 were used for additive, general, simplex alternative allele dominance, and simplex reference

allele dominance models, respectively. QQ-plots were constructed from association results to compare observed marker scores against nominal *P*-values.

Linkage Disequilibrium. Average decay of r^2 between SNPs was estimated internally in GWASpoly using a maximum number of 10,000 SNP pairs and eight degrees of freedom for spline plotting. Using the ldsep R package (Gerard, 2021), Lewontin's *D'* was estimated between a subsample of SNPs in each chromosome, with a minimum of 100 kb spacing between sampled SNPs. Heatmaps of chromosomal linkage disequilibrium (LD) matrices were constructed using the LDheatmap R package (Shin et al., 2006).

Candidate Gene Mining. For significant SNPs that did not reside on an annotated texture gene, genomic flanking regions of 1 Mb were investigated for the nearest biologically likely candidate gene. For markers that were in high LD with one another, candidate genes were collectively considered in the flanking regions of each marker. Seventy-two percent of the 38,503 predicted protein-coding genes in *R. argutus* were functionally annotated as described by Brůna et al. (2022). Genes with functions related to cell wall disassembly in other plant species were considered promising candidates.

Results

Phenotypic Data. Texture analysis was performed on 1,374 samples from 300 blackberry genotypes. Fruit firmness BLUPs were normally distributed (Figure 2.1) around a mean of 6.21 N, with values ranging from 3.38 - 10.29 N. The broad-sense entry-mean heritability fruit firmness was 0.68 (Table 2.1). Image analysis for RDR was performed on 1,370 samples from

299 blackberry genotypes. RDR values were right-skewed (Figure 2.1) with values ranging from 0.46% to 2.2% reverted pixels. The broad-sense entry-mean heritability of RDR was 0.31 (Table 2.1), less than half as heritable as fruit firmness. BLUPs for fruit firmness and RDR were weakly, but significantly correlated (r = - 0.28).

Genotypic Data. In total, 124,564 biallelic SNPs were discovered in initial variant calling across a larger panel of 502 genotypes. After removing genotypes not evaluated in this study and SNPs of unacceptable quality or frequency, 65,995 SNPs were used in association analyses. Over 99% of quality-passing SNPs were in annotated genic regions (Figure 2.2C) and 41% were located on coding sequences (CDS). About 60% of CDS polymorphisms were predicted to be missense mutations and 2% were predicted to be nonsense mutations. The filtered SNP set had an average alternative allele frequency of 0.25 and was somewhat unevenly distributed (Figure 2.3), as intergenic regions were avoided in the probe design stage.

Population Structure and LD. By comparing successive STRUCTURE simulations, K = 6 had the largest ΔK value of 93.4 (Appendix B) and clear differences were visible between the known subpopulations in the UA germplasm (Figure 2.4). These three subpopulations are primocane fruiting, floricane fruiting, and 'novel' or brachytic dwarf genotypes. Although crosses occur between these populations, they each align with specific market niches. Thus, a Q matrix assuming six admixed subpopulations was generated and used to reduce type I errors due to population structure in the GWAS model. LD associated with physical linkage between SNPs largely decayed within 5 Mb (Figure 2.5), but LD decay varied across the genome, with the most apparent high-LD block located at the distal end of chromosome Ra04 (Figure 2.6).

Genome Wide Associations. Fruit firmness was significantly associated with seven SNPs across chromosomes Ra01, Ra02, Ra03, and Ra06 (Table 2.2, Figure 2.7). All significant associations were identified under either additive or general dominance models, with general markers having the highest *LOD* scores. In a multi-SNP fruit firmness prediction model, Ra01:4352940_T/G, Ra02:6321387_T/C, and Ra06:17273160_A/G explained about 27% of all observed phenotypic variance in fruit firmness. The most significant association (*LOD* = 7.21) was observed under the general model at 17,273,160 bp on chromosome Ra06. Chromosomal QQ-plots of fruit firmness marker scores generally showed a gradual inflation in observed *LOD* scores compared to nominal values on chromosomes Ra01, Ra02, and Ra03 (Appendix B).

Red drupelet reversion was significantly associated with 220 SNPs (Figure 2.7), all of which were scattered across a 23.3 Mb region on chromosome Ra02. Interestingly, the RDR association analysis did not identify any of the same SNPs associated with fruit firmness, but 68 of the significant RDR markers were located on homologs of genes commonly associated with fruit texture (Table 2.2). Two hundred and eighteen RDR markers were discovered using the 1-dom ref model. However, the general model identified Ra02:13296902_C/A as the strongest marker for predicting RDR (*LOD* = 7.00; partial r^2 = 0.11) and was located on an intron region of Ra_g5949. As observed in fruit texture analysis, QQ-plots show gradual inflation of marker scores compared to nominal values on chromosome Ra02 (Appendix B).

Potential Candidate Genes. Four of the seven SNPs associated with fruit firmness were positioned directly on gene homologs associated with fruit texture, including PG, PME, and β-glucosidase (Table 2.2). On chromosome Ra06, a single silent PG variant on 17,273,160 bp

(Ra_g27483) had the highest *LOD* score, an r^2 of 11%, and was located less than 200 kb away from two additional PG homologs. The highest scoring marker on Ra01 was on an intron region of the PME homolog, Ra_g890. The 1 Mb region flanking this variant contained a large cluster of six other PME and PME inhibitor homologs, one PG, and eight other texture-related homologs. Two significant SNPs were found on the same β-glucosidase homolog on chromosome Ra02, with the variant on 6,321,387 bp functioning as a missense mutation. The SNP located at 3,633,404 bp on Ra03 was about 833 kb away from two β-glucosidase homologs. No additional candidates for fruit texture were identified in regions immediately surrounding the SNP located on 8,025,922 bp on Ra02.

Most of the 220 significant SNPs associated with RDR on Ra02 were in a state of very high LD with on another (Appendix B), even though not all of them were physically linked. Such widespread LD, combined with the large number of significant SNP associations, expanded the candidate gene search window to a region that covered much of chromosome Ra02. Nonsynonymous RDR SNPs located on texture homologs were reported in Table 2.2, and all other candidates neighboring the 23 Mb, high-LD region were compiled in Appendix B. Sixty-eight RDR-associated markers were located on just seven texture related homologs including one PG, one pectin lyase, two β-glucosidases, two expansins, and one β-glucanase. All seven putative texture homologs contained at least one nonsynonymous mutation. Notably, all nonsynonymous mutations on texture homologs were detected under the 1-dom tetraploid dominance model. Among the seven polymorphic texture homologs, the expansin-like Ra_g7125, was the only putative texture gene to contain a nonsense mutation. The PG homolog Ra_g5108 contained a nonsynonymous mutation with the highest *LOD* value (6.05) for RDR. The strongest SNP for predicting RDR (*LOD* = 7.00; partial r^2 = 0.11) was located on an intron

region of Ra_g5949, which is a homolog of 2-oxoglutarate-dependent dioxygenase 19 in rice. This SNP is not located within 1 Mb of any homologs with documented roles in cell wall disassembly.

Discussion

Insights into Genotypic Datasets. GWAS has been used to discover marker trait associations in many fruit crops, but to date there have been no studies on the genetic control of quantitative traits of economic importance in blackberry. In this study, we used Capture-Seq genotyping and GWASpoly (Rosyara et al., 2018) to identify genetic regions associated with fruit firmness and RDR in tetraploid, fresh-market blackberries. Similar approaches have already been implemented to successfully map traits related to productivity and fruit quality in tetraploid blueberry (Ferrão et al., 2018, 2020). In the present study, we attempted to improve mapping resolution by analyzing a set of 65,995 SNPs highly concentrated in genic regions (Figure 2.2C). Nearly half of these SNPs were in coding exon regions, increasing the likelihood of observing SNP associations on or near causal variants. Average read depths exceeded 150x and produced high-quality SNP dosage calls using the updog R package (Gerard et al., 2018). LD among this population decayed over relatively large distances (Figure 2.5), which is likely the result of breeding activity and relatedness among individuals compared to more diverse populations or landraces (Rahimi et al., 2019). The large LD block located at the end of Ra04 may also provide evidence of an important domestication gene and a corresponding selective sweep in this region (Kim and Stephan, 2002).

Insights into Phenotypic Datasets and Heritability. In general, blackberry fruit firmness and RDR appear to be highly polygenic traits associated with numerous small-effect QTL. However, several important underlying trends were observed that must be considered in the interpretation of marker trait association. The moderate heritability (H = 68%) of fruit firmness in our population (Table 2.1) suggests that environmental factors play an important role in determining firmness after storage; however, these estimates are not very different from those already reported in strawberry (Shaw et al., 1987) or blueberry (Cellon et al., 2018) breeding populations. Environmental factors contributing to variation in blackberry fruit firmness include the addition of water, N, or Ca, pressure from fungal pathogens, respiration rates, and pests such as spotted wing drosophila (Prange and DeEll, 1997; Lee et al., 2011).

With a broad-sense heritability of 0.32 across three years of data collection, RDR appears to be particularly subject to environmental influence, supporting the work of Edgley et al. (2019c, 2019b, 2019a). In addition, the right-skewed nature of the RDR phenotypes observed is likely to mask many true differences in postharvest quality towards the lower end of the distribution. In other words, genotypes with very low susceptibility to RDR probably performed no differently than those mildly prone to reversion due to the nature of the distribution. Mechanical damage during harvest and shipping increases the incidence and severity of red drupelet reversion (Edgley et al., 2019a). However, berries harvested in this study were harvested with much more care than is typical in commercial production and the vibration treatment implemented in 2020 and 2021 following Perez-Perez et al. (2018) did not increase RDR relative to 2019. Future studies should focus on experimental treatments to increase RDR in research plantings to levels more comparable with commercial conditions. Observed RDR was weakly explained by variation in fruit firmness (r = -0.28), which follows previously the reported

relationships between these traits (Salgado and Clark, 2016; Armour et al., 2021). The weakness of this correlation could indicate the presence of other factors contributing to RDR severity, such as anthocyanin content or composition. Armour et al. (2021) identified differences in cyanadin-3-rutinoside content among blackberry genotypes, also noting that 'Osage' had higher cyanadin-3-rutinoside content and low RDR. Other authors have provided strong evidence that the color changes brought on by RDR are the result of anthocyanin degradation (Edgley et al., 2019d; Kim et al., 2019). Following the methods outlined in this study, future GWAS should explore anthocyanin content to search for more heritable sources of resistance to RDR.

Fruit Firmness and its Genetic Associations. Based on a moderate broad sense heritability estimate (H = 0.68) and the presence of multiple significant marker-trait associations on four out of seven chromosomes (Ra01, Ra02, Ra03, and Ra06), the genetic control of fruit firmness appears to be highly polygenic. Major pathways for fruit-softening in other species are well-characterized in the literature. The two genes most frequently implicated in fruit softening are PG (Crookes and Grierson, 1983; Peace et al., 2005; Toivonen and Brummell, 2008) and PME (Marangoni et al., 1995; Wen et al., 2013; Xue et al., 2020), which act in unison to degrade pectin in the middle lamella. PME catalyzes the hydrolytic de-esterification of homogalacturonan (HG) regions of pectin molecules, while PG preferentially hydrolyzes α-1,4-D galacturonan linkages in HG regions of pectin molecules, leading to softening through a loss of cell adhesion. Hence, both enzymes are necessary for the biologically programmed process of softening to occur. Significant marker-trait associations for fruit firmness were detected on homologs of both PG (Ra06) and PME (Ra01), although both variants were synonymous mutations and are therefore not expected to impact protein function. These significant associations on

chromosomes Ra01 and Ra06 reside near larger surrounding clusters of linked PG and PME genes in flanking regions. Six PME, one PG, and eight additional homologs with documented roles in cell wall disassembly were located within 1 Mb of the significant SNP on Ra01. Two additional PG homologs were less than 200 kb away from the significant SNP on Ra06. The causal variants on these chromosomes are likely associated with at least one of these nearby homologs. In peach, a cluster of PG genes is responsible for the inheritance of melting flesh in peach (Callahan et al., 2004), and variable gene copy number is an important source of texture diversity (Gu et al., 2016). Slightly elevated LD levels surrounding the Ra01 locus (Figure 2.6) seems to indicate this gene cluster may have experienced high selection pressure through breeding activities. Fruit firmness in blackberry could be governed by gene clusters similar to the one reported in peach and the effects of gene copy number have not yet been explored.

Three significant fruit firmness SNPs were located on Ra02. The most important of these (*LOD* = 6.11) was a silent mutation on the β-glucosidase homolog Ra_g5252. Like PG, β-glucosidase degrades fruit texture by cleaving pectin molecules. Instead of hydrolyzing HG regions, β-glucosidase degrades the 'hairy' arabinogalactan side chains of the pectin macromolecule (de Vries et al., 1983), which are not targeted by PG. Therefore, β-glucosidases are thought to promote a more complete degradation of middle lamellar pectin molecules. A single β-glucosidase homolog (Ra_g5252) on Ra02 contained two SNPs significantly associated with fruit texture. This gene is the only candidate shared between fruit firmness and RDR association analyses, and it contains the only nonsynonymous mutation associated with fruit firmness discovered in this study (Table 2.2). The significant RDR associated SNP on Ra_g5252 was positioned only 1,355 bp from the closest fruit firmness SNP. Prupe.8G098000, a homolog Ra_g5252 found in peach, is a β-glucosidase that is upregulated by treatment with 1-MCP (Qian

et al., 2022), and the authors have speculated that it may be important in strengthening cell walls. Although the role of β-glucosidases in fruit texture has been well documented in several species (Gerardi et al., 2001; Konozy et al., 2012; Ortiz Araque et al., 2019), few studies have demonstrated genetic variation β-glucosidase and its potential connection to phenotypic variation for fruit texture. In sweet cherry, four β-glucosidase homologs were located on a fruit firmness QTL in chromosome four (Cai et al., 2019). In addition to their ability to modify pectin, β-glucosidases have a documented role in disease suppression (Kebede and Kebede, 2021), which may have the knock-on effect of preserving texture quality. It was more difficult to identify likely candidate genes for significant SNPs located at 8,025,922 bp on Ra02 and 3,633,404 bp on Ra03 were, as no known texture homologs appeared anywhere in the 1 Mb flanking regions. Interestingly, the SNP on 8,025,922 bp of Ra02 explained the most variation in fruit texture (12%) under a single marker prediction model, even though it was not located near any known texture homologs. This association could be the result of widespread LD between this SNP and the large, scattered group of texture genes associated with RDR (Appendix B).

RDR Associations and the Effects of LD. An inspection of QQ-plots identified a gradual inflation of *LOD* scores on some chromosomes compared to expected nominal values (Appendix B). This trend is especially apparent on chromosome Ra02 for both RDR and fruit firmness association analyses. In SNP sets with large numbers of intergenic variants these higher-than-expected *LOD* scores can be an indication of false discovery resulting from confounding factors that were not modeled, such as population structure or other covariates. In contrast, our models did account for relatedness and covariance through the inclusion of Q and K matrices and 99% of our SNPs were positioned on intron and exon regions. Schork et al. (2013), who referred to this

phenomenon as ‘enrichment’, reported how overrepresentation of SNPs in genic regions, such as introns and exons may result in higher numbers of significant *P*-values consistent with true polygenic effects. If this is indeed true in our own association analyses, the high number of postharvest QTL observed in this study would be consistent with findings in strawberry (Cockerton et al., 2021), which 24 QTL for fruit firmness widely distributed across the genome. In the case of blackberry, RDR may be a highly quantitative trait controlled by numerous low-effect genes on chromosome 2. Thus, future molecular breeding strategies for improving postharvest quality in blackberry should prioritize genomic prediction models over MAS approaches.

Despite the heavily right-skewed distribution of the RDR dataset, the genetic associations with this trait uncovered an interesting phenomenon on chromosome Ra02. Many widely distributed SNPs were significantly associated with RDR, and nearly all of them were in high LD (Supplementary Figure 4). Each of these SNPs explained nearly equivalent levels of phenotypic variance, with r^2 values ranging from 7.41% to 8.33% (Table 2.2). It is worth noting that these high LD SNPs were as far apart as 22 Mb, meaning this trend is not occurring due to physical linkage, but may instead be the result of heavy selection pressures. The relative importance of specific candidate genes may be obscured by the fact all seven RDR-associated genes containing nonsynonymous SNPs were in LD. Therefore, it could be true that only either one, a few, or indeed all RDR-associated genes may be important in their contributions to RDR resistance and postharvest quality.

Several gene candidates appear to be especially noteworthy. The SNP with the highest *LOD* score for RDR was a missense mutation on Ra_g5108, a polygalacturonase homolog (Table 2.2). The expansin-like gene, Ra_g7125, contained the only significantly associated nonsense

mutation, suggesting probable loss-of-function. Powell et al. (2003) reported that simultaneous transgenic suppression of PG and expansin genes in tomato synergistically prevented fruit softening, and the high LD between nonsynonymous mutations present on Ra_g5108 and Ra_g7125 suggests that similar multigenic model of control for RDR could be possible. The missense mutation at 6,320,015 bp of Ra02 was on Ra_g5252, the same β-glucosidase homolog identified in the fruit firmness association, providing a potential link between fruit firmness and RDR. In addition to PG, expansin, and β-glucosidase, significant associations with RDR were found on a pectate lyase (PL) homolog, Ra_g7552. In strawberry, transgenic antisense inhibition of PL has reduced fruit softening during ripening (Jiménez-Bermúdez et al., 2002).

Genetic Architecture of Postharvest Quality. The identification of numerous marker-trait associations with fruit firmness and RDR suggests that postharvest quality in blackberry is a complex and highly polygenic trait. These findings are consistent with similar findings in a raspberry biparental linkage mapping study, which identified three large fruit firmness QTL across two different linkage groups (Simpson et al., 2017). Similarly, we report significant SNPs in three chromosomes, with Ra02 appearing to be the most important overall in determining postharvest quality. Both RDR and fruit firmness associations draw attention to a large network of texture-related homologs on Ra02 that are in high LD. This network is scattered across the chromosome and contains PG, PL, β-glucosidases, and expansins which may all be synergistically contributing to postharvest quality. The association of both RDR and fruit firmness with this gene network may provide the genetic underpinning of the relationship previously reported between RDR and fruit firmness (Pérez-Pérez et al., 2018; Edgley et al., 2019b). The weakness of our observed phenotypic correlation between these traits is likely due

to environmental influences impacting phenotypic expression of RDR, but variation in anthocyanin composition between genotypes could also be a factor. The PME variant associated with fruit firmness on Ra01 was also located near a large cluster of 11 other texture-related homologs, providing further evidence of complex, polygenic control. Six of these genes were PME, suggesting that this locus could be important in the modification of pectin structure.

Limitations of GWAS. One of the key strengths of a traditional GWAS performed across diverse panels of heterogenous relatedness is in predicting common phenotypic variation with common genotypic variation (Myles et al., 2009). When important alleles are confined to a small number of individuals in the GWAS panel, detection of marker-trait associations becomes less likely. We expect this to be true in our own association analyses, considering the distribution of our phenotypic datasets. For instance, in our fruit firmness BLUP dataset, statistical outliers (1.5 x interquartile range) were present on both ends of the distribution, with A-2625T being the firmest and "Black Gem™" being the softest. Based on prior knowledge of these genotypes, these data seem valid. However, if these rare phenotypes are associated with rare underlying genotypes, statistical power will likely be insufficient to detect its source (Visscher et al., 2012). Such may be the case in detecting the cause of the rare 'crispy' texture phenotype documented in the UA breeding program (Salgado and Clark, 2016), which has only been observed in a small number of genotypes to date. This texture is a distinct phenotype that is not easily recovered through crossing and qualitative categorization of crispy genotypes is not easily achievable through the fruit firmness protocols employed in this study. For postharvest traits of unique importance like crispy texture, more targeted strategies such as biparental linkage mapping or

RNA sequencing should be considered along with modified phenotyping protocols to explore its biological mechanism and modes of inheritance.

Another important consideration following a GWAS is in developing a genome-informed strategy for promoting long-term genetic gain in a breeding program. Our work suggests that postharvest quality is a complex trait that is likely governed by numerous genes on multiple chromosomes. In this context, direct application of discovered QTL in MAS is unlikely to be sufficient. Instead, significant SNPs could be included in genomic selection models as fixed covariates based on their known importance (Rice and Lipka, 2019). In contrast with GWAS, genomic selection provides breeders with the ability to leverage the cumulative effects of many low-effect QTL in predicting the merit of new breeding selections. Furthermore, the large datasets accumulated in this study should provide an effective foundational training dataset for future genomic selection models. These data will allow breeders to predict blackberry fruit firmness and RDR susceptibility of genotypes and reduce the operational burdens of heavy phenotyping requirements. Such strategies are especially well-suited to complex and low-heritability traits like RDR and fruit firmness, which appear to be governed by numerous small-effect QTL (Bernardo, 2016).

Conclusion

This study is the first to report marker-trait associations in tetraploid blackberry, using a genome wide approach. We have identified numerous SNPs significantly associated with RDR on Ra02 and seven SNPs associated with fruit firmness across four out of seven chromosomes. Variants on a PME located on Ra01, a β-glucosidase on Ra02, and a PG on Ra06 explained 27% of variance in fruit firmness in this study. A variant on a PG homolog on Ra02 accounted for 8% of

variance in RDR, but this chromosome also contained a much larger network of significantly associated variants on texture homologs in high LD. A cluster of six PME and PME inhibitor homologs were also identified within 500 kb of markers associated with fruit firmness on Ra01. Best linear unbiased predictions of RDR and fruit firmness were only weakly correlated in these populations, but overlapping genetic associations with both traits were discovered on Ra02, suggesting that potential candidate genes in this region may have pleiotropic effects. Given the modest heritability of fruit firmness and RDR, combined with their apparent polygenic nature, we determine that genomic selection is the most promising long-term strategy for improvement of these traits. Significant QTL should be used as fixed covariates in a genomic selection model that utilizes existing datasets for model training. These findings represent the first large-scale genomic exploration of a diverse blackberry population and will provide a strong methodological and conceptual framework for continued genetic research in the crop and its relatives.

Literature Cited

Armour, M. E., Worthington, M., Clark, J. R., Threlfall, R. T., and Howard, L. (2021). Effect of harvest time and fruit firmness on red drupelet reversion in blackberry. HortScience 56, 889–896. doi: 10.21273/HORTSCI15853-21.

Bates, D., Mächler, M., Bolker, B., and Walker, S. (2015). Fitting linear mixed-effects models using lme4. J Stat Softw 67. doi: 10.18637/jss.v067.i01.

Bourke, P. M., Voorrips, R. E., Visser, R. G. F., and Maliepaard, C. (2018). Tools for genetic studies in experimental populations of polyploids. Front Plant Sci 9. doi: 10.3389/fpls.2018.00513.

Brůna, T., Aryal, R., Dudchenko, O., Sargent, D. J., Mead, D., Buti, M., et al. (2022). A chromosome-length genome assembly and annotation of blackberry (*Rubus argutus*, cv. 'Hillquist'). G3 Genes|Genomes|Genetics. doi: 10.1093/g3journal/jkac289.

Cai, L., Quero-García, J., Barreneche, T., Dirlewanger, E., Saski, C., and Iezzoni, A. (2019). A fruit firmness qtl identified on linkage group 4 in sweet cherry (*Prunus avium* l.) is associated with domesticated and bred germplasm. Sci Rep 9, 5008. doi: 10.1038/s41598-019-41484-8.

Callahan, A. M., Scorza, R., Bassett, C., Nickerson, M., and Abeles, F. B. (2004). Deletions in an endopolygalacturonase gene cluster correlate with non-melting flesh texture in peach. Functional Plant Biology 31, 159. doi: 10.1071/FP03131.

Cellon, C., Amadeu, R. R., Olmstead, J. W., Mattia, M. R., Ferrao, L. F. v., and Munoz, P. R. (2018). estimation of genetic parameters and prediction of breeding values in an

autotetraploid blueberry breeding population with extensive pedigree data. Euphytica 214, 87. doi: 10.1007/s10681-018-2165-8.

Clark, J. R., and Finn, C. E. (2011). Blackberry breeding and genetics. Fruit, Vegetable, and Cereal Science and Biotechnology 5, 27–43.

Cockerton, H. M., Karlström, A., Johnson, A. W., Li, B., Stavridou, E., Hopson, K. J., et al. (2021). Genomic informed breeding strategies for strawberry yield and fruit quality traits. Front Plant Sci 12. doi: 10.3389/fpls.2021.724847.

Crookes, P. R., and Grierson, D. (1983). Ultrastructure of tomato fruit ripening and the role of polygalacturonase isoenzymes in cell wall degradation. Plant Physiol 72, 1088–1093. doi: 10.1104/pp.72.4.1088.

Danecek, P., Auton, A., Abecasis, G., Albers, C. A., Banks, E., DePristo, M. A., et al. (2011). The variant call format and VCFtools. Bioinformatics 27, 2156–2158. doi: 10.1093/bioinformatics/btr330.

Devries, J., Denuijl, C., Voragen, A., Rombouts, F., and Pilnik, W. (1983). Structural features of the neutral sugar side chains of apple pectic substances. Carbohydr Polym 3, 193–205. doi: 10.1016/0144-8617(83)90018-8.

Edgley, M., Close, D. C., and Measham, P. F. (2019a). Effects of climatic conditions during harvest and handling on the postharvest expression of red drupelet reversion in blackberries. Sci Hortic 253, 399–404. doi: 10.1016/j.scienta.2019.04.052.

Edgley, M., Close, D. C., and Measham, P. F. (2019b). Flesh temperature during impact injury and subsequent storage conditions affect the severity of colour change caused by red

drupelet reversion in blackberries. Acta Hortic 1265, 129–134. doi: 10.17660/ActaHortic.2019.1265.18.

Edgley, M., Close, D. C., and Measham, P. F. (2019c). Nitrogen application rate and harvest date affect red drupelet reversion and postharvest quality in ‘Ouachita’ blackberries. Sci Hortic 256, 108543. doi: 10.1016/j.scienta.2019.108543.

Edgley, M., Close, D. C., Measham, P. F., and Nichols, D. S. (2019d). Physiochemistry of blackberries (*Rubus* L. subgenus *Rubus* Watson) affected by red drupelet reversion. Postharvest Biol Technol 153, 183–190. doi: 10.1016/j.postharvbio.2019.04.012.

Evanno, G., Regnaut, S., and Goudet, J. (2005). Detecting the number of clusters of individuals using the software STRUCTURE: A Simulation Study. Mol Ecol 14, 2611–2620. doi: 10.1111/j.1365-294X.2005.02553.x.

Ferrão, L. F. v., Benevenuto, J., Oliveira, I. de B., Cellon, C., Olmstead, J., Kirst, M., et al. (2018). Insights into the genetic basis of blueberry fruit-related traits using diploid and polyploid models in a GWAS context. Front Ecol Evol 6. doi: 10.3389/fevo.2018.00107.

Ferrão, L. F. v., Johnson, T. S., Benevenuto, J., Edger, P. P., Colquhoun, T. A., and Munoz, P. R. (2020). Genome-wide association of volatiles reveals candidate loci for blueberry flavor. New Phytologist 226, 1725–1737. doi: 10.1111/nph.16459.

Finn, C., and Clark, J. (2011). Emergence of blackberry as a world crop. Chron Horticult 51, 13–18.

Foster, T. M., Bassil, N. v., Dossett, M., Leigh Worthington, M., and Graham, J. (2019). Genetic and genomic resources for rubus breeding: a roadmap for the future. Hortic Res 6, 116. doi: 10.1038/s41438-019-0199-2.

Gerard, D. (2021). Pairwise linkage disequilibrium estimation for polyploids. Mol Ecol Resour 21, 1230–1242. doi: 10.1111/1755-0998.13349.

Gerard, D., Ferrão, L. F. V., Garcia, A. A. F., and Stephens, M. (2018). Genotyping polyploids from messy sequencing data. Genetics 210, 789–807. doi: 10.1534/genetics.118.301468.

Gerardi, C., Blando, F., Santino, A., and Zacheo, G. (2001). Purification and characterisation of a β-glucosidase abundantly expressed in ripe sweet cherry (*Prunus avium* L.) Fruit. Plant Science 160, 795–805. doi: 10.1016/S0168-9452(00)00423-4.

Gu, C., Wang, L., Wang, W., Zhou, H., Ma, B., Zheng, H., et al. (2016). Copy number variation of a gene cluster encoding endopolygalacturonase mediates flesh texture and stone adhesion in peach. J Exp Bot 67, 1993–2005. doi: 10.1093/jxb/erw021.

Jiménez-Bermúdez, S., Redondo-Nevado, J., Muñoz-Blanco, J., Caballero, J. L., López-Aranda, J. M., Valpuesta, V., et al. (2002). Manipulation of strawberry fruit softening by antisense expression of a pectate lyase gene. Plant Physiol 128, 751–759. doi: 10.1104/pp.010671.

Kebede, A., and Kebede, M. (2021). In silico analysis of promoter region and regulatory elements of glucan endo-1,3-beta-glucosidase encoding genes in *Solanum tuberosum*: cultivar DM 1-3 516 R44. Journal of Genetic Engineering and Biotechnology 19, 145. doi: 10.1186/s43141-021-00240-0.

Kim, M. J., Lee, M. Y., Shon, J. C., Kwon, Y. S., Liu, K. H., Lee, C. H., et al. (2019). Untargeted and targeted metabolomics analyses of blackberries – understanding postharvest red drupelet disorder. Food Chem 300, 125169. doi: 10.1016/j.foodchem.2019.125169.

Kim, Y., and Stephan, W. (2002). Detecting a local signature of genetic hitchhiking along a recombining chromosome. Genetics 160, 765–777. doi: 10.1093/genetics/160.2.765.

Konozy, E. H. E., Causse, M., and Faurobert, M. (2012). Cell wall glycosidase activities and protein content variations during fruit development and ripening in three texture contrasted tomato cultivars. Saudi J Biol Sci 19, 277–283. doi: 10.1016/j.sjbs.2012.04.006.

Lee, J. C., Bruck, D. J., Curry, H., Edwards, D., Haviland, D. R., van Steenwyk, R. A., et al. (2011). The susceptibility of small fruits and cherries to the spotted-wing drosophila, *Drosophila suzukii*. Pest Manag Sci 67, 1358–1367. doi: 10.1002/ps.2225.

Marangoni, A. G., Jackman, R. L., and Stanley, D. W. (1995). Chilling-associated softening of tomato fruit is related to increased pectinmethylesterase activity. J Food Sci 60, 1277–1281. doi: 10.1111/j.1365-2621.1995.tb04572.x.

Myles, S., Peiffer, J., Brown, P. J., Ersoz, E. S., Zhang, Z., Costich, D. E., et al. (2009). Association mapping: critical considerations shift from genotyping to experimental design. Plant Cell 21, 2194–2202. doi: 10.1105/tpc.109.068437.

Ortiz Araque, L. C., Ortiz, C. M., Darré, M., Rodoni, L. M., Civello, P. M., and Vicente, A. R. (2019). Role of UV-C irradiation scheme on cell wall disassembly and surface

mechanical properties in strawberry fruit. Postharvest Biol Technol 150, 122–128. doi: 10.1016/j.postharvbio.2019.01.002.

Peace, C. P., Crisosto, C. H., and Gradziel, T. M. (2005). Endopolygalacturonase: a candidate gene for freestone and melting fleshin peach. Molecular Breeding 16, 21–31. doi: 10.1007/s11032-005-0828-3.

Pérez-Pérez, G. A., Fabela-Gallegos, M. J., Vázquez-Barrios, M. E., Rivera-Pastrana, D. M., Palma-Tirado, L., Mercado-Silva, E., et al. (2018). Effect of the transport vibration on the generation of the color reversion in blackberry fruit. Acta Hortic 1194, 1329–1336. doi: 10.17660/ActaHortic.2018.1194.187.

Porebski, S., Bailey, L. G., and Baum, B. R. (1997). Modification of a CTAB DNA extraction protocol for plants containing high polysaccharide and polyphenol components. Plant Mol Biol Report 15, 8–15. doi: 10.1007/BF02772108.

Powell, A. L. T., Kalamaki, M. S., Kurien, P. A., Gurrieri, S., and Bennett, A. B. (2003). Simultaneous transgenic suppression of lepg and leexp1 influences fruit texture and juice viscosity in a fresh market tomato variety. J Agric Food Chem 51, 7450–7455. doi: 10.1021/jf034165d.

Prange, R. K., and DeEll, J. R. (1997). Preharvest factors affecting postharvest quality of berry crops. HortScience 32, 824–830. doi: 10.21273/HORTSCI.32.5.824.

Pritchard, J. K., Stephens, M., and Donnelly, P. (2000). Inference of population structure using multilocus genotype data. Genetics 155, 945–959. doi: 10.1093/genetics/155.2.945.

Qian, J., Zhao, Y., Shi, Y., and Chen, K. (2022). Transcriptome analysis of peach fruit under 1-mcp treatment provides insights into regulation network in melting peach softening. Food Quality and Safety 6. doi: 10.1093/fqsafe/fyac048.

R Core Team (2022). R: a language and environment for statistical computing. Available at: https://www.R-project.org/.

Rahimi, Y., Bihamta, M. R., Taleei, A., Alipour, H., and Ingvarsson, P. K. (2019). Genome-wide association study of agronomic traits in bread wheat reveals novel putative alleles for future breeding programs. BMC Plant Biol 19, 541. doi: 10.1186/s12870-019-2165-4.

Rice, B., and Lipka, A. E. (2019). Evaluation of RR-BLUP Genomic selection models that incorporate peak genome-wide association study signals in maize and sorghum. Plant Genome 12, 180052. doi: 10.3835/plantgenome2018.07.0052.

Rosyara, U. R., de Jong, W. S., Douches, D. S., and Endelman, J. B. (2016). Software for genome-wide association studies in autopolyploids and its application to potato. Plant Genome 9. doi: 10.3835/plantgenome2015.08.0073.

Salgado, A. A., and Clark, J. R. (2016). "'Crispy'" blackberry genotypes: a breeding innovation of the University of Arkansas blackberry breeding program.

Schork, A. J., Thompson, W. K., Pham, P., Torkamani, A., Roddey, J. C., Sullivan, P. F., et al. (2013). All SNPs are not created equal: genome-wide association studies reveal a consistent pattern of enrichment among functionally annotated SNPs. PLoS Genet 9. doi: 10.1371/journal.pgen.1003449.

Shaw, D. v, Bringhurst, R. S., and Voth, V. (1987). Genetic variation for quality traits in an advanced-cycle breeding population of strawberries.

Shin, J.-H., Blay, S., Graham, J., and McNeney, B. (2006). LDheatmap : an R function for graphical display of pairwise linkage disequilibria between single nucleotide polymorphisms. J Stat Softw 16. doi: 10.18637/jss.v016.c03.

Simpson, C. G., Cullen, D. W., Hackett, C. A., Smith, K., Hallett, P. D., McNicol, J., et al. (2017). Mapping and expression of genes associated with raspberry fruit ripening and softening. Theoretical and Applied Genetics 130, 557–572. doi: 10.1007/s00122-016-2835-7.

Threlfall, R. T., Dunteman, A. N., Clark, J. R., and Worthington, M. L. (2020). Using an online survey to determine consumer perceptions of fresh-market blackberries. Acta Hortic 1277, 469–476. doi: 10.17660/ActaHortic.2020.1277.67.

Toivonen, P. M. A., and Brummell, D. A. (2008). Biochemical bases of appearance and texture changes in fresh-cut fruit and vegetables. Postharvest Biol Technol 48, 1–14. doi: 10.1016/j.postharvbio.2007.09.004.

Visscher, P. M., Brown, M. A., McCarthy, M. I., and Yang, J. (2012). Five years of GWAS discovery. Am J Hum Genet 90, 7–24. doi: 10.1016/j.ajhg.2011.11.029.

Wen, B., Ström, A., Tasker, A., West, G., and Tucker, G. A. (2013). Effect of silencing the two major tomato fruit pectin methylesterase isoforms on cell wall pectin metabolism. Plant Biol 15, 1025–1032. doi: 10.1111/j.1438-8677.2012.00714.x.

Xue, C., Guan, S.-C., Chen, J.-Q., Wen, C.-J., Cai, J.-F., and Chen, X. (2020). Genome wide identification and functional characterization of strawberry pectin methylesterases related to fruit softening. BMC Plant Biol 20, 13. doi: 10.1186/s12870-019-2225-9.

Tables and Figures

Table 2.1. Variance components and broad-sense heritability of fruit firmness and red drupelet reversion (RDR) across 2019-2021

		Fruit firmness	RDR
Variance components	σ^2_g [i]	1.524	1.371
	σ^2_{gy} [ii]	0.323	0.405
	σ^2 [iii]	1.699	7.781
Heritability (%)	$H_{per\text{-}plot}$	0.430	0.143
	$H_{entry\text{-}mean}$	0.677	0.335

[i]genotypic variance
[ii]genotype by year variance
[iii]residual error variance

Table 2.2. SNP-trait associations and candidate genes for blackberry firmness and RDR detected across 2019-2021. All significant SNPs for fruit firmness are listed, but only 22 of 212 significant RDR SNPs were listed. All but one of these 22 SNPs with significant RDR associations were nonsynonymous mutations on genes with previously documented roles in cell wall modification/degradation.

Trait	Chromosome	Model	Position	Ref	Alt	*LOD*	r^2(%)[i]	Variant type	Gene	Annotation and *Arabidopsis* homolog[ii]
Fruit firmness	Ra01	additive	4352940	T	G	5.84	5.27	Intron variant	Ra_g890	Pectinesterase/pectinesterase inhibitor PPE8B; At3g43270
		additive	4422023	T	G	5.77	5.36	67,850 bp ds[iii]	Ra_g890	Pectinesterase/pectinesterase inhibitor PPE8B; At3g43270
	Ra02	additive	6321370	C	T	6.11	11.40	Silent	Ra_g5252	Glucan endo-1,3-beta-glucosidase 7; At4g34480
		additive	6321387	T	C	5.48	10.48	Missense	Ra_g5252	Glucan endo-1,3-beta-glucosidase 7; At4g34480
		general	8025922	G	T	5.55	12.70	NA		
	Ra03	general	3633404	G	A	6.34	8.76	833,124 bp us[iv]	Ra_g10675	Glucan endo-1,3-beta-D-glucosidase; At2g43670
	Ra06	general	17273160	A	G	7.21	11.47	Silent	Ra_g27483	Probable polygalacturonase; At3g15720
RDR	Ra02	1-dom-ref	5150596	G	A	6.05	8.26	Missense	Ra_g5108	Probable polygalacturonase; At3g15720
		1-dom-ref	5150747	G	T	5.63	7.66	Missense	Ra_g5108	Probable polygalacturonase; At3g15720
		1-dom-ref	6320015	C	A	5.52	7.44	Missense	Ra_g5252	Glucan endo-1,3-beta-glucosidase 7; At4g34480
		general	13296902[v]	C	A	7.00	11.13	Intron variant	Ra_g5949	2-oxoglutarate-dependent dioxygenase; AT2G36690.2
		1-dom-ref	21494838	C	T	5.55	7.64	Missense	Ra_g6621	Endo-1,3;1,4-beta-D-glucanase; At3g23600
		1-dom-ref	21495058	A	T	6.02	8.33	Missense	Ra_g6621	Endo-1,3;1,4-beta-D-glucanase; At3g23600
		1-dom-ref	24484457	T	C	5.76	7.97	Missense	Ra_g7012	Expansin-like A1; At3g45970
		1-dom-ref	24485338	T	C	5.38	7.41	Missense	Ra_g7012	Expansin-like A1; At3g45970
		1-dom-ref	24485380	C	A	5.38	7.41	Missense	Ra_g7012	Expansin-like A1; At3g45970
		1-dom-ref	25139841	T	C	5.46	7.47	Missense	Ra_g7125	Expansin-A20; At4g38210
		1-dom-ref	25140011	G	A	5.76	7.97	Nonsense	Ra_g7125	Expansin-A20; At4g38210
		1-dom-ref	25140131	T	A	5.76	7.97	Missense	Ra_g7125	Expansin-A20; At4g38210
		1-dom-ref	25140272	A	C	5.81	7.96	Missense	Ra_g7125	Expansin-A20; At4g38210
		1-dom-ref	26764458	T	C	5.38	7.51	Missense	Ra_g7381	Glucan endo-1,3-beta-glucosidase A6; At3g07320
		1-dom-ref	26765115	G	C	5.76	7.97	Missense	Ra_g7381	Glucan endo-1,3-beta-glucosidase A6; At3g07320
		1-dom-ref	26765139	A	G	5.38	7.51	Missense	Ra_g7381	Glucan endo-1,3-beta-glucosidase A6; At3g07320
		1-dom-ref	26765333	A	G	5.38	7.51	Missense	Ra_g7381	Glucan endo-1,3-beta-glucosidase A6; At3g07320
		1-dom-ref	26765357	G	A	5.76	7.97	Missense	Ra_g7381	Glucan endo-1,3-beta-glucosidase A6; At3g07320
		1-dom-ref	26765634	T	G	5.76	7.97	Missense	Ra_g7381	Glucan endo-1,3-beta-glucosidase A6; At3g07320
		1-dom-ref	27713275	A	G	5.38	7.41	Missense	Ra_g7552	Probable pectate lyase 8; At3g07010
		1-dom-ref	27715029	C	T	5.38	7.51	Missense	Ra_g7552	Probable pectate lyase 8; At3g07010
		1-dom-ref	27715116	A	G	5.76	7.97	Missense	Ra_g7552	Probable pectate lyase 8; At3g07010

[i]Phenotypic r^2 estimates were calculated based on single marker prediction models.
[ii]The SwissProt and Araport11 databases were interrogated for descriptions of gene homologs and the *Arabidopsis* homolog identifier following Brůna et al. 2022
[iii]Downstream from candidate end position
[iv]Upstream from candidate start position
[v]Not on or near any annotated gene with known role in cell wall dissassembly

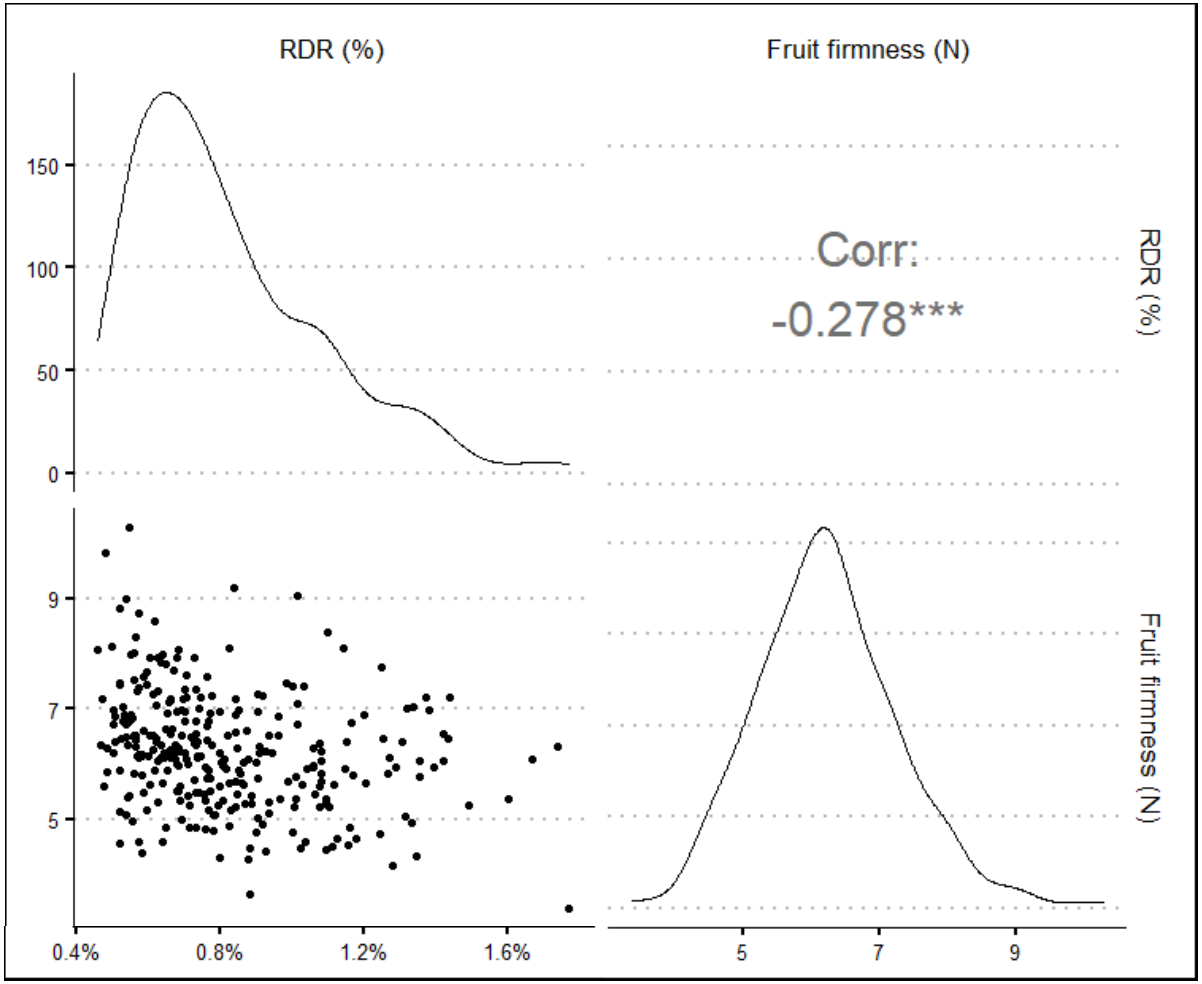

Figure 2.1. Phenotypic distributions and correlation of RDR measured by ShinyFruit and fruit firmness BLUPs across 300 tetraploid blackberry genotypes observed in 2019, 2020, and 2021.

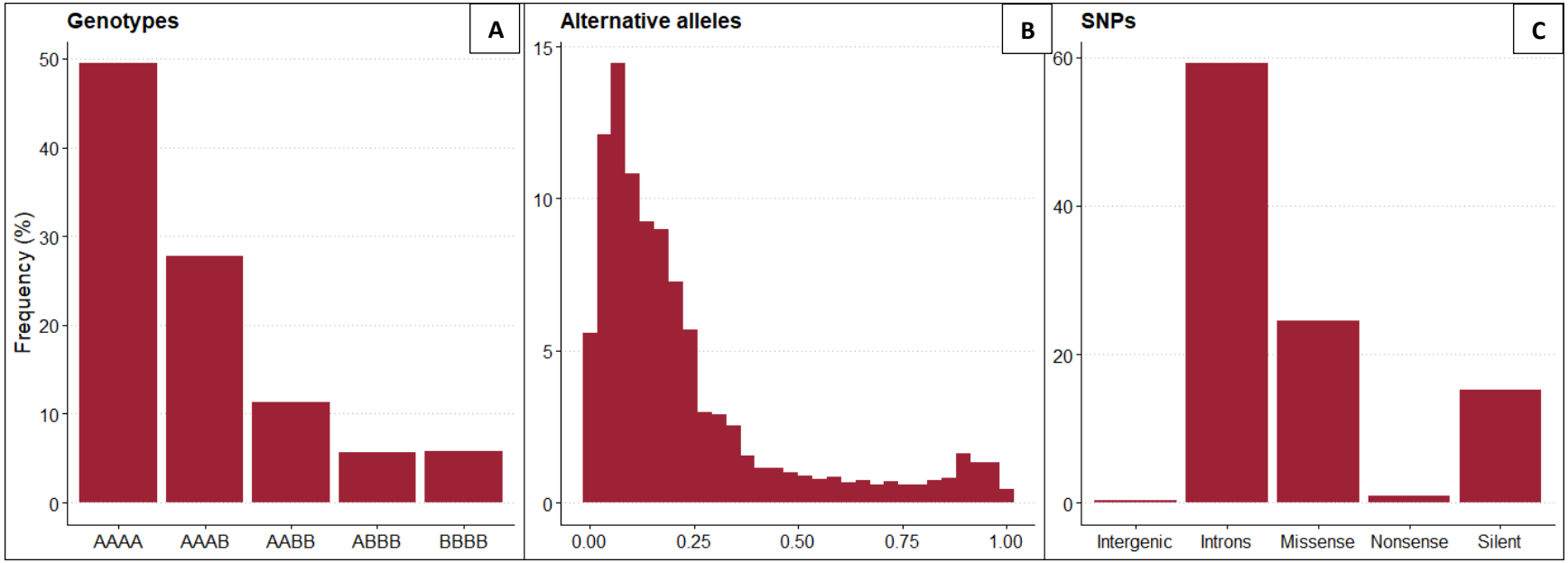

Figure 2. Distributions of genotypic frequencies across all loci in all individuals, where "A" represents the major allele and "B" represents the minor allele (A), minor allele frequencies (B), and variant class frequencies (C) of 65,995 SNPs used in association mapping.

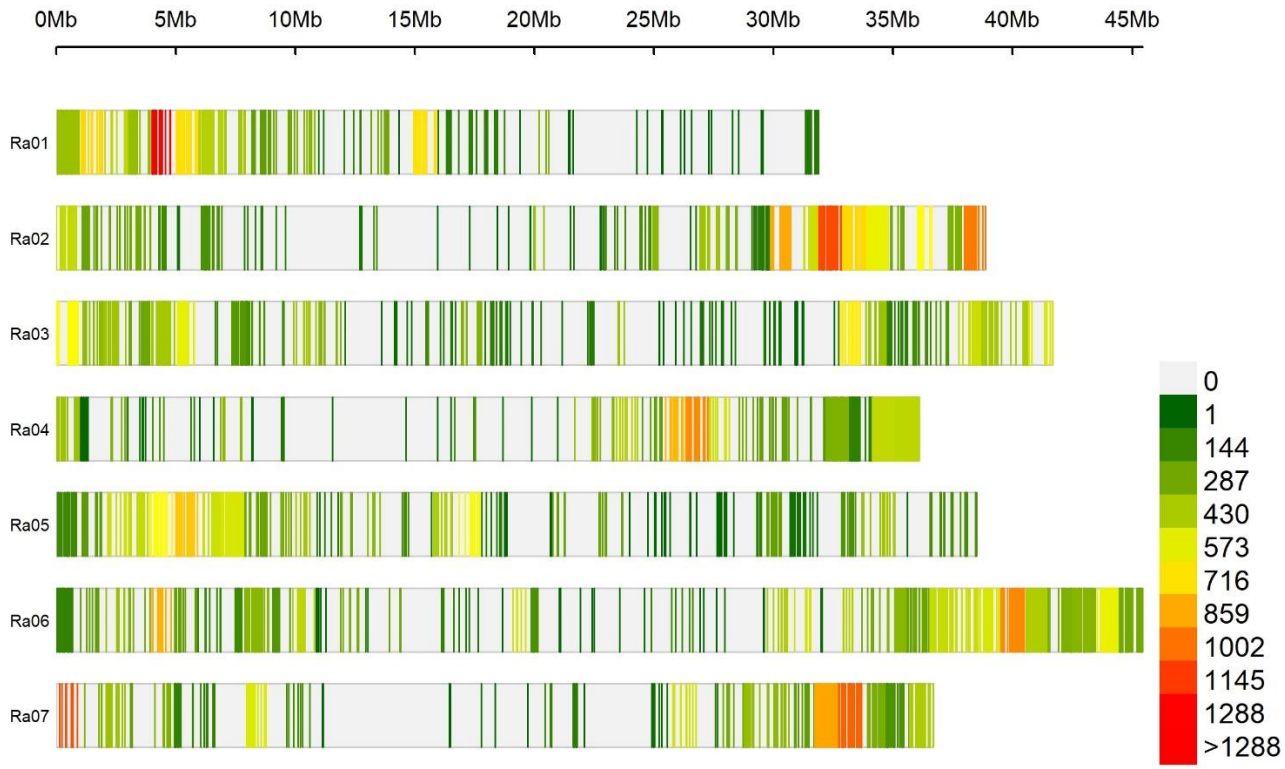

Figure 2.3. Distribution of 65,995 SNPs across the seven chromosomes contained in the *R. argutus* reference genome. Color bins are assigned based on the number of SNPs contained in a 1 Mb region.

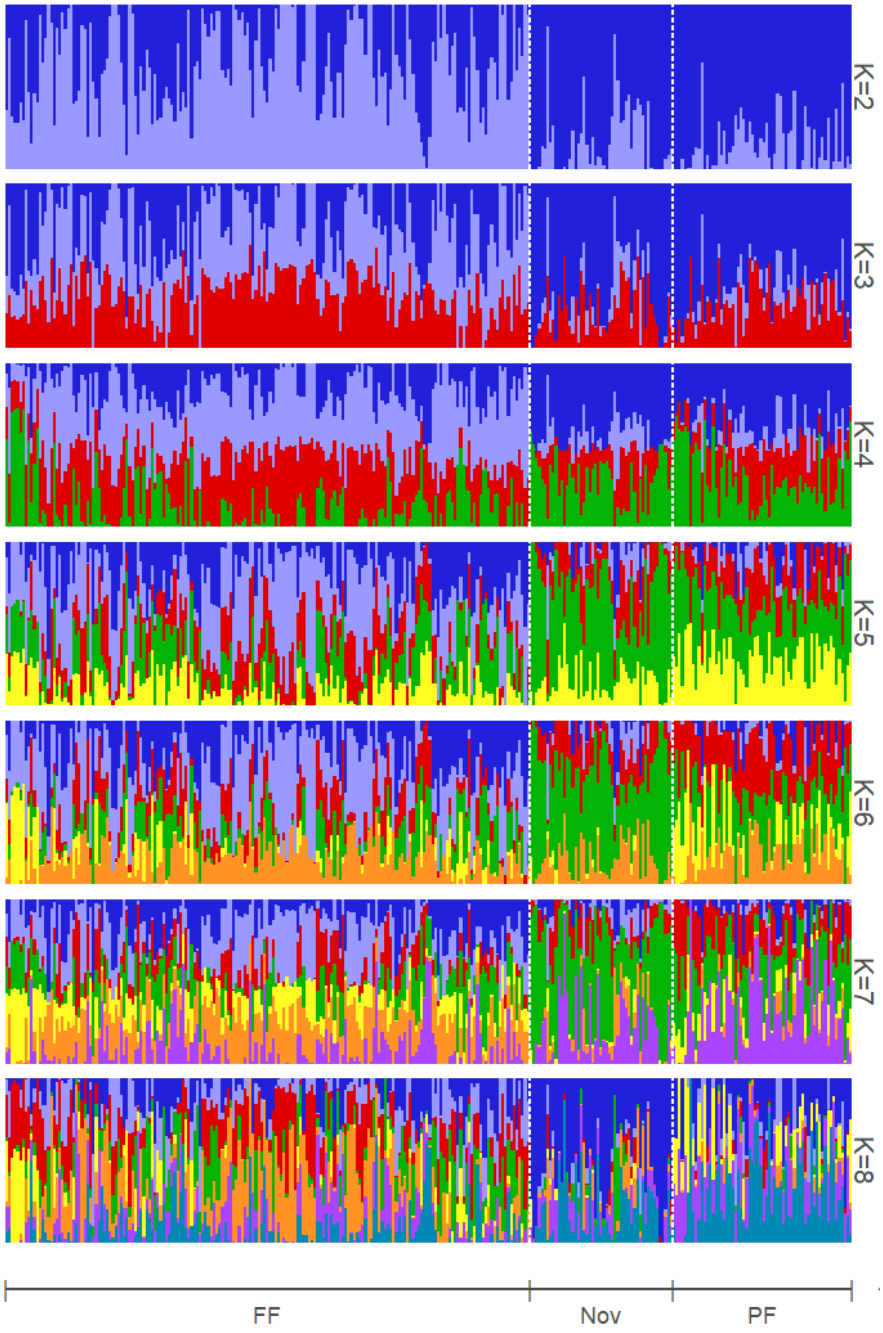

Figure 2.4. Structure estimation of admixed subpopulation proportions assuming numbers of subpopulations (K) ranging from two to eight. FF – floricane fruiting (non-primocane fruiting). Nov – Novels (brachytic dwarfing habit). PF – Primocane fruiting. K = 6 was optimal following Evanno et al. (2005).

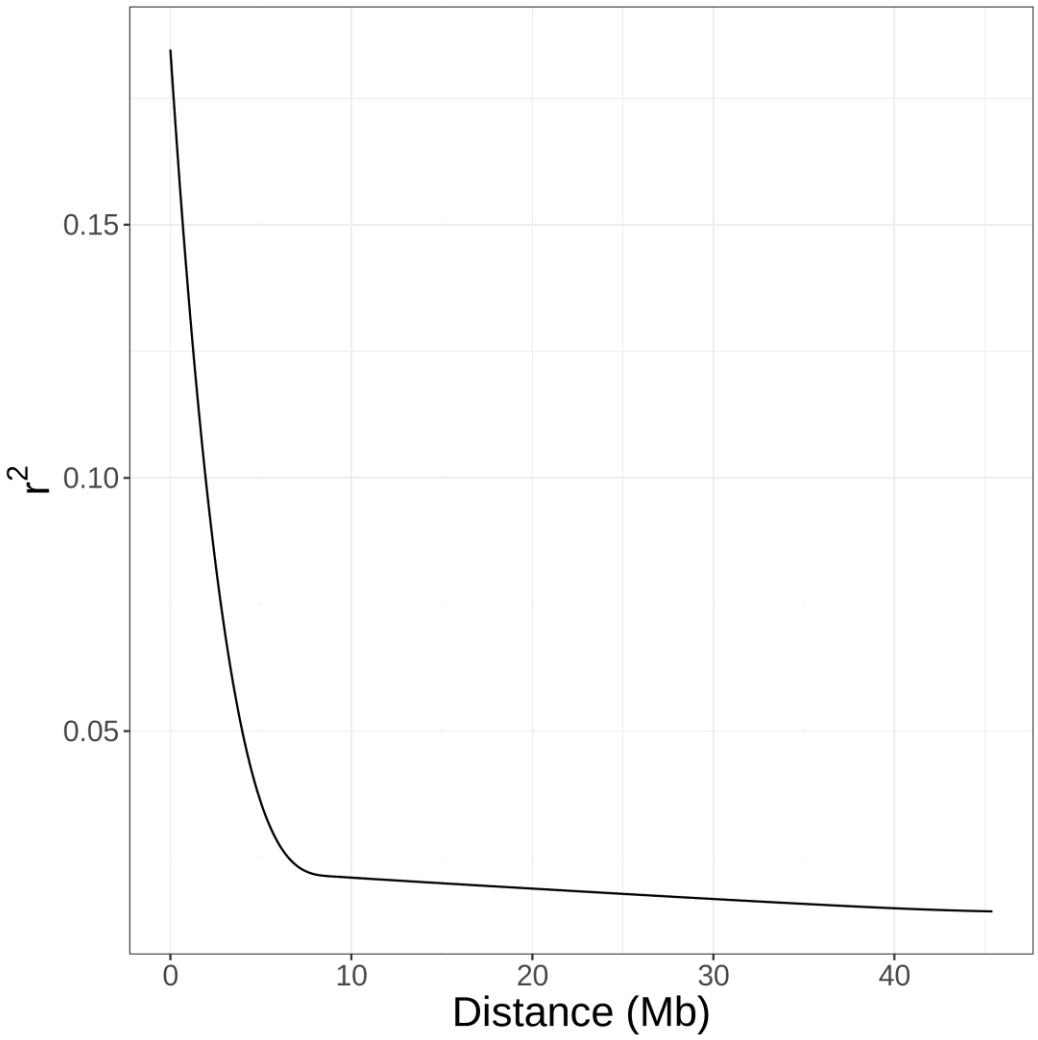

Figure 2.5. Average decay of linkage disequilibrium as estimated by squared correlation coefficients (r^2) between SNPs across the whole blackberry genome.

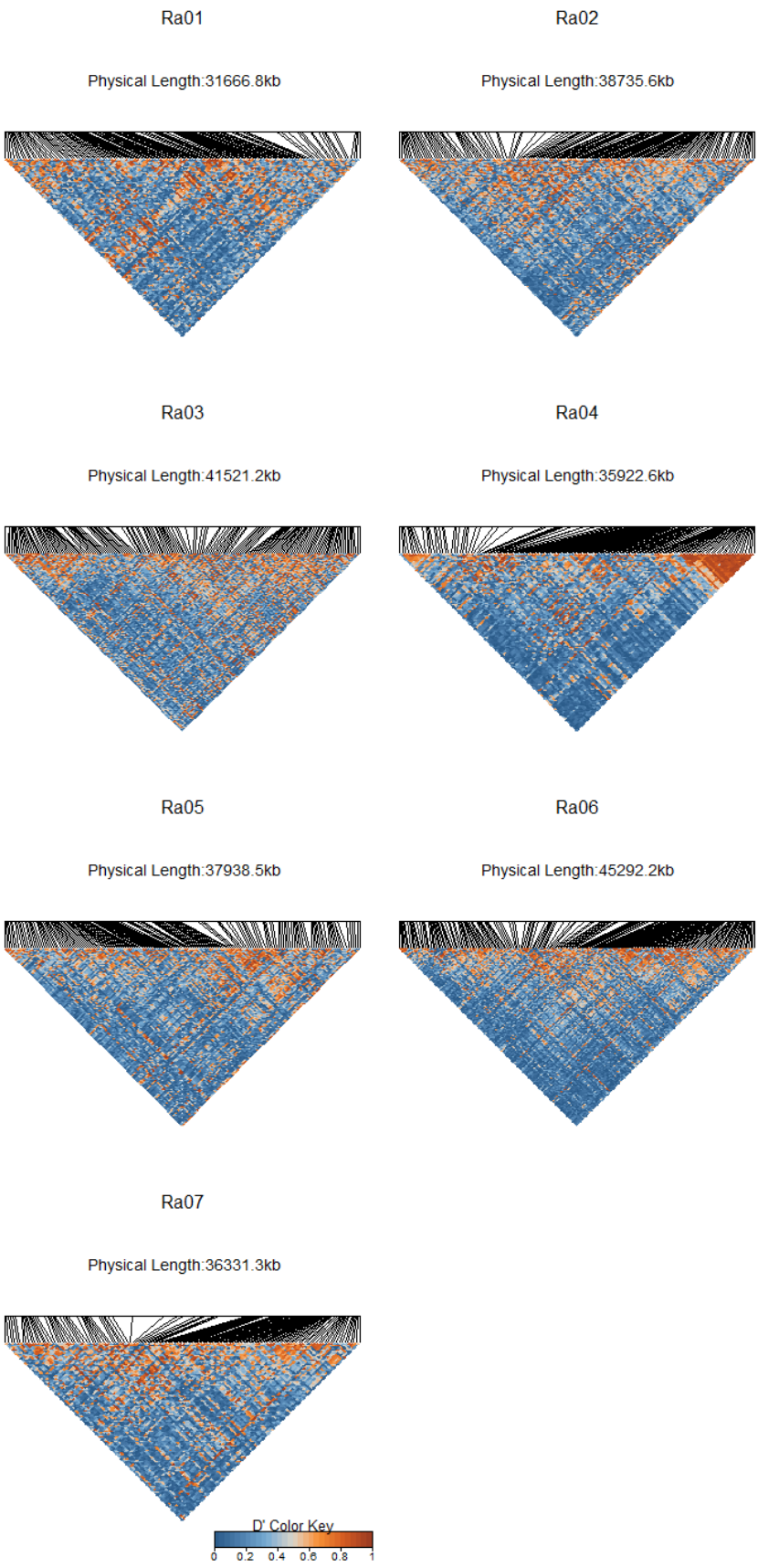

Figure 2.6. Heat maps of absolute values of Lewontin's D' estimated between SNP subsets in each chromosome of the *R. argutus* blackberry reference genome. SNPs were subsampled to have a minimum spacing of 100 kb.

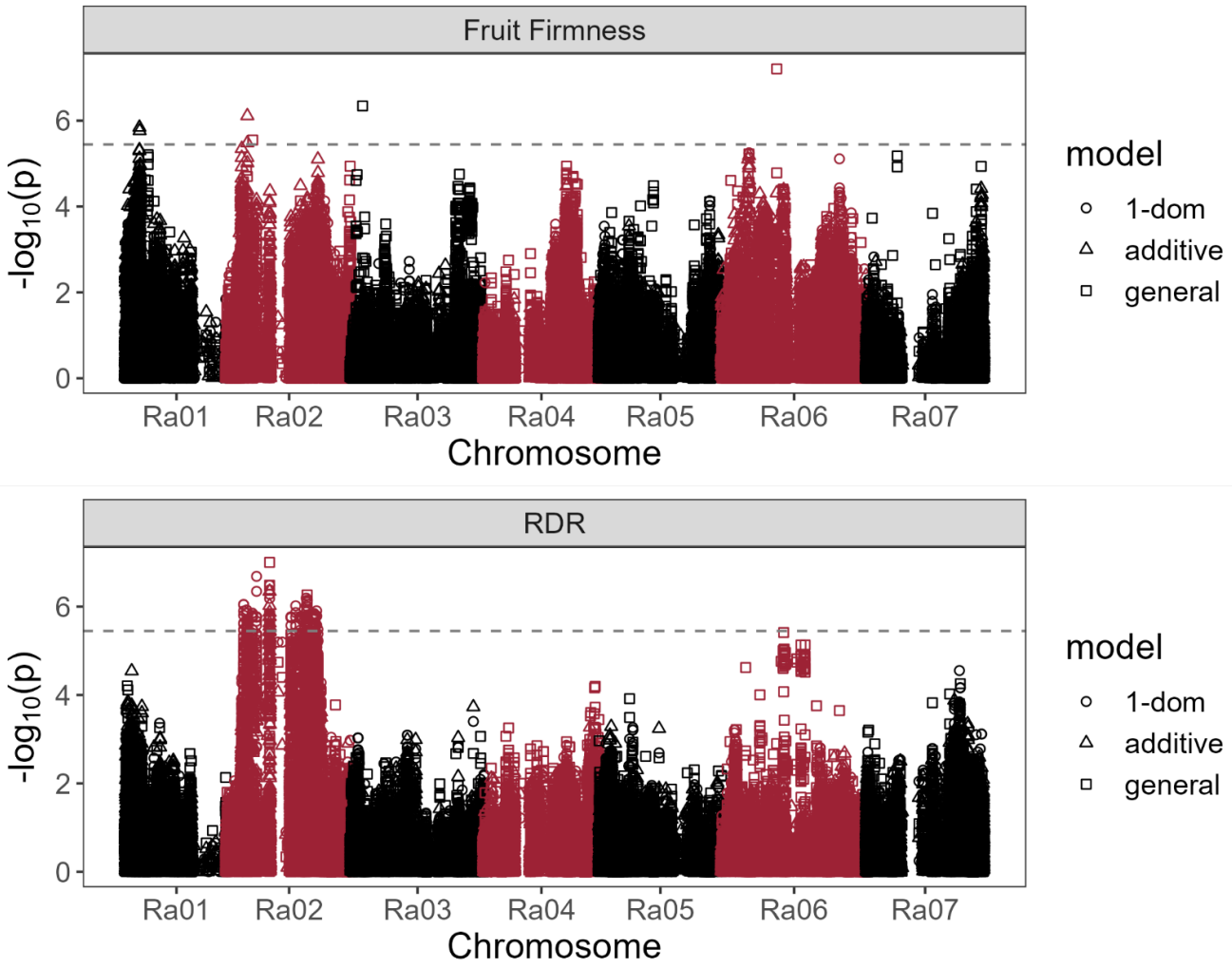

Figure 2.7. Manhattan plots of fruit firmness and red drupelet reversion (RDR) associations with 65,995 SNPs under additive, general, and simplex-dominance (1-dom) models. The dashed line indicates the lowest significance threshold used between tested models at $\alpha = 0.05$ using the GWASpoly M.eff method.

CHAPTER III

THE POTENTIAL ROLE OF POLYGALACTURONASE AND PECTIN METHYLESTERASE IN BLACKBERRY FRUIT SOFTENING PATTERNS

Abstract

Fresh market blackberries are considered one of the most challenging fruits to ship due to their soft texture and propensity for leakage, discoloration, deformation, and mold. Breeding programs have gradually developed new blackberry cultivars with improved shipping potential, but little is known about the specific proteins responsible for these genetic gains. By layering data from RNA sequencing, enzyme activity, and fruit softening patterns over three stages of berry development, we have developed insights into the potential roles of pectin methylesterase (PME) and polygalacturonase (PG) in mediating differential softening patterns between the soft fruited 'Black Gem™' and crispy-fruited A-2453T. 'Black Gem™' expressed both PME and PG at consistently higher levels than A-2453T during all stages of berry development ($Q \leq 0.05$). These expression levels may have corresponded with increased PG activity in 'Black Gem™' at the green stage of berry development ($P \leq 0.10$), and no significant differences in enzymatic activity were detected during the red and black stages. Unexpectedly, PME activity in A-2453T was significantly greater than in 'Black Gem™' during the green stage of berry development. These elevated levels of activity also appear to be inversely associated with the upregulation of PME inhibitors (PMEI) ($Q \leq 0.05$) as the fruit progresses to maturity. Expansin-like proteins may also fulfill a unique role in crispy blackberry texture, as greater levels were expressed in A-2453T. The softer texture of 'Black Gem™' during the mature black stage of fruit development appeared to be associated with elevated expression of PG, PME, and β-glucosidase, which may work synergistically to catalyze the degradation of complex pectin macromolecules.

Introduction

Year-round supply and distribution of fresh blackberries in the US is heavily dependent on international shipping lanes. In 2022, the US imported about 123,068 metric tons of fresh blackberries (USDA-ERS, 2023), with the highest volume shipped during winter months. Despite this dependency, blackberries are considered one of the most challenging fruits to ship. Soft-fruited blackberries often invite moisture loss, mold susceptibility, juice leakage, and discoloration (Perkins-Veazie, 2017; Segantini et al., 2017). The postharvest quality of blackberry is disadvantaged by fragile, thin skins and the notable lack of cuticle or protective rind, which allows moisture to escape more easily. However, fruit softening patterns in blackberry can vary drastically based on genotype (Perkins-Veazie et al., 1996; Perkins Veazie, 2017), and the genetic factors contributing to texture differences are not well understood.

In most horticulturally important fruit species, fruit softening occurs through a biologically programmed process whereby cell walls are disassembled during ripening. This process results in loss of cell adhesion and is achieved primarily through the degradation of pectic polysaccharides in the middle lamella region (Wang et al., 2018). These adhesive-like polysaccharides are structurally complex and are composed of both ‘smooth’ homogalacturonan (HG) regions and ‘hairy’ regions containing numerous rhamnogalacturonan sidechains (de Vries et al., 1983). Polygalacturonases (PG) degrade these pectic polysaccharides during ripening by hydrolyzing α-1,4-D galacturonan within the HG regions. However, newly synthesized HG is highly methylesterified (Wang et al., 2018), which prevents PG from accessing its substrate. Thus, the pectin-modifying enzyme, pectin methylesterase (PME), is often seen as an important enabler of PG activity for role in de-esterification of pectin HG. Powerful inhibitors of PMEs have also been reported in kiwi and tomato (Jolie et al., 2009; Reca et al., 2012), which are able

to downregulate modification of pectin molecules. Zhang et al. (2019) observed that the blackberry cultivar Arapaho had fruit with lower levels of PME enzyme activity between 30-39 days after flowering when compared the softer-fruited 'Boysen'. Similarly, 'Arapaho' had lower levels of PG enzyme activity between 24-36 days after flowering than 'Boysen'. Genetic diversity in PG and PME, or their regulators, appear to be present within blackberry germplasm. By selecting novel genotypes with low PG and PME activity, breeders may be able to improve blackberry shipping potential. However, the genetic framework underpinning the expression of these enzymes has not been as well-studied as in other species.

In strawberry, both PG and PME appear to play central roles in fruit softening. Antisense silencing of *FaPG1* increased the firmness of ripe fruit by 163% (Mercado et al., 2009). Xue et al. (2020) demonstrated the overexpression of either *FvPME38* or *FvPME39* produced significantly softer fruit, while RNAi-silencing of either of these genes produced significantly firmer fruit. Alternatively, the impact of PG and PME expression on tomato texture appears to be much less prominent. Schuch et al. (1991) reported no differences between fruit firmness of PG-silenced tomatoes and the wild-type control, and very little difference in softening was observed after silencing a PME gene, *Pmeu1* (Phan et al., 2007). In fact, there is a growing body of work in recent years that has demanded reevaluation of the traditional understanding of PME and its impact on fruit texture. In the presence of high calcium concentrations, the impact of PME on fruit texture appears to be reversed, promoting increased firmness through 'egg-box' calcium cross-linkages in de-esterified pectin molecules (Anthon et al., 2005; Sirijariyawat et al., 2012). Under these conditions, these cross-linkages may restrict access to the HG pectin backbone, preventing PG catalyzed degradation (Micheli, 2001). Transcriptomic investigations in apple have demonstrated that mealy texture is associated with lower levels of PME expression

(Segonne et al., 2014). In apricots, PME activity was reduced in a soft cultivar relative to a firm cultivar (Botondi et al., 2003). This trend differs from the findings reported in blackberry (Zhang et al., 2019), but a transcriptome-level validation for the expression trends of PME and PG has not yet been attempted in diverse blackberry genotypes.

Transcriptomic research in *Rubus* is less developed than in other rosaceous fruit crops like strawberry, but recent advances have provided a strong foundation for continued research. The *R. occidentalis* genome was the first annotated *Rubus* genome to be sequenced (VanBuren et al., 2016; VanBuren et al., 2018) followed by the *R. idaeus* genome (Davik et al., 2022). Even more recently, the *R. argutus* diploid blackberry genome was assembled and annotated (Brůna et al., 2022). At the time of writing, the *R. argutus* 'Hillquist' v1.0 genome is the reference genome that is most closely related to the cultivated blackberry and it is predicted to contain 81 PG homologs and 67 PME homologs (Brůna et al., 2022). Genome wide association of postharvest-related traits has drawn attention to potential quantitative trait loci (QTL) on or around these homologs in chromosomes Ra01, Ra02, and Ra06 (Chizk et al., 2023). In raspberry, multiple QTLs have also been identified on a linkage group collinear with Ra06 through a biparental linkage map of fruit firmness (Simpson et al., 2017). Several of these loci are located near dense clusters of texture related homologs, and sequencing of the fruit transcriptome may provide a better understanding of the relative importance of these genes.

The blackberry germplasm in the University of Arkansas (UA) System Division of Agriculture Fruit Breeding Program contains a diverse range of softening patterns, including a uniquely firm phenotype described as 'crispy' (Salgado & Clark, 2016). Despite efforts to introgress crispy texture into improved breeding selections, the phenotype has proven difficult to recover, and only a small number of crispy genotypes are present in UA germplasm today. These

crispy genotypes have displayed exceptional firmness and are resistant to red drupelet reversion (RDR) (Salgado & Clark, 2016). A better understanding of the crispy texture trait may inform future efforts to improve texture quality and shipping potential in fresh-market blackberries. In the present study, we examine expression-level evidence, enzyme activity, and fruit softening patterns throughout fruit maturation to characterize softening patterns in two texturally diverse blackberry genotypes. By comparing crispy-textured and soft-textured genotypes, we gain insight to the factors that may be responsible for the unique crispy phenotype.

Materials and Methods.

Plant Materials and Harvest. Two genotypes chosen to represent the range of textures present in UA blackberry breeding germplasm (soft = 'Black Gem^{TM}', crispy = A-2453T) were each harvested from 6 m plots at the UA Fruit Research Station (FRS) in Clarksville, AR in 2020. 'Black Gem^{TM}' is very soft textured during the shiny black stage of fruit development and is unsuitable for shipping. In contrast, A-2453T produces 'crispy' fruit at the black stage. The FRS site is located at 35º31'5"N and long. 93º24'12"W, in USDA hardiness zone 7b (USDA, 2021), on Linker fine sandy loam. Both plots were treated with standard production practices including an early spring application of ammonium nitrate (56 kg.ha^{-1} N) and a biweekly fertigation application of 20N-4.4P-17K from flowering to harvest. Liquid lime sulfur fungicide (94 L.ha^{-1}) was applied during bud break, five weeks before first harvest, and three weeks before first harvest to minimize anthracnose [*Elsinoë veneta* (Burkh.) Jenkins], botrytis fruit rot (*Botrytis cinerea* Pers.: Fr), and cane and leaf rust [*Kuehneola uredines* (Link) Arthur]. Multiple pesticides containing active ingredients zeta-cypermethrin, bifenthrin, and malathion were applied weekly from flowering until floricane harvest in June to control spotted wing drosophila (*Drosophila*

suzukii Matsumura) populations. A bifenthrin-containing insecticide was also applied annually in October to control raspberry crown borer (*Pennisetia marginata* Harris). All plants were trained to a four-wire, horizontal T-trellis with low and high wires 0.5 m and 1.0 m off the ground, respectively. Plants were tipped to 1.1 m height in mid-May and lateral branches were pruned in August. Plots were grown in black plastic mulch to reduce weed pressure. Fruit from single plots were harvested at three different growth stages: large green, full red, and full shiny black (ripe) (Perkins-Veazie et al., 2000). About 80 berries from each sample were immediately flash-frozen in liquid nitrogen and transported to the laboratory for storage at -80 °C.

Fruit Firmness. Following harvest, ten randomly selected berries per sample were assessed for firmness using a Stable Micro Systems TA.XT.Plus Texture Analyzer (Texture Technologies Corporation, Hamilton, MA). A fruit compression test was performed by placing individual berries horizontally on a flat surface using a cylindrical plane probe of 7.6 cm diameter at a rate of 2 $mm.s^{-1}$ with a trigger force of 0.02 N. The probe travelled 5 mm after first contact, and the peak force (N) was recorded as berry firmness.

RNA Extraction. RNA was extracted from berry tissue in triplicate using a method adapted from Poudel et al. (2013). Approximately 50 mg of berry tissue for each development stage, genotype, and individual berry were ground using a mortar and pestle in two sequential aliquots of RNA extraction buffer (2.42% Tris base, 1.27% LiCl, 1.50% lithium dodecylsulphate, 0.29% ethylenediaminetetra-acetic acid [EDTA], 1% sodium deoxycholate, 1% NP-40, and 1% w/v β-mercaptoethanol [vol/vol] added just before use) and collected in a 2 mL tube. Eight hundred and fifty microliters of supernatant were placed into a new 2 mL tube with 850 µL of potassium

acetate solution (3.8 M potassium and 5.8 M acetate). The tube containing crude RNA extract and potassium acetate mix were inverted several times and centrifuged at 15,000 × g for 10 min to pellet and remove cell debris. Supernatant was equally divided into two 2 mL tubes and vortexed with equal volumes of phenol:chloroform:IAA (25:24:1) to minimize interference from inhibitors (Vennapusa et al., 2020). Mixtures were centrifuged at 15,890 × g for seven minutes at 4 ℃. Supernatant was collected in new tubes and vortexed with an additional 200 µL of phenol:chloroform:IAA. Solutions were centrifuged again at 15,890 × g for seven minutes at 4 ℃. Supernatant was poured into new 1.5 mL tubes and mixed with 160 µL of 8 M LiCl and 60 µl of 3M CH_3COONa by inversion. Crude extracts were incubated overnight at -20 ℃ and centrifuged at 15,890 × g for seven minutes at 4 ℃. Supernatant was discarded and pellets were resuspended in 50 µL of autoclaved water. To each tube, 500 µL RNA wash buffer (10.0 mM Tris–HCl, pH 7.5, 0.5 mM EDTA, 50.0 mM NaCl, 50% ethanol) and 20 µL of silica milk glass preparation (66.7% Sigma S5631 silica particles [pH 2]) for nucleic acid binding. Each tube was vortexed for 10 to 15 seconds and pulse centrifuged to reach 10,000 × g. Supernatant was discarded and resuspended in 500 µL of wash buffer by vortex for 15 seconds. Extracts were centrifuged at 15,000 × g for 30 seconds to pellet the silica. The pellets were allowed to dry at room temperature (20 ℃) for 15 minutes and then resuspended in 150 µL of 0.01 M sodium citrate by incubation for five minutes at room temperature. Extracts were centrifuged once more at 15,000 × g for one minute to pellet any residual silica. One hundred microliters of the RNA extract were transferred from each tube into a single 1.5 mL tube and stored at -80 ℃.

RNA-Seq, Quality Filtering, Alignment, and Quantification. Library preparation and sequencing was conducted at RAPiD Genomics LLC (Gainesville, FL). RNA libraries were sequenced with

Illumina HiSeq to achieve an average of 33.5 million 150bp paired-end reads per sample. Paired-end Illumina adapter sequences were trimmed from fastq files using Trimmomatic (Bolger et al., 2014). Fastq formatted sequences were aligned to the 'Hillquist' v1.0 reference genome with HISAT2 (Zhang et al., 2021). Sequence alignment maps (SAMs) were sorted and compressed in SAMtools (Li et al., 2009). Binary alignment maps (BAMs) and the 'Hillquist' v1.0 general feature format file (gff) were used to assembled transcripts with StringTie (Pertea et al., 2015) in expression estimation mode. The Ballgown R package (Frazee et al., 2015) was used to quantify RNA expression levels and test for differential expression between genotypes and berry development stage. Genes with *Q-values* ≤ 0.05 and $|\log_2(\text{fold-change})| \geq 1$ were considered differentially expressed.

Crude PG Extraction and Activity Assay. PG was extracted once and assayed in triplicate following Buescher (1973). Ten grams of fruit were homogenized in a 30 mL 0.5 M NaCl solution containing 1% polyvinylpyrrolidone (PVP). Homogenate was centrifuged at 11,000 × g for 10 minutes at 4 ℃. The supernatant was decanted and adjusted to pH 5 with 0.1 N NaOH. Ten mL of crude PG extract were mixed with 20 mL of 1% pectin in citrate buffer at pH 5 and 30 ℃. The solution was rapidly stirred and poured into two separate viscometers (Cannon-Fenske Series 200, State College, PA) that were emerged in 30 ℃ water baths. Viscosity was determined at 0 and 20 minutes of reaction time. PG activity was estimated to be the change in viscosity over 20 minutes.

Crude PME Extraction and Activity Assay. PME was extracted following the same protocol used for PG extraction. Following the decanting step, 10 mL of extract was combined with 100 mL of

1% citrus pectin. The pH of the solution was adjusted to 7.5 with 0.2 N NaOH. The solution was titrated in a 30°C water bath for five minutes by maintaining a pH of 7.5 with 0.05 N NaOH. The volume of 0.05 N NaOH added at the end of the five-minute titration was recorded. PME activity was reported in microequivalents per gram of fresh fruit and calculated as follows.

$$PME = \frac{ml\ NaOH\ x\ N}{g\ extract\ x\ min}\ x\ 10^4$$

Results.

Fruit Firmness. The fruit of 'Black Gem™' was relatively firm at the green stage, with a mean firmness of 147.5 N (Figure 3.1). The green fruit of A-2453T were significantly softer than 'Black Gem™', having a firmness of only 95.9 N. No differences were detected between firmness of the two genotypes at the red stage of fruit maturity, and the mean firmness values ranged from 42.7-43.8 N. At the black stage of development, 'Black Gem™' became significantly softer than the crispy genotype, with a firmness of 5.5 N compared to 11.8 N in A-2453T.

Differential expression with RNA-Seq. Of the 18 replicated factorial combinations of genotypes and berry development stages, one green A-2453T sample and one red 'Black Gem™' sample failed during the sequencing step due to poor sample quality. Due to this imbalance and resulting loss of statistical power, almost no DEGs were detectable between factorial combinations of genotype and development stage. For this reason, genotypic effects were tested by pooling development stages, and development effects were tested by pooling genotypes. Nineteen DEGs with texture related annotations were identified between 'Black Gem™' and A-2453T (Table

3.1; Figure 3.2) including 10 β-glucosidases, two PMEs, two PGs, two pectin methylesterase inhibitors (PMEI), and three expansins. Expression of both PGs and both PMEs was higher in 'Black Gem™' than A-2453T. Of the two PG genes that were more highly expressed in 'Black Gem™', Ra_g19697 was expressed at higher levels in the red and green stages, while Ra_g27485 was expressed more highly in the black stage of fruit development (Figure 3.3; Figure3. 4). In 'Black Gem™', the PME genes Ra_g8929 and Ra_g23523 both had three-fold or greater expression than A-2453T in all stages. In contrast, expression of PMEI and expansin was higher in the crispy-textured breeding selection, A-2453T (Table 3.1; Figure 3.2). In A-2453T, the PMEI gene Ra_g888 on chromosome Ra01 was expressed at very high levels in the red and black stages (Figure 3.5) with mean fragments per kilobase of exon per million mapped fragments (FPKM) values exceeding 125 in the black stage of fruit development compared to and FPKM of 10 in 'Black Gem™'.

Many more texture related DEGs were observed between fruit development stages (Figure 3.4), with 52 DEGs between green and red stages, and 45 DEGs between red and black stages. The functions of these genes include ethylene signaling, pectin modification, pectin degradation, and enzyme inhibition. All three differentially expressed PMEs were incrementally downregulated throughout berry development. PGs, ethylene response factors, and β-glucosidases followed a similar trend of downregulation throughout berry development, although a small number were upregulated. Three pectin lyases (PL) were upregulated through berry development and only one was downregulated. Inhibitors of PG and PME were most frequently downregulated between green and red stages, but they were upregulated between red and black stages.

Enzyme Activity. Standard error values for PG activity (Δ viscosity) measurements were large, and differences between 'Black Gem™' and A-2453T were not apparent at $P < 0.05$ (Figure 3.3) , but mean values for 'Black Gem™' were consistently highest. Mean PG activity values for A-2453T were highest in the red development stage, but mean PG activity values for 'Black Gem™' were higher in the green and black stages. PME activity (microequivalents/g fresh fruit) at the green stage was higher in A-2453T than 'Black Gem™' ($P \leq 0.05$), but no significant genotypic differences were observed in the red and black stages. PME activity in A-2453T followed a nearly linear decrease in expression through fruit development (Figure 3.5).

Discussion.

The firmness observed in black stage fruit were generally consistent with expectations. The black fruit of A-2453T were about 50% firmer than that of 'Black Gem™'. Armour et al. (2021) observed firmness in A-2453T and 'Black Magic™', the soft-fruited female parent of 'Black Gem™', and found that A-2453T was up to 500% more firm than the soft-fruited genotype. This difference may partially be explained by the alternate soft-fruited genotype, but in 2018, Armour et al. (2021) observed that the mean firmness of A-2453T was about 3 N firmer than reported in the present study. More interestingly, the large gap in firmness observed by Armour et al. (2021) could also be the effect of softening patterns and enzyme activity that occurred over the seven days of storage they allowed before recording firmness. In contrast, we observed firmness immediately after harvest, preventing softening that might have occurred during storage.

The patterns of PME activity observed between 'Black Gem™' and A-2453T suggest that pectin modification by PME in blackberry may be more nuanced than previously thought. Unlike Zhang et al. (2019), who observed gradual increases in PME activity through fruit development for the soft-fruited 'Boysen', we found lower levels of PME activity in the green

stage in the soft-fruited 'Black Gem^{TM}' and no differences in PME activity between soft- and crispy-textured genotypes at the black stage (Figure 3.5). Zhang et al. (2019) also observed that the firmer-fruited 'Arapaho' maintained consistent levels of PME activity, but instead our crispy-fruited selection, A-2453T, gradually declined in PME activity. Neither of the genotypes compared by Zhang et al. (2019) had crispy texture, which may account somewhat for these discrepancies. Zhang et al. (2019) also observed a sharp increase in PG activity in the black stage of berry development, which we did not observe for either genotype (Figure 3.3). This may be the result of differing methods used in the PG activity assay.

In the RNA-Seq analysis, two PMEs (Ra_g8929 and Ra_g23523) were more highly expressed in soft-fruited 'Black Gem^{TM}', but these higher expression levels did not correspond with a proportional increase in PME activity in the enzymatic assay. In the crispy-fruited A-2453T, PME activity appeared to be inversely associated with expression of two inhibitors of PME (Table 3.3; Ra_g888 and Ra_g8326). The most highly expressed PMEI, Ra_g888, was on chromosome Ra01 (Table 3.1), less than 7 kb from a SNP significantly associated with fruit firmness in a GWAS analysis of 300 fresh-market blackberry genotypes (Table 2.2), which could indicate an important role for PMEIs in the regulation of pectin modification across more diverse populations of tetraploid blackberry. Ra_g888 closely resembles an important PMEI in tomato (Reca, 2012) and in A-2453T it expressed a fold-change of 10 over 'Black Gem^{TM}' overall and a fold-change of about 15 in the black stage. Indeed, the inhibition of PME activity in the green stage of fruit development may regulate softening patterns by preventing the formation of 'eggbox' calcium cross-linkages. This 'eggbox' phenomenon has been well-reported in apple and fig (Botondi et al., 2003; Segonne et al., 2014) and could be an important factor in the crispy blackberry phenotype. Future studies could attempt to investigate the role of these cross-linkages

in blackberry by observing the effects of Ca^{2+} abundance on crispy and non-crispy genotypes. Unlike A-2453T, the PME activity soft-fruited 'Black Gem™' seems to correspond with both lower expression of PMEIs and greater expression of the two PMEs on chromosomes Ra02 and Ra05 (Figure 3.5). Diversity in both PME and PMEI expression appear to be present in blackberry germplasm, but inhibition of pectin modification by PME may be an important factor associated with crispy fruit texture. Silencing of the PMEI on Ra01 (Ra_g888) may provide additional insight into this hypothesis. However, based on our work and results of GWAS for fruit firmness in a large panel of diverse fresh-market blackberries (Chizk et al., 2023), it is likely that texture quality in *Rubus* is a highly multigenic and complex trait.

Both PG activity and gene expression analyses provide evidence supporting its role as an important fruit softening enzyme in blackberry. The soft-fruited 'Black Gem™' expressed two PGs (Ra_g19687 and Ra_g27485) more highly than the crispy-fruited A-2453T. Considering the pooled expression of these two genes, 'Black Gem™' expressed PG at levels 300% greater than A-2453T in each stage of berry development (Figure 3.3), although differences in PG activity were only apparent at the green stage according to the viscosity-based enzyme assay. 'Black Gem™' softened at a much faster rate than A-2453T throughout berry development (Figure 3.1), but based on our observations this does not appear to be driven by a detectable increase in PG activity (Figure 3.3). The failure to detect differences in PG activity at the red and black stages appears inconsistent with observed fruit softening patterns, in which 'Black Gem™' rapidly softened throughout berry development. This could be the result of poor sensitivity and high standard error in the viscosity assay used. Initial viscosity of all reaction mixtures was very low (viscosity ≤ 1.9), and the manual timing method used may have resulted in low precision of viscosity measurements.

Of the two PGs identified by differential expression analysis, Ra_g27485 appears to be an especially promising candidate with proximity to fruit firmness QTLs identified in two previous *Rubus* experiments. In a previously reported genome wide association of fruit firmness in 300 blackberry genotypes, we identified a significant marker-trait association located about 25 kb upstream from the start codon of Ra_g27485 on chromosome Ra06 (Table 2.2). In that GWAS panel, the Ra06 QTL explained 11.5% of observed variance in fruit texture. Additionally, a QTL for fruit firmness was identified on a homologous chromosome in a biparental red raspberry population (Simpson et al., 2017). Thus, the importance of Ra_g27485 as a source of diversity for fruit texture may extend to an even wider range of *Rubus* species. Antisense silencing of this gene in soft-fruited genotypes, such as 'Black Gem^{TM}', may provide further insight into its contribution to blackberry fruit softening. Similar silencing of a PG in strawberry resulted in a 163% increase in firmness compared to the wild type (Mercado et al., 2009).

In addition to PG and PME, several expansins and β-glucosidases were expressed differentially between 'Black Gem^{TM}' and A-2453T (Figure 3.2). These genes are less frequently discussed in fruit softening literature, but a trend between the two blackberry genotypes observed seems apparent. Expansins were more highly expressed in the crispy genotype, while β-glucosidases were more highly expressed in the soft genotype. The higher expression of β-glucosidases in soft-fruited blackberries is consistent with the hypothetical role of this enzyme in degradation of pectin sidechains (Gerardi et al., 2001). It is likely that β-glucosidases act synergistically with other cell wall degrading enzymes such as PG and PL to attack specific regions of the macromolecule. On the other hand, higher expression level of three expansins in A-2453T was somewhat unexpected, since these proteins are thought to loosen the cell wall by

facilitating pH-dependent extension (Cosgrove, 2015), and transgenic overexpression of expansin in tomato has accelerated fruit softening (Chen et al., 2022). The specific interactions formed between expansin proteins and cell wall components are not well understood in plant species and it is possible that these proteins could behave in unexpected ways. The differentially expressed expansin, Ra_g7012, on chromosome Ra02 was also previously identified as a potential candidate gene for red drupelet reversion (RDR), a postharvest disorder often associated with soft fruit texture (Table 2.2). No differentially expressed ethylene response factors, PLs, cellulases, or PG inhibitors were found among the two blackberry genotypes in this study. Transcriptomic investigation of more diverse germplasm should be conducted for validation, but based on our work, these classes of enzymes seem to be less important sources of diversity in blackberry softening patterns.

We hypothesize that texturally diverse blackberry genotypes regulate modification of cell wall pectin at key stages of berry development, mediated by differential expression of both PMEs and PMEIs. Based on the timing of pectin de-esterification, pectin may form ‘eggbox’ structures that promote crisp texture, or alternatively, pectin may be exposed to degradation by fruit-softening PGs. Diverse blackberry genotypes may also express varying levels of both PG and β-glucosidase, mediating the rate of pectin degradation directly. The role of expansin in blackberry softening is less clear, but its expression could be associated with crispy texture. Future studies should investigate the effects of gene silencing of key DEGs on fruit softening to validate their role in blackberry.

Conclusion.

The soft texture of mature 'Black Gem™' fruits was associated with increased expression of two PGs, two PMEs, and seven β-glucosidases. The PG, Ra_g27485, appears to be of particular importance as it is located in a QTL region previously associated with fruit texture in a blackberry GWAS panel and is most highly expressed during the critical black stage of fruit development in the soft-fruited 'Black Gem™'. The PMEI gene, Ra_g888, appears to be an important mediator of PME activity in the red and black stage of development for A-2453T and may be associated with crispy texture. Three expansin genes were also expressed at unexpectedly high levels in the crispy A-2453T genotype, suggesting a potentially unique role for these proteins in blackberry softening. Future work should investigate the relative contributions of these transcripts to fruit softening through gene silencing, especially as they relate to crispy textured phenotypes.

References Cited.

Anthon GE, Blot L, Barrett DM. 2005. Improved firmness in calcified diced tomatoes by temperature activation of mectin methylesterase. Journal of Food Science. 70(5):C342–C347. https://doi.org/10.1111/j.1365-2621.2005.tb09964.x

Armour M, Worthington M, Clark JR. 2021. Effect of harvest time and fruit firmness on red drupelet reversion in blackberry. HortScience. 56(8):889-896.

Bolger AM, Lohse M, Usadel B. 2014. Trimmomatic: A flexible trimmer for Illumina sequence data. Bioinformatics. 30(15):2114–2120. https://doi.org/10.1093/bioinformatics/btu170

Botondi R, DeSantis D, Bellincontro A, Vizovitis K, Mencarelli F. 2003. Influence of ethylene inhibition by 1-methylcyclopropene on apricot quality, volatile production, and glycosidase activity of low- and high-aroma varieties of apricots. Journal of Agricultural and Food Chemistry. 51(5):1189–1200. https://doi.org/10.1021/jf025893o

Brůna T, Aryal R, Dudchenko O, Sargent DJ, Mead D, Buti M, Cavallini A, Hytönen T, Andrés J, Pham M, Weisz D, Mascagni F, Usai G, Natali L, Bassil N, Fernandez GE, Lomsadze A, Armour M, Olukolu B, Poorten T, Britton C, Davik J, Ashrafi H, Aiden E, Borodovsky S, Worthington, M. 2022. A chromosome-length genome assembly and annotation of blackberry (*Rubus argutus*, cv. 'Hillquist'). G3 Genes|Genomes|Genetics. 13(2):1-14. https://doi.org/10.1093/g3journal/jkac289

Buescher RW. 1973. Physiological and biochemical alterations in tomato fruit induced by chilling temperatures (PhD Diss). Purdue University. West Lafayette, Indiana, USA.

Chen Y, Xie B, An X, Ma R, Zhao D, Cheng C, Li E, Zhou J, Kang G, Zhang Y. 2022. Overexpression of the apple expansin-like gene MdEXLB1 accelerates the softening of fruit texture in tomato. Journal of Integrative Agriculture. 21(12):3578-3588. https://doi.org/10.1016/j.jia.2022.08.030

Cosgrove DJ. 2015. Plant expansins: diversity and interactions with plant cell walls. Current Opinion in Plant Biology. 25:162–172. Elsevier Ltd. https://doi.org/10.1016/j.pbi.2015.05.014

Devries J, Denuijl C, Voragen A, Rombouts F, Pilnik W. 1983. Structural features of the neutral sugar side chains of apple pectic substances. Carbohydrate Polymers. 3(3):193–205. https://doi.org/10.1016/0144-8617(83)90018-8

Frazee AC, Pertea G, Jaffe AE, Langmead B, Salzberg SL, Leek JT. 2015. Ballgown bridges the gap between transcriptome assembly and expression analysis. Nature Biotechnology 33(3):243–246. https://doi.org/10.1038/nbt.3172

Gerardi C, Blando F, Santino A, Zacheo G. 2001. Purification and characterisation of a β-glucosidase abundantly expressed in ripe sweet cherry (*Prunus avium* L.) fruit. Plant Science. 160(5):795–805. https://doi.org/10.1016/S0168-9452(00)00423-4

Jolie RP, Duvetter T, Houben K, Clynen E, Sila DN, Van Loey AM, Hendrickx ME. 2009. Carrot pectin methylesterase and its inhibitor from kiwi fruit: study of activity, stabililty, and inhibition. Innovative Food Science & Emerging Technologies. 10(4):601-609.

Li H, Handsaker B, Wysoker A, Fennell T, Ruan J, Homer N, Marth G, Abecasis G, Durbin R. 2009. The Sequence Alignment/Map format and SAMtools. Bioinformatics, 25(16):2078–2079. https://doi.org/10.1093/bioinformatics/btp352

Mercado JA, Quesada MA, Blanco-Portales R, Pose S, García-Gago JA, Jiménez-Bermúdez S, Muñoz-Serrano A, Caballero JL, Pliego-Alfaro F, Muñoz-Blanco J. 2009. Antisense down-regulation of the *FaPG1* gene reveals an unexpected central role for polygalacturonase in strawberry fruit softening. Plant Physiology. 150(2):1022–1032. https://doi.org/10.1104/pp.109.138297

Micheli F. 2001. Pectin methylesterases: cell wall enzymes with important roles in plant physiology. Trends in Plant Science, 6(9):414–419. https://doi.org/10.1016/S1360-1385(01)02045-3

Perkins-Veazie P. 2017. Postharvest storage and transport of blackberries. p. 266-282. In. Blackberries and their hybrids. Wallingford UK: CABI.

Perkins-Veazie P, Clark JR, Huber DJ, Baldwin EA. 2000. Ripening physiology in 'Navaho' thornless blackberries: color, respiration, ethylene production, softening, and compositional changes. J of the American Soc for Hortic. 125(3):357-363.

Perkins-Veazie P, Collins J, Clark J. 1996. Cultivar and maturity affect postharvest quality of fruit from erect blackberries. HortScience. 31(2):258-261.

Pertea M, Pertea GM, Antonescu CM, Chang TC, Mendell JT, Salzberg SL. 2015. StringTie enables improved reconstruction of a transcriptome from RNA-seq reads. Nature Biotechnology. 33(3):290–295. https://doi.org/10.1038/nbt.3122

Phan TD, Bo W, West G, Lycett GW, Tucker GA. 2007. Silencing of the major salt-dependent isoform of pectinesterase in tomato alters fruit softening. Plant Physiology. 144(4):1960–1967. https://doi.org/10.1104/pp.107.096347

Poudel B, Wintermantel WM, Cortez AA, Ho T, Khadgi A, Tzanetakis IE. 2013. Epidemiology of blackberry yellow vein associated virus. Plant Disease. 97(10):1352–1357. https://doi.org/10.1094/PDIS-01-13-0018-RE

Reca IB, Lionetti V, Camardella L, D'Avino R, Giardina T, Cervone F, Bellincampi D. 2012. A functional pectin methylesterase inhibitor (SolyPMEI) is expressed during tomato fruit ripening and interacts with PME-1. Plant Molecular Biology. 79:429-442.

Salgado AA, Clark JR. 2016. "'Crispy'" blackberry genotypes: a breeding innovation of the University of Arkansas blackberry breeding program. HortScience. 51(5):468-471.

Schuch W, Kanczler J, Robertson D, Hobson G, Tucker G, Grierson D, Bright S, Bird C. 1991. Fruit quality characteristics of transgenic tomato fruit with altered polygalacturonase activity. HortScience. 26(12):1517–1520. https://doi.org/10.21273/HORTSCI.26.12.1517

Segantini D, Threlfall R, Clark J, Brownmiller C, Howard L, Lawless L. 2017. Changes in fresh-market and sensory attributes of blackberry genotypes after postharvest storage. J Berry Research. 7(2):129-145.

Segonne SM, Bruneau M, Celton JM, le Gall S, Francin-Allami M, Juchaux M, Laurens F, Orsel M, Renou JP. 2014. Multiscale investigation of mealiness in apple: an atypical role for a pectin methylesterase during fruit maturation. BMC Plant Biology. 14(1):375. https://doi.org/10.1186/s12870-014-0375-3

Simpson CG, Cullen DW, Hackett CA, Smith K, Hallett PD, McNicol J, Woodhead M, Graham J. 2017. Mapping and expression of genes associated with raspberry fruit ripening and softening. Theoretical and Applied Genetics. 130(3):557–572. https://doi.org/10.1007/s00122-016-2835-7

Sirijariyawat A, Charoenrein S, Barrett DM. 2012. Texture improvement of fresh and frozen mangoes with pectin methylesterase and calcium infusion. Journal of the Science of Food and Agriculture. 92(13):2581–2586. https://doi.org/10.1002/jsfa.5791

USDA-ARS. 2021. USDA plant hardiness zone map. https://planthardiness.ars.usda.gov/. [accessed 15 Feb 2023].

USDA-ERS. 2023. Fruit and tree nuts data. https://data.ers.usda.gov/reports.aspx?programArea=fruit&top=5&HardCopy=True&RowsPerPage=25&groupName=Noncitrus&commodityName=Blackberries&ID=17851. [accessed 15 Feb 2023]

VanBuren R, Bryant D, Bushakra JM, Vining KJ, Edger PP, Rowley ER, Priest HD, Michael TP, Lyons E, Filichkin SA, Dossett M, Finn CE, Bassil N, Mockler TC. 2016. The genome of black raspberry (*Rubus occidentalis*). The Plant Journal. 87(6):535–547. https://doi.org/10.1111/tpj.13215

VanBuren R, Wai CM, Colle M, Wang J, Sullivan Shawn, Bushakra JM, Liachko I, Vining KJ, Dossett M, Finn CE, Jibran R, Chagne D, Childs K, Edger PP, Mockler TC, Bassil NV. 2018. A near complete, chromosome-scale assembly of the black raspberry (*Rubus occidentalis*) genome. Gigascience. 7(8):1–9. https://doi.org/10.1093/gigascience/giy094

Vennapusa AR, Somayanda IM, Doherty CJ, Jagadish SVK. 2020. A universal method for high-quality RNA extraction from plant tissues rich in starch, proteins and fiber. Scientific Reports. 10(1):1-13. https://doi.org/10.1038/s41598-020-73958-5

Wang D, Yeats TH, Uluisik S, Rose JKC, Seymour GB. 2018. Fruit softening: revisiting the role of pectin. Trends in Plant Science. 23(4):302–310. https://doi.org/10.1016/j.tplants.2018.01.006

Xue C, Guan SC, Chen JQ, Wen CJ, Cai JF, Chen X. 2020. Genome wide identification and functional characterization of strawberry pectin methylesterases related to fruit softening. BMC Plant Biology. 20(1):13. https://doi.org/10.1186/s12870-019-2225-9

Zhang C, Xiong Z, Yang H, Wu W. 2019. Changes in pericarp morphology, physiology, and cell wall composition account for flesh firmness during the ripening of blackberry (*Rubus* spp.) fruit. Scientia Horticulturae. 250:59–68. https://doi.org/10.1016/j.scienta.2019.02.015

Zhang Y, Park C, Bennett C, Thornton M, Kim D. 2021. Rapid and accurate alignment of nucleotide conversion sequencing reads with HISAT-3N. Genome Research. 31(7):1290–1295. https://doi.org/10.1101/gr.275193.120

Tables and Figures

Table 3.1. Fruit texture related DEGs[i] across all stages of fruit development between soft-fruited 'Black Gem™' and crispy-fruited A-2453T.

Gene	Fold change[ii]	*Q-value*	Chromosome	Start position	End position	Orientation	Functional prediction[iii]
Ra_g888	0.15	0.030	Ra01	4344303	4346316	-	Probable pectinesterase/pectinesterase inhibitor 12; AT2G26440.1
Ra_g4207	0.22	<0.001	Ra01	30677175	30679926	-	Beta-glucosidase BoGH3B; AT5G20950.3
Ra_g7012	0.04	0.002	Ra02	24484112	24485569	+	Expansin-like A1; AT3G45970.1
Ra_g8326	0.37	0.026	Ra02	31637403	31639325	-	Probable pectinesterase/pectinesterase inhibitor 7; AT1G02810.1
Ra_g8929	2.07	0.016	Ra02	34910046	34912339	-	Probable pectin methylesterase CGR3; AT5G65810.1
Ra_g9454	0.05	0.021	Ra02	37476510	37477458	+	Expansin-A11; AT1G20190.1
Ra_g12497	2.43	<0.001	Ra03	17643760	17657930	+	Beta-glucosidase 11; AT1G02850.2
Ra_g13397	3.24	0.014	Ra03	27835177	27836821	+	Glucan endo-1,3-beta-glucosidase; AT4G16260.1
Ra_g13398	7.18	0.043	Ra03	27843063	27844693	+	Glucan endo-1,3-beta-glucosidase; AT4G16260.1
Ra_g13400	2.51	<0.001	Ra03	27858367	27868137	+	Glucan endo-1,3-beta-glucosidase; AT4G16260.1
Ra_g19697	2.10	0.038	Ra04	34580547	34584307	+	Polygalacturonase; AT1G48100.1
Ra_g23523	3.93	<0.001	Ra05	26316537	26318858	+	Probable pectin methylesterase CGR2; AT3G49720.3
Ra_g27224	4.74	<0.001	Ra06	14390847	14394620	+	Beta-glucosidase 13; AT5G44640.1
Ra_g27485	2.53	0.025	Ra06	17298261	17304692	+	Polygalacturonase; AT3G57510.1
Ra_g27744	0.22	<0.001	Ra06	20008828	20010242	-	Glucan endo-1,3-beta-glucosidase; AT1G75800.1
Ra_g31086	3.25	0.032	Ra07	246435	249951	+	Beta-glucosidase; AT2G44480.4
Ra_g33184	0.25	0.001	Ra07	19507248	19507897	-	Beta-glucosidase BoGH3B-like; AT5G04885.2

[i]Differentially expressed genes with *Q-values* ≤ 0.05 and $|\log_2(\text{fold change})| \geq 1$.
[ii]Fold changes > 1 indicates greater expression in 'Black Gem™' and fold changes < 1 indicates greater expression in A-2453T
[iii]The SwissProt and Araport11 databases were interrogated for descriptions of gene homologs and *Arabidopsis* homolog identifiers following Brůna et al. (2022)

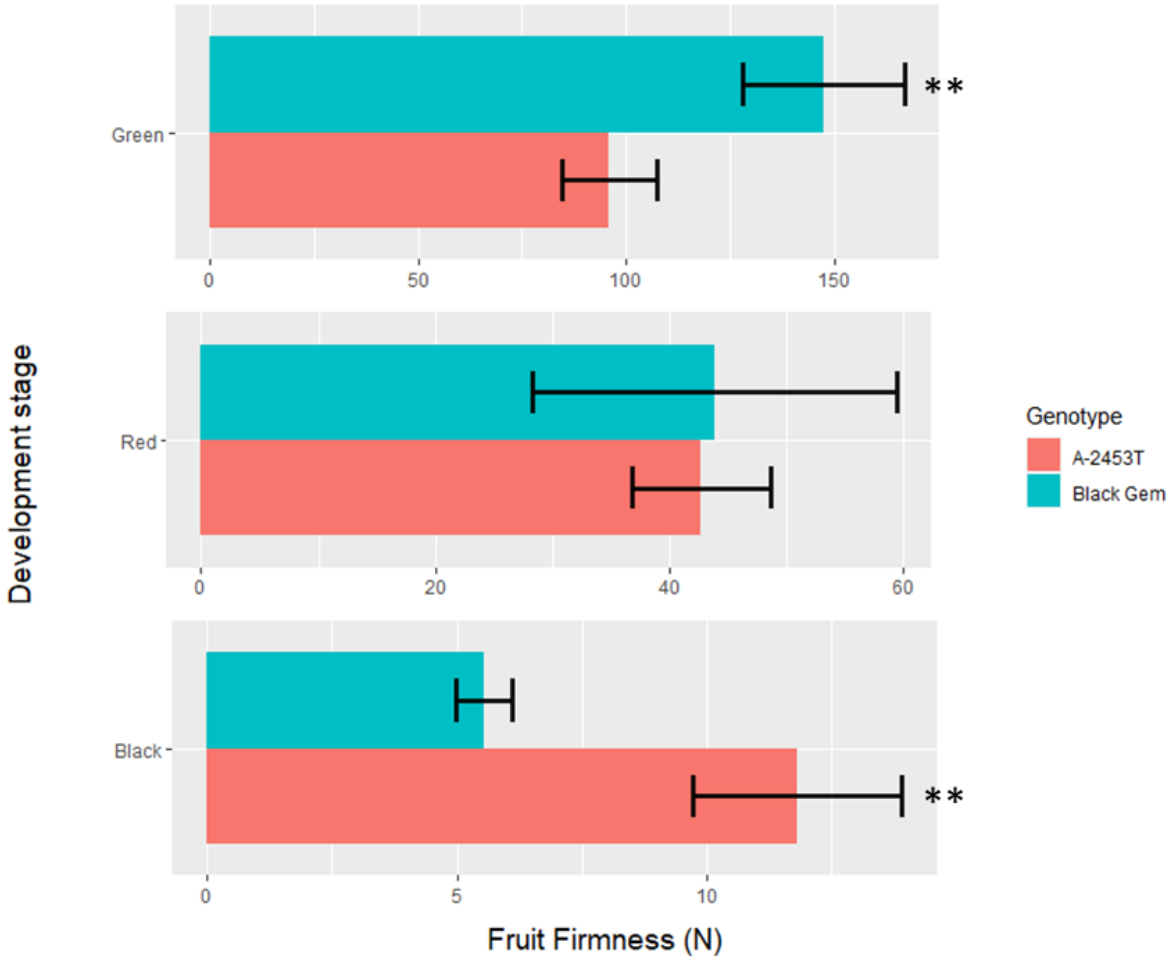

Figure 3.1. Fruit firmness of A-2453T and 'Black Gem^{TM}' at each stage of berry development. Error bars indicate a 90% confidence interval. Double asterisks indicate significant differences between genotypes at $P \leq 0.01$.

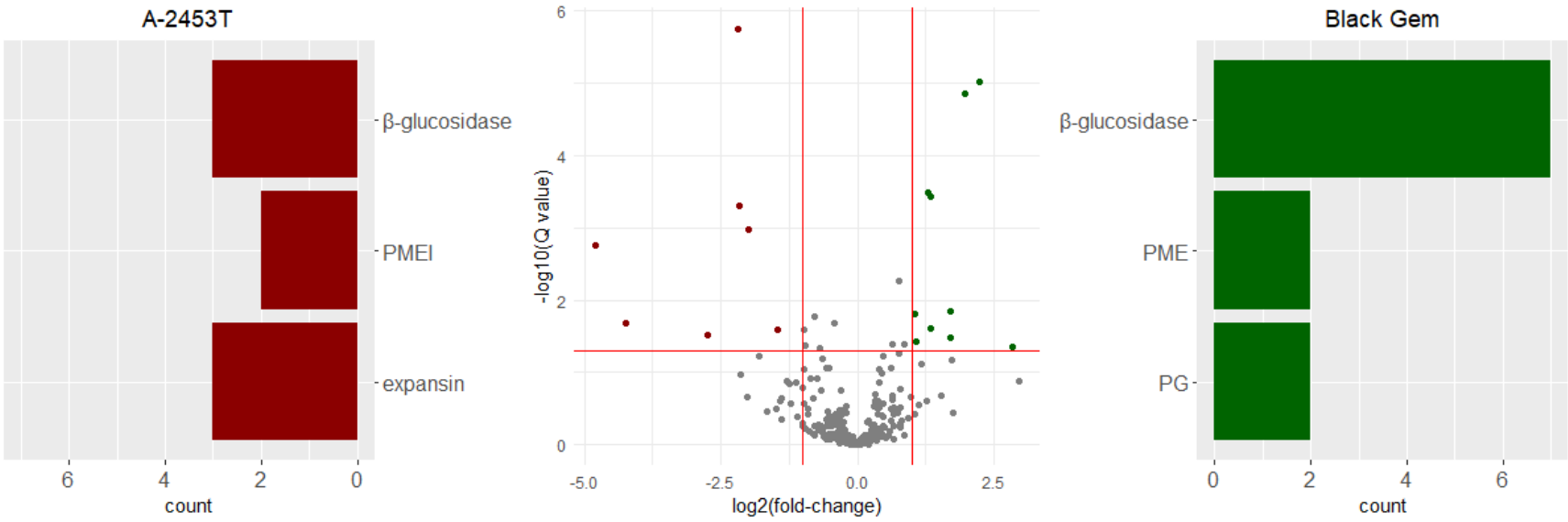

Figure 3.2. Differentially expressed genes (DEGs) with functional annotations related to fruit texture across all fruit development stages for crispy-fruited A-2453T (left) and soft-fruited 'Black Gem™' (right) and volcano plot (middle) of transcript fold changes against *Q-values*. Histogram bins of DEGs are based on functional predictions of annotated genes in the *R. argutus* reference genome. Counts represent transcripts that are more highly expressed in the respective genotype. Threshold values for DEG fold change and *Q-values* (red lines) are -log10(0.05) and ±log2(1) respectively. PG = polygalacturonase, PME = pectin methylesterase, PMEI = pectin methylesterase inhibitor.

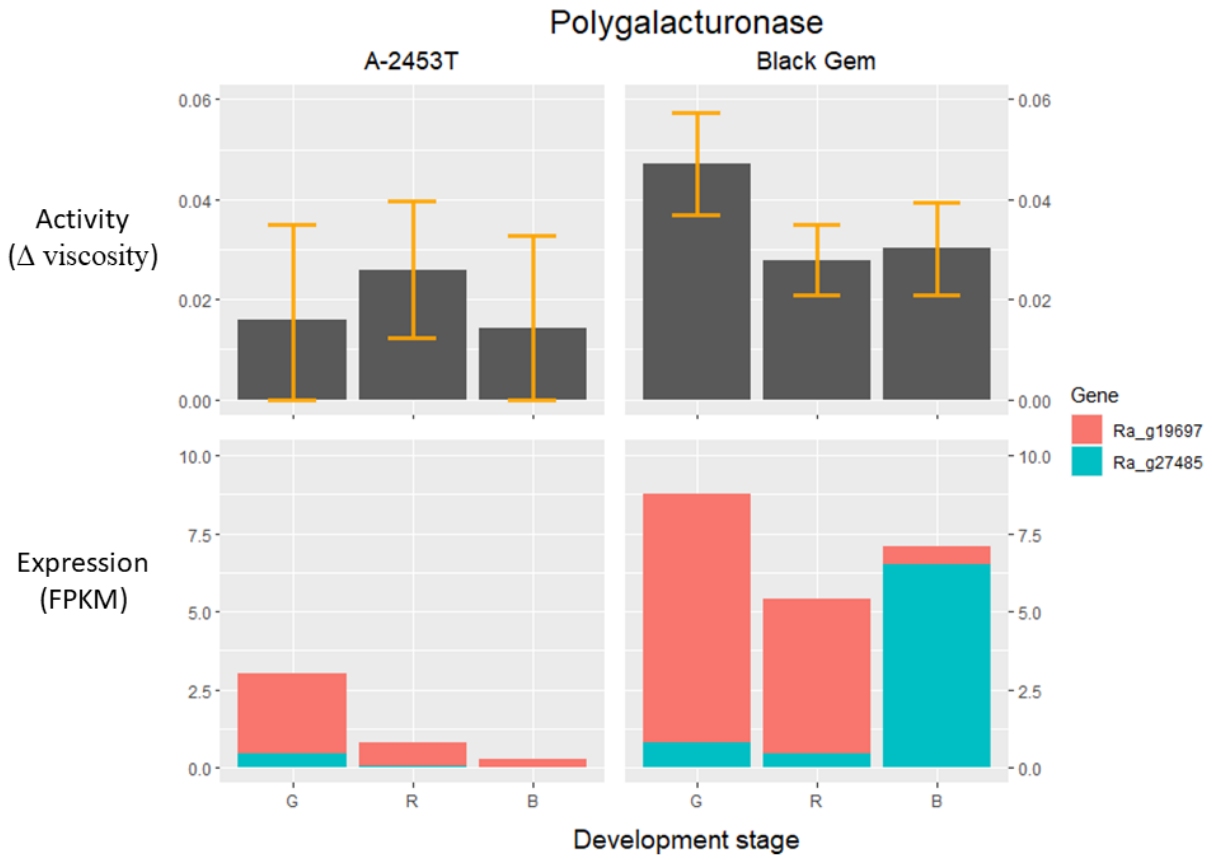

Figure 3.3. Polygalacturonase (PG) activity across each berry development stage of A-2453T (left) and 'Black Gem™' (right) observed through viscosity change (top row; 90% confidence interval) compared with differential expression levels of two PG transcripts, Ra_g19697 and Ra_g27485 (bottom row).

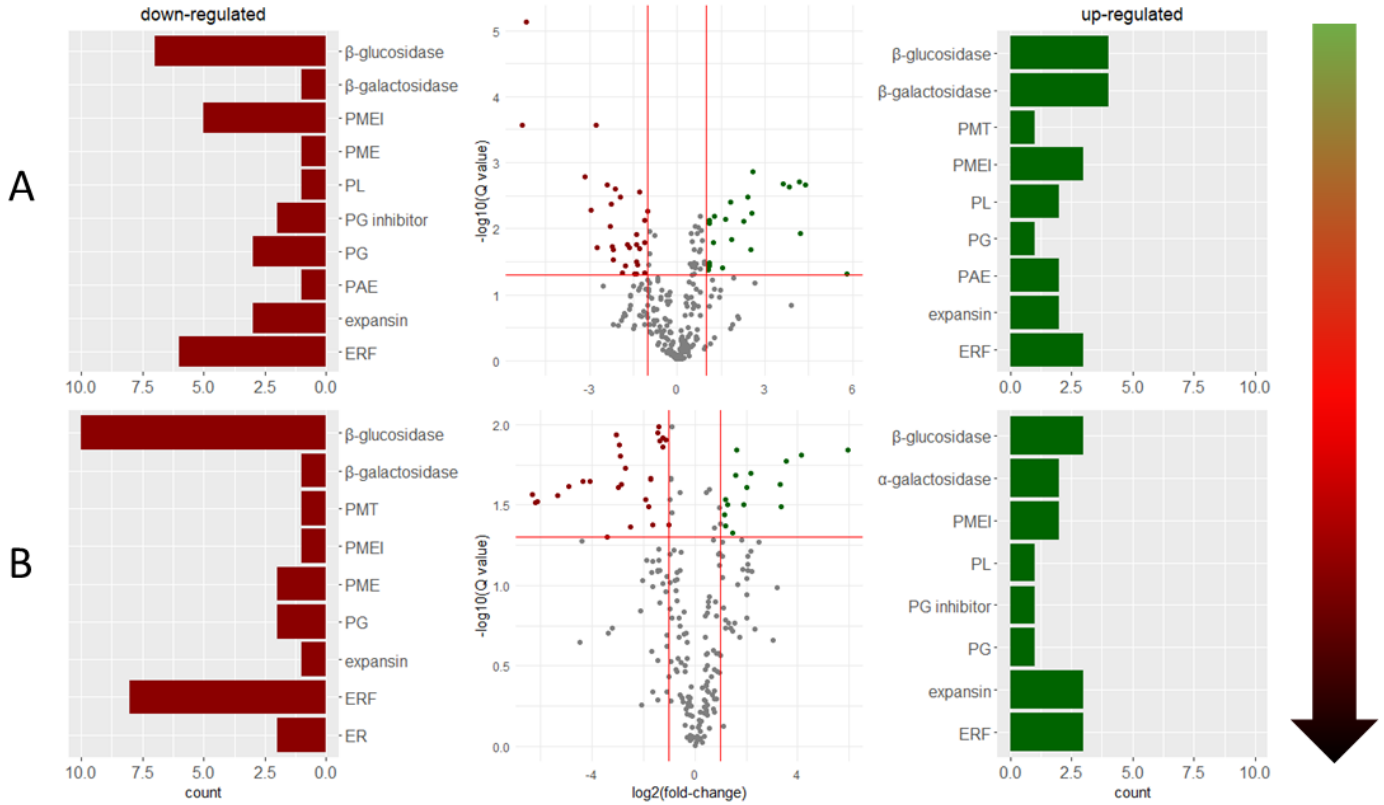

Figure 3.4. A. Genes up-regulated (right) or down-regulated (left) from green to red stage across both A-2453T and 'Black Gem' and volcano plot (middle) of transcript fold changes plotted against *Q-values*. B. Genes upregulated (right) or downregulated (left) from red to black stage across both A-2453T and 'Black Gem™' and volcano plot (middle) of transcript fold changes plotted against *Q-values*. Histogram bins of differentially expressed genes are based on functional predictions of annotated genes in the *R. argutus* reference genome. Threshold values for DEG fold change and *Q-values* (red lines) are -log10(0.05) and ±log2(1) respectively. ER = ethylene receptor, ERF = ethylene response factor, PAE = pectin acetylesterase, PG = polygalacturonase, PL = pectin lyase, PME = pectin methylesterase, PMEI = pectin methylesterase inhibitor, PMT = pectin

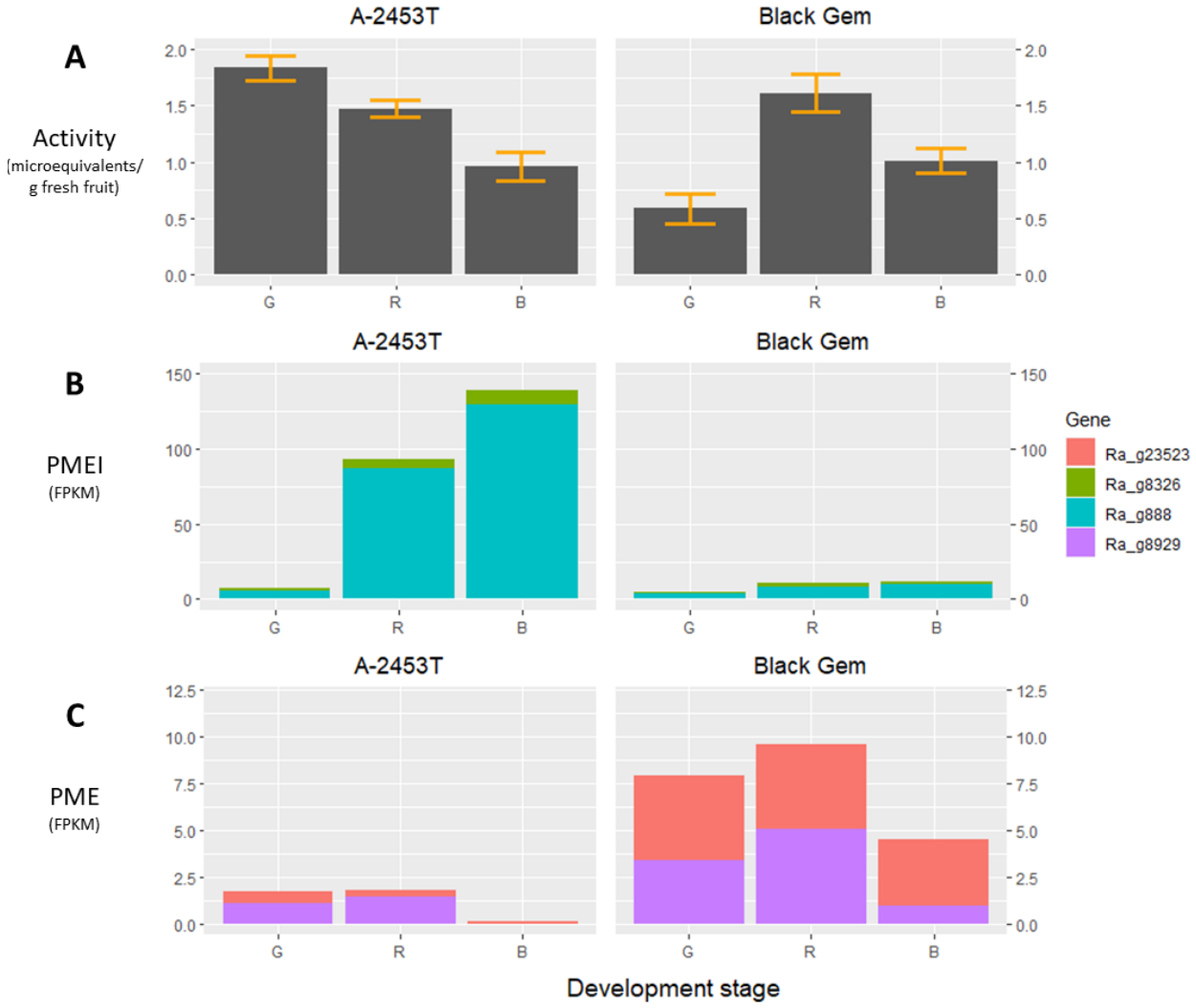

Figure 3.5. (A) Pectin methylesterase (PME) activity across each berry development stage of A-2453T (left) and 'Black Gem™' (right) observed through manual titration (90% confidence interval) compared with differential expression levels of (B) two pectin methylesterase inhibitor (PMEI) transcripts, Ra_g888 and Ra_g8326, and (C) two PME transcripts, Ra_g8929 and Ra_g23523.

CHAPTER IV

INSTRUMENTAL AND SENSORY METHODS FOR TEXTURE EVALUATION IN MUSCADINE GRAPES

Abstract

Muscadine grapes (*Vitis rotundifolia*) are enjoyed as a specialty crop in the southeast United States, but consumer acceptance is hindered by their tough skins and soft gummy flesh. Improved textural quality of muscadine grapes has been a major objective of breeding programs for many years and may contribute to market expansion. Multiple methods have been developed to measure textural quality in muscadine, including descriptive sensory panels, instrumental texture analysis, and breeders' field ratings, but few studies have examined the relationships between these methods and many more methods remain untested. The primary objective of the present study is to build a recommended phenotyping method for selection of improved texture quality in muscadine breeding programs. Texture data from six instrumental analysis protocols were correlated with ten descriptive sensory panel characteristics and three breeders' field ratings across seven texturally diverse muscadine genotypes and one table grape. By combining data collected using breeders' field ratings, a 2 mm cylinder probe, and a Kramer shear cell (KSC), regression models were constructed to predict awareness of skins, crispness, hardness, and visual separation explaining 85%, 91%, 82%, and 83% of variance respectively. Breeders' scores for overall texture quality were most strongly correlated with visual separation in 2019 (r = -0.83) and 2020 (r = -0.89). Genotypes that scored most highly in breeders' ratings of overall texture had soft skins and firm flesh, suggesting that both qualities are important targets for texture improvement in muscadine.

Introduction

Muscadine grapes (*Vitis rotundifolia*) are native to the southern United States and are the only commercially produced species in the subgenus *Muscadinia*. Muscadines are often used for wine and juice production, but they are also sold as fresh market table grapes. They possess a strong following in their native region and are a well-adapted, disease resistant option for fruit producers in the humid, temperate region of the southeastern United States. Muscadines are notable for their unique flavor and challenging texture profile. Most muscadine cultivars have a thick, leathery exocarp that slips easily (commonly referred to as 'slipskin') from a gummy, mucilaginous mesocarp (Conner 2013; Olien 1990). This texture starkly contrasts with the thin, tender exocarp and meaty mesocarp that is observed among preferred table-type *Vitis vinifera* cultivars (Sato et al. 1997). Consumer panelists have indicated that the overall liking of a muscadine cultivar is heavily influenced by both skin thickness and pulp texture, and that even panelists familiar with muscadines prefer thinner skins (Brown et al. 2016). Substantial variation in texture has been reported among muscadine germplasm, with flesh textures ranging from soft and melting to tough and stringy (Conner and Worthington 2023). Moreover, variation in muscadine texture may be associated with postharvest quality and storability. Barchenger et al. (2015) observed that the force required to penetrate the skin of a muscadine reduced over time in cold storage, but that the rate of this reduction varied significantly between genotypes. Conner (2012) reported similar findings, noting that 'Supreme' maintained exceptional firmness in storage compared to other genotypes.

Despite evidence that muscadine fruit texture influences both storability and consumer acceptance, little is known about relationships between human-perceived texture qualities and objective measurements of texture-related attributes through lab instrumentation. Food texture is

defined as “all the mechanical, geometrical, surface and body attributes of a product perceptible by means of kinesthetic and somesthetic receptors, and (where appropriate) visual and auditory receptors from first bite to final swallowing” (ISO 5492:2008). Human perception of food texture is implicit in the definition itself. Thus, investigators of grape and muscadine texture have often relied on randomly sampled consumer panels (Brown et al. 2016) or trained and standardized descriptive sensory panels (Cliff and Bejaei 2018; Felts et al. 2018) to gather texture data from human panelists. Felts et al. (2018) established a standard lexicon of terms for descriptive sensory analysis of muscadine texture, flavor, and appearance. Of the nine texture-related characteristics included in the lexicon, panelists were only able to differentiate genotypes based on visual separation of skins. Both consumer panels and trained sensory panels are costly and difficult to scale for routine screening of breeding materials. Instead, breeders often assess texture quality using ad hoc numeric rating scales. Specific implementations of breeders’ field ratings may vary, but all are subjective and presumably influenced by fatigue when large numbers of genotypes are observed over short periods of time.

Many breeders have determined that laboratory instruments like the Stable Micro Systems TA.XT Texture Analyzer (Texture Technologies Corporation, Hamilton, MA) are an effective alternative or complement to panel-based texture analyses and breeders’ field ratings (Conner 2013; Rolle et al. 2012). *V. vinifera* researchers have already tested and reported uses for a range of probes with diverse shapes and functions (Rolle et al. 2012). For instance, flat, cylindrical compression probes have been used to estimate traits like hardness, cohesiveness, springiness, and chewiness (Cefola et al. 2011; Martinez-Romero et al. 2003; Rolle et al. 2011). The needle-like 2mm cylinder probe has been used to measure elasticity, rupture force, and skin thickness (Rolle et al. 2011; Vargas et al. 2001). Other experiments in *V. vinifera* have explored

uses for spring clamps (Deng et al. 2005), conical probes (Letaief et al. 2008), and rounded probes (Maury et al. 2009). Instrumental texture research in muscadine is much less mature. At the time of writing, all published work in muscadine has relied solely on the 2 mm and 5 mm cylinder probes (Barchenger et al. 2015, Brown et al. 2016, Conner 2013, Felts et al. 2018). Conner (2013) used both probes to evaluate texture in 26 muscadine genotypes using four different measurement protocols. Conner (2013) used the 2 mm cylinder probe to measure berry deformation at first peak and berry maximum force. The 5 mm cylinder probe was used to measure flesh maximum force and skin break force. Using these four protocols, Conner (2013) suggested that berry penetration work estimated with the 2 mm probe and flesh maximum force estimated with the 5 mm probe would be most useful in routine texture screening. Still, many texture analysis protocols and attachments remain untested in the muscadine literature. The Kramer Shear Cell (KSC), for instance, has been recommended as a supplement or replacement to the 2 mm probe penetration tests (Harker et al. 1997). This instrument consists of five parallel blades positioned over a metal box with five grates at the bottom. Bulk fruit samples are placed in the box and macerated by the blades to simulate one or more cycles of chewing.

The objective of the present study is to expand on the work of Brown et al. (2016) and Felts et al. (2018), who compared instrumental and consumer or descriptive sensory data collected on a group of muscadine genotypes. Felts et al. (2018) provided the methodological framework for a descriptive sensory analysis in fresh muscadine, and Brown et al. (2016) found that consumers' overall liking of a muscadine genotype was negatively correlated with the instrumental traits of elasticity and berry puncture force using the 2mm probe. To build on previous work, this study implements a more comprehensive selection of instrumental probes than any reported to date in muscadine. In addition, we modify methods established by Felts et

al. (2018), who recommended the inclusion of fewer attributes and adjustment of texture standards in descriptive sensory analysis of muscadines. By correlating descriptive sensory panelist scores, breeders' ratings, and instrumental measurements in a group of texturally diverse muscadines and a *V. vinifera* check, we seek to develop a robust strategy for routine screening of muscadine texture profiles through cost-effective instrumentation.

Materials and Methods

Plant Materials and Harvest. Three advanced selections from the University of Arkansas System Division of Agriculture (UA) breeding program (AM-9, AM-135, and AM-195), one breeding selection from the North Carolina State University muscadine breeding program (NC67015-26), and three commercially available muscadine cultivars (Carlos, Ison, and Tara) were used for sensory and texture analysis in 2019 and 2020. These genotypes were selected based on their diverse texture characteristics and availability of sufficient quantities of ripe fruit. 'Carlos' (Brooks and Olmo 1997) is popular processing cultivar with poor texture quality for fresh-market. NC67015-26 is a breeding selection with both fresh-market and processing cultivars in its pedigree. 'Ison' and 'Tara' are both fresh-market cultivars (Brooks and Olmo 1997). AM-135, AM-195, and AM-9 are breeding selections with improved texture quality. Ten 500 g clamshells of each cultivar were harvested from the UA Fruit Research Station (FRS) in Clarksville, AR [west-central Arkansas, lat. 35°31'58"N and long. 93°24'12"W; U.S. Department of Agriculture hardiness zone 7a; soil type: Linker fine sandy loam (Typic Hapludult)] on 11 Sep 2019 and 16 Sep 2020. Vines harvested at FRS were planted at 6.1 m plant spacing and with 3.0 m row spacing. All vines ranged from five to 25 years in age and were trained to a bilateral, high-cordon/curtain system and were pruned to three or four node spurs. Annual fertilization of vines with nitrogen fertilizer occurred in March and April, and weed pressure was minimized using

preemergent and postemergent herbicides as needed. Fungicides were also applied as needed. Additionally, ten 500 g clamshells of the seeded table grape cultivar Red Globe were taken from storebought bags of grapes to provide a check representing ideal table-grape texture qualities for reference during the analysis. After harvest, fruit was transported from FRS to the UA Department of Food Science in Fayetteville, AR. Fruit from each genotype was mixed and re-sorted into seven 500 g clamshells which were randomly assigned to the five analytical texture analysis methods and sensory analysis. Berries that were immature, overripe, or that displayed obvious deformity, wet stem scar, or other damage were discarded during randomization. Instrumental texture analyses were performed on the day of harvest. All remaining fruit designated for descriptive sensory analysis was stored in a refrigerator at 2 ℃ and 85% to 89% relative humidity until analysis could begin the following day.

Descriptive Sensory Analysis. Descriptive sensory analyses of AM-9, AM-135, AM-195, NC67015-26, 'Carlos', 'Ison', 'Tara', and 'Red Globe' were conducted at the UA Sensory Science Center on 12 Sep 2019 and 17 Sep 2020. The panelists (n=9 in 2019; n=6 in 2020) used a modified Sensory Spectrum® method, an objective method for describing the intensity of attributes in products using references for the attributes. The descriptive panel evaluated each sample for 10 texture attributes (Table 4.1) using a 15-point scale (0=less of an attribute, 15=more of an attribute). A slightly modified version of the descriptive sensory lexicon described by Felts et al. (2018) was implemented for sensory analysis. Edamame in pods were included as an upper limit standard for the 'awareness of skins' scale (15 points), where Felts et al. (2018) had previously used medium lima beans (8 points) as an upper limit. The fruit was removed from cold storage, washed, and placed on trays to air-dry before it was presented to the descriptive sensory panelists. The descriptive sensory evaluation was performed in duplicate in

2019 and triplicate in 2020, following a randomized complete block design with randomized presentation order of each of the seven muscadine genotypes and ‘Red Globe’ within each replication. Five fully intact berries of each genotype were assigned to each panelist per replicate. Only the first berry was used for visually rated characteristics (visual separation, amount of seeds, and seed size), and the remaining four berries were used in the remaining physically evaluated sensory characteristics. Panelists were instructed to cleanse their palates between samples by consuming water and unsalted crackers. The fruit was served at room temperature on plates marked with anonymized three-digit codes and knives were provided to each panelist for cutting berries and rating visual characteristics.

Breeders’ Ratings. Three researchers familiar with the UA muscadine breeding germplasm rated all seven muscadine genotypes and ‘Red Globe’ for skin texture, flesh texture, and overall texture desirability. The skin texture scale ranged from 1 = extremely thick skin to 9 = extremely thin, tender skin. The flesh texture scale ranged from 1 = extremely soft, mucilaginous flesh to 9 = extremely firm, meaty flesh. The overall desirability scale ranged from 1 = highly undesirable texture to 9 = highly desirable texture.

Instrumental Analysis – General Description. All instrumental analyses were performed using a TA.XTPlus Texture Analyzer (Texture Technologies Corporation, Hamilton, MA) with a 5 kg load cell. Detailed specifications used with each protocol are provided in Supplemental Table 1. Probe attachments tested include a 2 mm cylindrical probe, an 8 mm cylindrical probe, a 7.62 cm cylinder compression probe, a 45° chisel probe, and a Kramer shear cell. Fifteen randomly

selected berries of each genotype were used for each analysis, except for the Kramer shear cell, which consisted of three runs per genotype and six berries per run.

Instrumental Analysis - Penetration. Fruit firmness was measured by penetration using a 2 mm flat cylindrical probe. Penetrations were made on the equatorial plane of each berry with the stem scar facing the right-hand side at a probe speed of 1 $mm.sec^{-1}$ (Appendix C). Berry skin break force (N) was calculated as the force required to rupture the berry skin. Elasticity was calculated as the distance (mm) the berry was compressed before the skin was ruptured. Skin firmness was calculated as skin break force (N) / elasticity (mm) following Felts et al. (2018). Berry penetration work (mJ) was calculated as the area under the curve from zero to the point of berry maximum force following Conner (2013).

Instrumental Analysis - Skin and Flesh. To evaluate skin and flesh properties individually, a small circular section of skin was carefully removed from the equatorial surface of each berry using a razor blade. Both the removed skin and exposed berry were used to perform separate tests for skin thickness and flesh firmness. The removed sections of skin were trimmed of any excess flesh clinging to the interior surface and penetrated using a 2 mm flat cylindrical probe (Appendix C). The distance traveled from first contact to the work surface was recorded as skin thickness. The exposed flesh of the entire berry was then probed using an 8 mm flat cylindrical probe. The probe traveled 3 mm at a speed of 0.5 $mm.sec^{-1}$ after first contact (Appendix C), and the peak force was recorded as flesh firmness (N).

Instrumental Analysis - Compression. Compression tests were performed using a 7.62 cm mm flat cylindrical probe and were conducted on the equatorial plane of each berry with the stem scar facing the right-hand side at a probe speed of 1 $mm.sec^{-1}$ (Appendix C). After the probe contacted the berry surface, it traveled halfway to the work surface, achieving a strain of 50%. Peak force (N) was recorded as compression firmness. The area under the texture curve was also recorded as compression work (mJ).

Instrumental Analysis - Single Blade. Tests were performed using a knife blade attachment with a 45-degree chisel end. Compressions were conducted on the equatorial plane of each berry with the stem scar facing the right-hand side at a probe speed of 1 $mm.sec^{-1}$ (Appendix C). After the probe contacted the berry surface, it traveled halfway to the work surface, achieving 50% strain. Peak force (N) and work (mJ) measurements were reported as knife firmness and knife work respectively.

Instrumental Analysis - Kramer Shear Cell. Kramer shear tests were performed using a Kramer shear cell (KSC). The box at the cell base was filled with six berries. The sample was then macerated in two cycles with a probe speed of 1 $mm.sec^{-1}$ (Appendix C).

Statistical Analysis. Instrumental and breeders' ratings were analyzed using PROC MIXED in SAS 9.4 (SAS Institute Inc., Cary, NC) with genotype as a fixed effect and year and genotype by year interactions treated as random effects. Sensory texture data were also analyzed using PROC MIXED with genotype considered as a fixed effect and with year, panelist, and their interactions treated as random. The panelist factor was nested within year since panelists changed from year

to year. Mean separation for significant factors was conducted using Fisher's F-protected Least Significant Difference. PROC CORR was used to conduct Pearson correlations between the instrumental, sensory, and breeders' ratings data.

Nineteen instrumental measurements and one generalized breeders' rating for overall texture quality were used to construct multiple regression models predictive of awareness of skins, crispness, hardness, visual separation, and overall breeders' ratings. A stepwise method of model testing was used to select candidate models having the lowest Akaike information criterion (*AIC*) within years. Models were selected on the basis of low *AIC* scores and high r^2 values. Three separate principal component analyses (PCAs) were conducted with base R across years to heuristically compare the variance explained and genotypic clustering patterns in models including all 19 instrumental measurements for which genotypic differences were observed in either year, all six instrumental measurements that were included in regression models, and all descriptive sensory and visual traits except for those relating to seeds or in which genotypic differences were not reported (R Core Team, 2022).

Results

Descriptive Sensory Panel. The seeded table grape *V. vinifera* check, 'Red Globe', was a frequent, yet anticipated outlier for most attributes measured. Its disproportionate statistical leverage on the analysis and its inherently non-muscadine qualities would have likely produced misleading conclusions about instrumental methods for texture evaluation as they pertain to muscadine populations. Therefore, 'Red Globe' was excluded from analyses of variance (ANOVA), mean separations, and correlation analyses, but it was presented elsewhere in the results as a baseline comparison to an ideal texture profile for table consumption. Any mention

of ‘Red Globe’ in these results is considered only in this specific context. Genotype by year interactions were significant among six out of ten descriptive sensory traits, two out of three breeders’ ratings, and fifteen out of twenty-three instrumental attributes. Thus, all means comparisons and downstream analyses were considered within years. Descriptive sensory panel and breeders’ ratings differed significantly (Tables 4.2-4.3, $P \leq 0.05$) between genotypes for all attributes measured, except moisture release in 2019 and 2020 and detachability in 2020 (Table 4.2).

Among the seven sensory panel attributes (excluding seed size and number) for which genotypic differences were observed in 2019 and 2020 (Table 4.2, $P \leq 0.05$), visual separation displayed the widest ranges of variation between muscadine genotypes according the 15-point scale. In both years, the genotypic means of visual separation were strongly correlated to those of awareness of skins (r = 0.84-0.96, $P \leq 0.001$, data not shown), with AM-135 and AM-195 both having skins that adhered more strongly to the flesh (Table 4.2) than the other five muscadine genotypes. A very strong correlation between visual separation and detachability was observed in 2019 (r = 0.98, $P \leq 0.001$, data not shown), but in 2020 panelists were unable to differentiate genotypes based on detachability (Table 4.2). The mean visual separation scores of the two improved genotypes (AM-135 and AM-195), which ranged from 7.33-9.78 (Table 4.2), were nearly twice as large as those of ‘Red Globe’ (3.67-3.75), but at least two points lower than all other *V. rotundifolia* genotypes (12.36-14.06). Similarly, panelists in both years were significantly less aware of skins on AM-135 compared to all other genotypes except for AM-195 and ‘Tara’ (Table 4.2). In all descriptive sensory attributes, differences were present among the individual panelists (Table 4.2) indicating that, even with food standards and training, panelists' interpretations of the scales were varied. Significant interactions between genotype and panelist

for visual separation (Table 4.2) demonstrate that panelists had difficulty ranking genotypes consistently for this trait.

Means for seed separation varied greatly between years, but NC67A015-26 and ‘Ison’ both had seeds that were significantly more difficult to separate compared the highest scoring muscadines (Table 4.2). In 2020, NC67A015-26 had seeds that were at least 40% more resistant to separation than all other genotypes (Table 4.2). Like seed separation, seed size varied widely between years. AM-9 had the largest mean seed size in 2019, but the smallest in 2020 (Table 4.2). Similarly, AM-135 had the smallest mean seed size in 2019, but it was significantly larger than ‘Tara’ and AM-9 in 2020 (Table 4.2). AM-195 consistently had the lowest mean number of seeds with significantly fewer than ‘Carlos’, ‘Ison’, and ‘Tara’ in both years (Table 4.2, $P \leq 0.05$). The strong influence of year on seed number is evidenced by a nearly two-fold increase in seed number from 2019 to 2020 for most genotypes (Table 4.2).

In 2019, the mean hardness and crispness of the ‘Red Globe’ check was at least 30% lower than all muscadine genotypes, but in 2020, its mean hardness was more similar to those of muscadines (Table 4.2). Both processing-types, ‘Carlos’ and NC67A015-26, also had lower mean hardness and crispness ratings than all other muscadine genotypes in 2019 (Table 4.2). The genotypic means of crispness and hardness were strongly correlated in both years ($P \leq 0.01$), with Pearson correlations ranging from $r = 0.96$ - 0.98. AM-9 and AM-195 both consistently grouped with the hardest and crispest genotypes, along with AM-135 in 2019 (Table 4.2). In 2019, the improved fresh market selection, AM-135, had one of the hardest, most crispy berries (Table 4.2). Genotypic rankings for fibrousness varied greatly between years, but the processing-quality breeding selection, NC67A015-26, consistently grouped with the most fibrous genotypes (Table 2).

Breeders' Ratings. Breeders were able to distinguish significant genotypic differences (Table 4.3) in ratings for overall texture, skin texture, and flesh texture. The mean breeder's ratings for skin texture, flesh texture, and overall desirability in 2019 and 2020 were highly correlated to one another (Table 4.6, $P \leq 0.01$), with AM-135 and AM-195 consistently ranking among the most texturally desirable genotypes for all three ratings. AM-135 and AM-195 were most like the breeders' ratings of 'Red Globe', which greatly exceeded breeders' ratings of all others. For all three breeder attributes, 'Carlos' and NC67A015-26 performed similarly and were in the lowest rated group in both years (Table 4.3). None of the breeders' ratings were correlated with hardness or crispness (Table 4.6), but breeders did consistently prefer skin, flesh, and overall texture of genotypes with low scores for visual separation (r = -0.79 to -0.92).

Instrumental Analysis. Using the five TA.XT probes described, 22 unique, instrumentally measured attributes were included in the final statistical analyses. Genotypic differences were present in all instrumental analyses performed in 2019 (Tables 4.4-4.5). In 2020, KSC peak force, skin thickness using the 2 mm cylinder, and strain to rupture using the 7.62 cm cylinder did not detect genotypic differences (Tables 4.4-4.5).

For all attributes measured by the 2 mm cylinder probe, muscadine genotypes required greater force, work, and distance to penetrate berries and skins than 'Red Globe' (Table 4.4). Skin thickness of 'Red Globe', as measured by penetration with the 2 mm cylinder probe, was disproportionately affected by year, being twice as thick in 2020, possibly resulting from different sources of fruit in each year (Table 4.4). No significant differences for muscadine skin thickness were observed in 2020 (Table 4.4), but both processing-quality muscadine genotypes, Carlos and NC67A015-26, had significantly thinner skins than all other muscadines in 2019.

‘Tara’, AM-9, and the table-type, AM-135 all appeared in the thickest-skinned group in 2019 (Table 4.4). In both years, NC67A015-26 had skins that required significantly more force and work to penetrate when tested apart from the flesh than all other muscadine genotypes (Table 4.4). AM-195, a table-type breeding selection, had skins that required significantly less force to penetrate than all other genotypes in both years (Table 4.4). Breeders in both years favored skins, flesh, and overall texture quality of genotypes with skins that required less force or work to penetrate, as evidenced by Pearson correlations ranging from 0.70 to 0.96 (Table 4.6).

In the whole-berry penetration test conducted with the 2 mm cylinder probe, NC67A015-26 consistently grouped with those genotypes requiring the largest amount of force and work to rupture whole berries (Table 4.4). AM-135 had the lowest work to rupture, rupture force, and elasticity of all genotypes observed, with values that were 48%, 32%, and 28% lower than those for NC67A015-26, respectively. AM-135 had significantly lower rupture force and work to rupture in both years than all other muscadine genotypes (Table 4.4). In 2019, elasticity measured by the 2 mm cylinder held a tight negative correlation (Table 4.6, $P \leq 0.01$, $r = 0.91$ - 0.97) with all breeders’ ratings and a positive correlation (Table 4.6, $P \leq 0.01$, $r = 0.92$ -0.94) with visual separation and detachability. Of all probes tested, only the 2 mm cylinder provided measurements that were consistently correlated with all three breeders’ ratings in both years (Table 4.6). Breeders favored the skins, flesh, and overall texture of genotypes that required less work or force to rupture whole berries, with significant Pearson correlations ranging from -0.65 to -0.95 (Table 4.6).

Work and peak force measured by the 8 mm probe on the exposed mesocarp of individual berries, were tightly correlated with detachability and visual separation in 2019 (Table 4.6, $P \leq 0.01$). Using this probe, work and peak force were also so strongly correlated with one

another (r = 0.98 – 1.00, data not shown) that they are likely colinear predictors of the same descriptive sensory attributes. Additionally, the flesh analyses conducted with the 8 mm probe demonstrated that AM-195 had flesh that was significantly firmer than all other genotypes in both 2019 and 2020 (Table 4.4), while 'Carlos' consistently grouped in the lowest categories for flesh firmness. In 2019, both improved table-type muscadines, AM-195 and AM-135, had flesh that was even more firm than 'Red Globe', but in 2020 only AM-195 had flesh firmer than 'Red Globe'.

The means of analogous attributes measured by the 7.62 cm cylinder and the 45° chisel probe analyses were highly correlated (r = 0.87 – 0.98, data not shown), and thus expected to be collinear predictors of sensory texture attributes. In addition, the chisel often caused muscadines with low skin adherence to pop open, releasing the mesocarp and producing inconsistencies in results. For the sake of simplification and the two reasons previously mentioned, the results produced by the chisel probe were excluded from post-ANOVA regression analyses. Instead, the cylinder probe will be discussed primarily as the most promising of the two options. Force required to rupture berries with the 7.62 cm cylinder probe had significant correlations with hardness and crispness in both years (Table 4.6, $P \leq 0.01$). AM-9 consistently required the most force to rupture using the 7.62 cm cylinder. The processing cultivar, Carlos, consistently grouped with the lowest scoring muscadines for all attributes measured by the 7.62 cm cylinder (Table 4.5). In 2019, work to rupture with the 7.62 cm probe was positively correlated with skin thickness (r = 0.67, data not shown), but in 2020 it was positively correlated with flesh peak force (r = 0.68, data not shown) and flesh total work (r = 0.70) measured using the 8 mm cylinder.

During preliminary experiments with the KSC, it was observed that cycle one of maceration caused the smaller, more slip-skin genotypes to be pushed through the openings in the base of the KSC. This was especially common for ‘Carlos’ and NC67A015-26. For this reason, it was determined that multi-cycle KSC protocols are infeasible in muscadine panels that include processing-quality muscadines. By using a single cycle maceration protocol to measure total work and peak puncture force, genotypic differences were observed (Table 4.5) in 2019, but only total work produced genotypic differences in 2020. The small-fruited, processing genotypes (‘Carlos’ and NC67A015-26) had significantly lower total work than all other genotypes in both years and were among the group of genotypes with lowest peak puncture force in 2019 (Table 4.5). In years when genotypic differences were present, both total work and peak force measured by KSC were most tightly correlated with crispness and hardness (Table 4.6; r = 0.86 - 0.95).

Multiple Regression and PCA. Predictive regression models with adjusted r^2 values greater than 0.60 were identified and presented (Table 4.7) for four of the descriptive sensory and visual traits analyzed. These included awareness of skins, crispness, hardness, and visual separation. The most predictive model (Table 4.7; adjusted r^2 = 0.85) for awareness of skins included berry elasticity and rupture force to puncture, as measured by the 2 mm cylinder probe. Inclusion of a general breeders’ rating did not improve model prediction. Variance in crispness and hardness were best explained by a model including total work measured by the KSC, berry rupture force measured by the 2 mm cylinder probe, and generalized breeders’ ratings (Table 4.7; adjusted r^2 = 0.91 and 0.82 respectively). Visual separation was the only descriptive trait that was predicted by breeders’ ratings in a single regression model (Table 4.7; adjusted r^2 = 0.70). For every point assigned by the breeder to overall liking of texture quality, the sensory panel ratings for visual

separation of skins were predicted to decrease by 1.31 points (Table 4.7). The most predictive instrumental model for visual separation included work to puncture berry skin (removed from berry) with the 2 mm cylinder and maximum force measured on exposed flesh with the 8 mm cylinder (Table 4.7; adjusted $r^2 = 0.85$). Breeders' ratings for overall texture quality were best explained by a model including berry rupture force using the 2 mm cylinder and peak force of flesh compression using the 8 mm cylinder (Table 4.7; adjusted $r^2 = 0.83$). No models using the 7.62 cm cylinder or the 45° chisel were identified as consistently high-performing for prediction of sensory traits. PCAs for regression models (Figure 4.1B) and descriptive sensory traits (Figure 4.1C) clustered genotypes very similarly explaining 87.18% and 88.76% of the variance in the first two principal components, respectively. In both analyses, 'Red Globe' presented as an extreme outlier. Improved selections AM-135 and AM-195 formed a distinct cluster. 'Tara', 'Ison', and AM-9 formed an intermediate texture quality cluster. Finally, the processing cultivar 'Carlos' and NC67A015-26 formed a poor-quality cluster. The PCA that considered all 19 instrumental measurements (Figure 4.1A) explained less variance in the first two principal components (72.75%) than the selected regression model or descriptive sensory model, and it clustered genotypes differently.

Discussion

After designing and testing the descriptive sensory lexicon used in this study, Felts et al. (2018) only observed genotypic differences in visual separation of skins among the six fresh-market muscadine cultivars and breeding selections included in that study, and they made several recommendations for improvements in future work. These recommendations included the re-establishment of texture standards and the reduction of lexicon size to contain only texture-

related attributes. By implementing these suggestions, our work has demonstrated the ability of descriptive sensory panels to detect genotypic differences in texture quality for all attributes except for moisture release. Differences observed in the present study are likely explained by several modifications to the protocol used by Felts et al. (2018), including our selection of texturally diverse genotypes, which ranged from slip-skin processing types to improved table-type breeding selections. Our inclusion of only texture-related attributes likely reduced error from panelist fatigue compared to the evaluation of a larger lexicon. Additionally, the inclusion of a new upper-limit food standard for the awareness of skins scale may have helped panelists to distinguish differences in this attribute more effectively. Numerous tight correlations between descriptive sensory traits, instrumental traits, and breeders' scores demonstrated the broad predictive ability of texture analyzers and breeders in evaluating sensory characteristics.

Previous work has already established the presence of broad diversity among muscadine germplasm for texture quality (Brown et al. 2016) and the improvement of this trait in recently released fresh-market cultivars (Conner 2020). Based on the genotypes we have examined, fresh-market muscadine breeders appear to have selected for superior texture primarily on the basis of slip-skin related qualities like visual separation of skins. Indeed, AM-135 and AM-195 scored significantly lower than all other genotypes for visual separation and detachability (Table 4.2) and significantly higher than others for breeders' ratings of skin and overall quality (Table 4.3). Seventy percent of variance in visual separation was explained by regressing against the breeders' overall rating of texture quality (Table 4.7). By using an instrumental model of visual separation prediction that included total skin work measured with the 2 mm cylinder and flesh maximum force with the 8 mm cylinder, the adjusted r^2 was increased to 85% (Table 4.7), although this model requires the time-consuming task of excising muscadine skins for separate

skin puncture and flesh work analysis. This model expands on the findings of Conner (2013) who also reported broad diversity for muscadine skin break force. Conner (2013) recommended the combination of berry penetration work with a 2 mm cylinder and flesh maximum force with a 5 mm cylinder for characterizing muscadine texture profiles. This recommendation closely mirrors our best performing model for the prediction of overall breeders' scores, which included berry penetration force with a 2 mm cylinder and flesh maximum force with an 8 mm cylinder. In our dataset, Conner's recommended model explained 80% of variance in general breeders' ratings of texture (Table 4.7), and our chosen model explained 84% of variance in general breeders' ratings. However, our sampling of genotypes could be partially responsible for these differences in model performance, and Conner used a 5 mm cylinder for flesh analysis rather than the 8 mm cylinder that we report. Regardless of phenotyping method, imrovement of skin toughness is an important breeding objective. Breeders' field ratings were significantly correlated with skin puncture force (r = -0.70 to -0.95) and may provide a much more practical option for routine screening purposes. Breeders' ratings for skin, flesh, and overall quality were not consistently correlated to any other descriptive sensory characteristics, but breeders may gain a more comprehensive and objective understanding of texture diversity within their own germplasm by having defined instrumental protocols. Standardized phenotyping protocols should create opportunities in genomic exploration by allowing breeders to evaluate a wider range of traits. These data may also be used complement or enhance established breeders' ratings through the elimination of error from fatigue.

Hardness and crispness both provide potential examples of texture attributes that may be overlooked when breeders rely exclusively on field ratings for texture quality. Neither of these characteristics were strongly correlated to any breeders' field rating, but they were correlated to

total work measured by KSC (r = 0.86 - 0.92) and penetration rupture force measured with the 2 mm cylinder (r = 0.76 - 0.78). Interestingly, the KSC, which has not yet been reported for use in muscadine, was most highly predictive of crispness and hardness. When used alongside 2 mm rupture force and breeders' scores for overall texture, 90% of variance in crispness could be explained across years (Table 7). Using the same 2 mm probe and penetration test that we report, Brown et al. (2016) found a significant negative correlation between berry rupture force and the consumer panel's liking of skin texture and liking of pulp texture. If consumers' texture preferences reported in Brown et al. (2016) are assumed to be consistent with breeders' preferences, our selection of genotypes has shown no such trend. One striking example of this is AM-195, which is an improved table-type muscadine that grouped with the genotypes having the highest rupture force in 2019 (Table 4.4). AM-195 simultaneously grouped with the most preferred texture quality for breeders (Table 4.3) and the hardest, crispest genotypes for descriptive sensory panelists (Table 4.2). NC67A015-26 also grouped with those requiring the greatest force to rupture (Table 4.4), but it grouped with the poorest quality texture in breeders' scores (Table 4.3) and with the softest, least crisp genotypes according to descriptive sensory panelists (Table 4.2). Indeed, descriptive sensory panelists' ratings of hardness and crispness were highly correlated (data not shown). The high hardness scores assigned to genotypes that are preferred by breeders appears to contradict the findings of Brown et al. (2016), suggesting that hardness may be a desirable quality in muscadine texture, assuming minimal separation of skins.

To better understand this relationship between muscadine texture and hardness, it may be helpful to consider the individual contributions of muscadine flesh and skin. According to instrumental measurements with the 8 mm cylinder and the 2 mm cylinder, the flesh of AM-195 was significantly firmer than all other genotypes (Table 4.4), but it also grouped with those

having the softest skins. In contrast, NC67A015-26 had the toughest skins (Table 4.4) and grouped with those having the softest flesh. Yet, both genotypes grouped with those requiring the greatest force to rupture with the 2 mm cylinder (Table 4.4). Conner (2013) similarly identified a negative correlation between flesh maximum force and berry rupture force, and a positive correlation between skin break force and berry rupture force. Additionally, breeders preferred genotypes that had high instrumental measurements for flesh compression force and low instrumental measurements of skin work (Table 4.4), indicating that hard berries with tender skin and firm flesh are considered superior in texture quality while berries with hard skin and soft flesh are considered to be poor quality. It was encouraging to find that even within the narrow selection of genotypes observed, the UA muscadine germplasm had flesh that was as firm or firmer than the 'Red Globe' *V. vinifera* comparison. In contrast, the skins of all muscadine genotypes required at least 300% more work to penetrate with the 2 mm cylinder than 'Red Globe' (Table 4.4). Thus, the improvement of skin tenderness may require sustained selection strategies from breeders to promote gradual enrichment of muscadine germplasm. Skin tenderness and seedlessness may be the two most important long-term breeding objectives achieving texture quality palatable for consumers.

Awareness of skins may provide another perspective for understanding muscadine skin texture and it may be predicted with a very simple and scalable instrumental texture analysis protocol. The best performing multiple regression model for predicting awareness of skins used a whole-berry puncture test with the 2 mm cylinder probe, which has been widely reported in muscadine literature (Brown et al. 2016; Conner 2013; Felts et al., 2018). Importantly, this puncture test did not require the time-consuming manipulation of samples by removal of skins. By performing a berry puncture test to evaluate elasticity and rupture force, 85% of variance in

awareness of skins could be explained (Table 4.7). Brown et al. (2016) reported a negative correlation between consumers' liking of skins and berry rupture force using the 2 mm probe. This appears to be consistent with the descriptive sensory panel's interpretation of awareness of skins, which was positively correlated to berry rupture force in both years (r = 0.92 - 0.95) and negatively correlated with breeders' ratings for skin texture quality in 2020 (r = -0.88). It appears to be true that breeders and consumers both prefer the texture of muscadines with inconspicuous, tender skins that cling to the flesh, as evidenced by correlations between awareness of skins and visual separation of skins (r = 0.84 - 0.96). Brown et al. (2016) asked untrained consumers to preference of skin thickness based on a five-point JAR scale where 1 = too thin, 3 = just about right, and 5 = too thick. They observed that muscadine genotypes were generally too thick and that the table-type *V. vinifera* check was closer to 3 (just about right). In contrast, our instrumental measurements of skin thickness did not appear uniformly indicative of breeders' liking of skin texture or descriptive sensory panelists' awareness of skins. This point is evidenced by AM-135, which consistently grouped with the least awareness of skins (Table 4.2), but the thickest skins (Table 4.4). This deviation from the consumer ratings reported by Brown et al. (2016) may have occurred because consumers were more aware of tough skins. If so, an untrained consumer may be more likely to equate skin toughness with skin thickness, even when tougher skins could be thinner.

Predictive regression models were not identified for the remaining descriptive sensory characteristics, which included detachability, moisture release, and seed separation. Just as Felts et al. (2018) observed, genotypic differences were not consistently observed for detachability or moisture release. This may either be due to differences in the understanding of how to score these traits among descriptive sensory panelists, or because little phenotypic diversity was

present for these traits among the genotypes tested. The 7.62 cm cylinder probe and the 45º chisel probe were heavily correlated in most measurements (data not shown), such that one could likely be used in place of the other. Both probes produced measurements that were correlated with crispness and hardness (Table 4.6), however neither probe outperformed the KSC in construction of regression models for these traits (Table 4.7). Therefore, these probes could be used in estimation of crispness and hardness in muscadines, but should not be adopted as a preferred method.

Conclusion

Our findings have substantiated the value of the 2 mm cylinder probe in predicting awareness of skins in muscadine based on the regression model presented. Similarly, the 8 mm cylinder may help to predict visual separation of skins, or slip-skins, by measuring the flesh tenderness in a protocol following Conner (2013). Additionally, the KSC attachment was more capable of predicting hardness and crispness than any other instrumental methods previously documented. The 7.62 cm cylinder and the 45º chisel were correlated with many descriptive sensory traits, but neither protocol yielded regression models more predictive of sensory traits than the 2 mm cylinder, the 8 mm cylinder, or the KSC. Breeders' ratings of skin, flesh, and overall texture quality were so closely correlated in both years ($r \geq 0.96$), that collecting independent ratings for skin and flesh would probably be redundant and unnecessary for routine screening of germplasm. These breeders' ratings best predicted visual separation of skins, but by including measurements from the KSC and 2 mm cylinder, it may be possible to screen germplasm based on instrumental prediction of awareness of skins, crispness, hardness, and visual separation. The proposed regression models should continue to be tested across a more

diverse range of breeding materials and compared with consumer sensory panels as in Brown et al. (2016). This work adds to a growing body of evidence that suggests continued improvement of muscadine texture should focus both on the tenderness of skins and firmness of flesh.

References Cited

Barchenger DW, Clark JR, Threlfall RT, Howard LR, Brownmiller CR. 2015. Evaluation of physicochemical and storability attributes of muscadine grapes (*Vitis rotundifolia* Michx.), HortScience. 50(1):104-111.

Brooks RM, Olmo HP. 1997. Brooks and Olmo register fruit & nut varieties. (3rd ed). ASHS Press, Alexandria, VA, USA.

Brown K, Sims C, Odabasi A, Bartoshuk L, Conner P, Gray D. 2016. Consumer acceptability of fresh-market muscadine grapes. J Food Sci. 81(11):S2808–S2816.

Cefola M, Pace B, Buttaro D, Santamaria P, Serio F. 2011. Postharvest evaluation of soilless-grown table grape during storage in modified atmosphere. J Sci Food Agric. 91:2153-2159.

Cliff MA, Bejaei M. 2018. Inter-correlation of apple firmness determinations and development of cross-validated regression models for prediction of sensory attributes from instrumental and compositional analyses. Food Research International 106:752–762.

Conner PJ. 2012. Evaluation of muscadine genotypes for storage ability (abstr). HortScience. 47(9):S386

Conner PJ. 2013. Instrumental textural analysis of muscadine grape germplasm. HortScience. 48(9):1130–1134.

Conner PJ. 2020. 'RubyCrisp' muscadine grape. HortScience. 55(6):961-964.

Conner PJ, Worthington ML. 2023. Muscadine grape breeding. Plant Breeding Reviews. 46:30-117.

Deng Y, Wu Y, Li Y. 2005. Effects of high O2 levels on post-harvest quality and shelf life of table grapes during long-term storage. European Food Research and Technology. 221(6):834–834.

Felts M, Threlfall RT, Clark JR, Worthington ML. 2018. Physiochemical and descriptive sensory analysis of Arkansas muscadine grapes. HortScience. 53(11):1570–1578.

Harker FR, Redgewell RJ, Hallett IC, Murray SH. 1997. Texture of fresh fruit. Horticultural Reviews. 20:121-224.

Letaief H, Rolle L, Gerbi V. 2008. Mechanical behavior of winegrapes under compression tests. Am J Enol Vitic. 59(3):323–329.

Martinez-Romero D, Guillen F, Castillo S, Valero D, Serrano M. 2003. Modified atmosphere packaging maintains quality of table grapes. J Food Sci. 68(5):1838–1843.

Maury C, Madieta E, le Moigne M, Mehinagic E, Siret R, Jourfon F. 2009. Development of a mechanical texture test to evaluate the ripening process of Cabernet Franc grapes. J Texture Stud 40(5):511–535.

Olien WC. 1990. The muscadine grape: botany, viticulture, history, and current industry. HortScience. 25(7):732–739.

R Core Team. 2022. R-4.2.1 for Windows. R Foundation for Statistical Computing, Vienna, Austria. https://cran.r-project.org/bin/windows/base/old/4.2.1/. [accessed 20 Jan 2023].

Rolle L, Giacosa S, Gerbi V, Novello V. 2011. Comparative study of texture properties, color characteristics, and chemical composition of ten white table-grape varieties. Am J Enol Vitic 62(1):49–56.

Rolle L, Siret R, Segade SRS, Maury C, Gerbi V, Jourjon F. 2012. Instrumental texture analysis parameters as markers of table-grape and winegrape quality: A review. Am J Enol Vitic. 63(1):11-28.

Sato A, Yamane H, Hirakawa N, Otobe K, Yamadai M. 1997. Varietal differences in the texture of grape berries measured by penetration tests. Vitis. 36(1):7-10.

Vargas A, Perez J, Zoffoli P, Perez A. 2001. Comparacion de variables de textura la medicion de firmeza de bayas de uva Thompson Seedless. Cienc Investig Agrar. 28(1):37–42.

Tables and Figures

Table 4.1. 2019-2020 Descriptive sensory lexicon for evaluation of muscadine grapes for texture.

Term	Definition	Technique	Reference	
Appearance (pulp of one berry cut in half)				
Visual separation	Detachability of pulp from skin of berry	Squeeze half of berry and observe the extent of which the pulp detaches from the skin. (None=*does not detach* to Much=*completely detaches*)	None Much	0.0 15.0
Amount of seeds	Number of seeds in the whole berry	Count the number of seeds in the whole berry.	Number of seeds	
Seed size	Visual size of the seeds	Observe the seeds and determine the overall size. (Small to Large)	Photo reference of size A=12 (5.3 x 8.5 mm) B=7 (4.9 x 7.1 mm) C=3 (3.9 x 6.1 mm)	
Texture (whole berry for 4 berries)				
Berry hardness	Force required to compress the sample.	Place the sample in the mouth. Compress or bite through the sample one time with molars or incisors. (Soft to Hard)	Cream Cheese[1] Egg White Am Cheese Beef Frank Olive Peanut Almond	1.0 2.5 4.5 5.5 7.0 9.5 11.0

[1] Philadelphia cream cheese, cut into ½" cubes (Kraft, Chicago, IL); Egg White, jumbo eggs, boiled for 5 minutes, cut into ½" cubes; American cheese, cut into ½" cubes (Boars Head, Brooklyn, NY); Hebrew National beef frank, boiled for 5 minutes and cut into ½" slices (ConAgra Foods, Indianapolis, IN); Great Value queen olives, with pimentos removed (Walmart, Bentonville, AR); Planters peanuts, whole pieces (Kraft, Chicago, IL); Almonds were not used for this evaluation

Crispness	Unique, strong, clean, and acute sound produced in first bite of the food with incisors and open lips.	Place the sample in the mouth. Compress or bite through the sample one time with molars or incisors. Evaluate the sound intensity produced at the first bite. (None=*not crisp* to Much=*extremely crisp*)	Ripe Banana[2] Granny Smith Apple Carrot	0.0 7.5 15.0

Table 1. Continued.

Moisture release	Amount of wetness or moistness felt in the mouth after one bite or chew.	Compress the sample with molars one time only. (Dry to Wet)	Banana[3] Carrot Mushroom Snap beans Cucumber Apple Honeydew Orange (Chew refs 5 times)	1.0 2.0 4.0 7.0 8.0 10.0 12.0 15.0
Awareness of skins	How aware are you of the skins during mastication of the sample?	Place sample in mouth and chew 3-5 times. Can also be evaluated in first bite stage. (None=*cannot tell skins are there* to Much=*extremely aware of skins*)	Baked beans[4] Medium lima beans Edamame	4.0 8.0 15.0
Detachability	Ease with which the pulp separates from the skin of the berries	Place the sample in the mouth. Compress or bite through the sample one time with molars or incisors. Evaluate the ease that the pulp separates from the skin.	None Much	0.0 15.0

[2] Ripe banana, cut into ½" cubes; Granny smith apple, peeled and cut into ½" cubes; Carrot, peeled and cut into ½" cubes

[3] Ripe banana, cut into ½" cubes; Carrot, peeled and cut into ½" cubes; Button mushrooms, destemmed and cut into ½" cubes; Snap beans were not used for this evaluation; Cucumber, peeled, deseeded, and cut into ½" cubes; Pink lady apple, peeled and cut into ½" cubes; Honeydew, peeled and cut into ½" cubes; Dole mandarin orange piece (Dole Foods, Westlake Village, CA)

[4] Bush's baked beans (Bush Brothers and Company, Knoxville, TN); Medium lima beans; Edamame in pods

		(None=*does not detach* to Much=*completely detaches*)		
Fibrousness between teeth	Amount of grinding of fibers required to chew through the sample (not including skins)	Place sample between molars and chew 3-5 times. Evaluate during chewing, but ignore the skin. (None=*not fibrous at all* to Much=*extremely fibrous*)	Apple[5] Apricot Salami Celery Toasted oats Bacon Beef jerky	2.0 5.0 7.0 9.0 10.0 12.0 20.0

Table 1. Continued.

Seed separation	The ease with which the seeds separate from the pulp of the berry	Manipulate the pulp in the mouth for ease to separate seeds from pulp. (None=*hard to separate seeds from pulp* to Much=*seeds easily separate from pulp*)	None Much	0.0 15.0

[5] Pink lady apple, peeled and cut into ½" cubes; Mariani apricots, sliced in half (Mariani, Vacaville, CA); Hard salami, cut into ½" cubes (Boars Head, Brooklyn, NY); Celery, cut into ½" pieces; Oats, toasted for 5 minutes at 350 F; Bacon and beef jerky were not used for this evaluation

Table 4.2. Least square means of descriptive sensory attributes for seven muscadine genotypes and 'Red Globe' measured in 2019 and 2020.

Year	Genotype	Descriptive sensory attributes (1-15 scale)												Visual attributes					
		Awareness of skin		Crispness		Detachability		Fibrousness		Hardness		Moisture release		Seed separation		Seed number		Seed size (mm)		Visual separation (1-15 scale)	
2019	AM-135	12.06	B[i]	7.00	AB	8.50	B	4.27	D	6.81	A	11.59	ns[ii]	8.78	AB	3.50	B	3.96	D	9.08	B
	AM-195	13.17	A	7.47	A	8.17	B	4.11	D	7.14	A	11.56	ns	9.64	A	2.72	D	4.38	CD	7.33	B
	AM-9	13.82	A	7.08	AB	13.81	A	4.92	BC	7.36	A	12.11	ns	9.30	A	3.00	CD	6.11	A	12.36	A
	Carlos	13.21	A	5.36	C	13.66	A	4.36	CD	5.91	B	10.97	ns	9.31	A	3.66	AB	5.31	ABC	13.41	A
	Ison	13.81	A	7.33	A	14.11	A	5.64	A	7.01	A	11.78	ns	6.31	C	3.66	AB	5.72	AB	12.80	A
	NC67AO15	13.78	A	6.11	BC	14.03	A	5.49	AB	6.06	B	11.11	ns	6.75	BC	3.99	A	4.25	CD	14.06	A
	Tara	13.51	A	6.58	AB	13.47	A	5.01	B	6.81	A	12.31	ns	9.08	A	3.33	BC	4.75	BCD	12.94	A
	Red Globe[iii]	6.29		2.92		4.11		2.72		3.72		11.72		9.75		2.78		4.28		3.75	
	LSD[iv]	0.91		1.06		1.73		0.62		0.65		0.85		2.08		0.43		1.13		1.80	
	P_G[v]	0.001		0.007		<0.001		<0.001		<0.001		0.098		0.012		<0.001		<0.001		<0.001	
	P_P[vi]	<0.001		<0.001		0.004		<0.001		<0.001		<0.001		<0.001		0.029		<0.001		<0.001	
	P_{GP}[vii]	<0.001		0.043		<0.001		0.093		1.000		0.203		0.424		0.456		0.854		0.138	
2020	AM-135	11.93	B	6.45	AB	11.51	ns	5.63	B	6.70	BC	12.28	ns	13.34	A	5.95	BCD	3.67	ABC	9.78	B
	AM-195	11.14	B	7.22	A	11.52	ns	5.20	B	7.26	AB	11.53	ns	11.94	AB	4.88	D	3.36	CD	9.34	B
	AM-9	13.46	A	7.27	A	12.46	ns	4.19	B	7.78	A	11.93	ns	12.07	AB	6.16	BCD	3.00	D	13.57	A
	Carlos	13.85	A	5.38	B	11.71	ns	8.06	A	6.54	BC	11.12	ns	9.24	C	8.54	A	3.44	BCD	12.73	A
	Ison	13.62	A	5.90	AB	11.96	ns	5.44	B	6.20	C	11.95	ns	10.32	BC	7.18	AB	4.00	AB	13.48	A
	NC67AO15	13.57	A	5.66	AB	12.47	ns	8.49	A	6.36	C	11.09	ns	5.27	D	5.23	CD	4.22	A	13.35	A
	Tara	13.22	AB	5.52	AB	10.78	ns	3.89	B	6.19	C	12.41	ns	12.21	AB	6.42	BC	3.06	D	13.16	A
	Red Globe	2.63		2.68		6.38		2.17		6.38		10.71		13.44		4.81		3.22		3.67	
	LSD	1.34		1.76		1.27		1.78		0.84		0.96		2.31		1.49		0.57		1.42	
	P_G	0.006		0.029		0.146		<0.001		<0.001		0.064		<0.001		<0.001		0.036		<0.001	
	P_P	0.002		<0.001		<0.001		0.006		<0.001		0.001		0.002		<0.001		0.585		0.022	
	P_{GP}	0.075		0.643		<0.001		<0.001		0.153		0.024		0.019		0.257		0.012		0.028	

[i]Means with different letters indicate significant differences ($P < 0.05$) between genotypes using Fisher's LSD

[ii]No significant genotypic differences ($P \geq 0.05$)

[iii]Red Globe was excluded from ANOVA and means comparisons analysis, but is presented here as a reference for *V. vinifera* fresh market qualities

[iv]Least significant difference between genotypes assuming $P < 0.05$

[v]*P* values for genotypes

[vi]*P* values for panelists

[vii]*P* values for genotype by panelist interactions

Table 4.3. Least square means of breeders' field ratings for seven muscadine genotypes and 'Red Globe' collected in 2019 and 2020.

Year	Genotype	Breeders' ratings (1-9 scale)					
		Flesh		Skin		All	
2019	AM-135	6.67	A[i]	8.00	A	8.00	A
	AM-195	6.00	AB	8.00	A	7.67	A
	AM-9	6.00	AB	5.33	B	5.67	B
	Carlos	2.00	D	2.33	C	2.00	C
	Ison	5.00	C	5.67	B	5.33	B
	NC67AO15-26	2.33	D	2.00	C	2.33	C
	Tara	5.33	BC	6.00	B	6.00	B
	Red Globe[ii]	8.00		9.00		8.67	
	LSD[iii]	0.88		0.88		0.95	
	P_G[iv]	<0.001		<0.001		<0.001	
	P_B[v]	0.065		0.929		0.422	
2020	AM-135	6.00	A	6.33	A	6.33	A
	AM-195	5.67	A	6.00	AB	6.00	AB
	AM-9	3.67	CD	3.67	CDE	3.67	DE
	Carlos	3.00	DE	3.33	DE	2.67	E
	Ison	4.00	BC	5.00	ABC	4.67	CD
	NC67AO15-26	2.67	E	2.67	E	2.67	E
	Tara	4.67	B	4.67	BCD	5.00	BC
	Red Globe	7.67		9.00		8.67	
	LSD	0.84		1.56		1.16	
	P_G	<0.001		<0.001		<0.001	
	P_B	0.009		0.018		0.002	

[i]Means with different letters indicate significant differences ($P < 0.05$) between genotypes using Fisher's LSD

[ii]Red Globe was excluded from ANOVA and means comparisons analysis, but is presented here as a reference for *V. vinifera* fresh market qualities

[iii]Least significant difference between genotypes assuming $P < 0.05$

[iv]*P* values for genotypes

[v]*P* values for breeders

Table 4.4. Least square means of instrumental texture analysis conducted with the 2 mm and 8 mm cylinder probes on seven muscadine genotypes and 'Red Globe' in 2019 and 2020.

Year	Genotype	2 mm cylinder (berry penetration)			2 mm cylinder (skin penetration)			8 mm cylinder (flesh)	
		Work to rupture (mJ)	Elasticity (mm)	Rupture force (N)	Total work (mJ)	Skin thickness (mm)	Peak force (N)	Peak force (N)	Total work (mJ)
2019									
	AM-135	19.47 D[i]	6.28 C	7.22 E	6.09 C	1.43 AB	30.77 C	2.12 B	2.81 B
	AM-195	27.82 C	6.30 C	10.03 AB	4.59 E	1.36 B	24.25 E	2.35 A	3.24 A
	AM-9	29.59 C	7.71 B	9.09 C	6.10 C	1.50 A	30.48 C	1.28 C	1.67 CD
	Carlos	34.50 B	8.50 A	9.50 BC	6.63 B	1.14 C	33.15 B	1.00 D	1.29 E
	Ison	28.22 C	7.43 B	9.23 C	6.72 B	1.36 B	33.53 B	1.28 C	1.76 CD
	NC67AO15-26	37.52 A	8.52 A	10.18 A	7.29 A	1.04 C	36.43 A	1.18 CD	1.53 DE
	Tara	27.44 C	7.52 B	8.15 D	5.42 D	1.40 AB	27.03 D	1.35 C	1.82 C
	Red Globe[ii]	7.64	5.50	2.89	1.25	0.51	6.2801	1.92	2.57
	LSD[iii]	2.74	0.38	0.60	0.45	0.12	2.33	0.20	0.29
	P_G[iv]	<0.001	<0.001	<0.001	<0.001	<0.001	<0.001	<0.001	<0.001
2020									
	AM-135	15.20 D	5.79 D	6.42 D	5.39 C	1.31 ns[v]	20.07 E	1.50 BC	4.10 B
	AM-195	23.31 BC	6.30 CD	8.73 BC	4.67 D	1.24 ns	18.34 F	1.83 A	5.21 A
	AM-9	25.04 B	6.54 BC	9.63 AB	6.00 B	1.39 ns	23.89 B	1.50 BC	4.08 B
	Carlos	31.87 A	7.72 A	9.72 A	6.41 B	1.12 ns	24.31 B	1.06 E	2.92 D
	Ison	20.74 C	6.60 BC	8.08 C	5.07 CD	1.45 ns	22.29 C	1.29 D	3.79 BC
	NC67AO15-26	30.54 A	8.25 A	9.86 A	7.72 A	1.20 ns	25.87 A	1.31 CD	3.48 C
	Tara	22.02 BC	7.04 B	7.89 C	5.37 C	1.48 ns	21.21 D	1.55 B	4.32 B
	Red Globe	5.01	8.13	2.03	0.60	1.13	8.67	1.55	4.60
	LSD	3.53	0.54	0.95	0.57	0.25	1.04	0.20	0.55
	P_G	<0.001	<0.001	<0.001	<0.001	0.369	<0.001	<0.001	<0.001

[i]Means with different letters indicate significant differences ($P < 0.05$) between genotypes using Fisher's LSD

[ii]Red Globe was excluded from ANOVA and means comparisons analysis, but is presented here as a reference for *V. vinifera* fresh market qualities

[iii]Least significant difference between genotypes assuming $P < 0.05$

[iv]*P* values for genotypes

[v]No significant genotypic differences ($P \geq 0.05$)

Table 4.5. Least square means of instrumental texture analysis conducted with 7.62 cm compression probe and Kramer Shear Cell (KSC) on seven muscadine genotypes and 'Red Globe' in 2019 and 2020.

Year	Genotype	7.62 cm cylinder (compression)										Kramer Shear Cell			
		Work to rupture (mJ)		Total work (mJ)		Elasticity (mm)		Strain to rupture (%)		Peak force (N)		Rupture force (N)		Cycle 1: total work (mJ)		Cycle 1: peak force (N)	
2019	AM-135	191.04	B[i]	92.86	CD	7.97	C	32.32	C	35.57	B	27.79	BC	3350.07	A	225.20	AB
	AM-195	259.27	A	118.40	BC	8.08	C	31.13	C	44.27	A	34.31	B	2946.89	BC	200.17	BC
	AM-9	201.83	B	187.86	A	11.22	A	41.15	A	44.87	A	44.48	A	3151.29	AB	221.59	AB
	Carlos	46.90	E	46.95	E	6.71	D	33.00	C	17.11	D	17.11	D	1705.11	D	154.78	D
	Ison	151.46	C	129.15	B	9.50	B	38.25	AB	35.65	B	34.33	B	3086.12	AB	241.43	A
	NC67AO15-26	78.79	D	75.06	D	7.77	C	40.11	A	22.34	CD	22.27	CD	1941.13	D	169.11	CD
	Tara	153.30	C	108.29	BC	9.49	B	36.52	B	28.55	C	25.85	C	2665.49	C	181.29	CD
	Red Globe[ii]	78.04		75.69		10.30		46.70		15.91		15.82		1309.93		82.26	
	LSD[iii]	28.01		27.49		0.82		3.42		6.62		6.56		368.87		31.58	
	P_G[iv]	<0.001		<0.001		<0.001		<0.001		<0.001		<0.001		<0.001		0.008	
2020	AM-135	100.69	B	83.48	B	7.85	B	33.23	ns[v]	28.86	B	27.25	B	3391.20	B	182.32	ns
	AM-195	116.77	B	67.63	BC	7.31	BC	30.12	ns	26.92	B	22.27	BC	3703.84	B	216.97	ns
	AM-9	140.59	A	108.64	A	8.09	AB	33.06	ns	35.29	A	33.68	A	4428.29	A	223.19	ns
	Carlos	44.10	C	44.14	D	6.44	CD	32.41	ns	17.35	C	17.35	C	2130.01	C	154.10	ns
	Ison	99.12	B	71.28	B	6.78	CD	28.22	ns	27.56	B	26.81	B	3348.44	B	199.76	ns
	NC67AO15-26	47.72	C	47.77	CD	6.32	D	32.85	ns	20.08	C	20.08	C	2606.00	C	157.74	ns
	Tara	106.74	B	74.28	B	8.84	A	36.05	ns	20.58	C	18.86	C	3524.88	B	231.48	ns
	Red Globe	84.99		56.51		10.05		48.03		21.80		11.50		887.00		41.51	
	LSD	22.30		22.06		0.91		3.97		5.10		5.41		492.29		45.61	
	P_G	<0.001		0.002		<0.001		0.170		<0.001		<0.001		<0.001		0.111	

[i]Means with different letters indicate significant differences ($P < 0.05$) between genotypes using Fisher's LSD

[ii]Red Globe was excluded from ANOVA and means comparisons analysis, but is presented here as a reference for *V. vinifera* fresh market qualities

[iii]Least significant difference between genotypes assuming $P < 0.05$

[iv]*P* values for genotypes

[v]No significant genotypic differences ($P \geq 0.05$)

Table 4.6. Pairwise Pearson correlations of sensory descriptive characteristics with breeders' ratings and instrumental measurements for seven muscadine genotypes and 'Red Globe' in 2019 and 2020.

Probe	Measurement	Flesh		Skin		Overall		Hardness		Awareness of skin		Crispness		Detach[i]	Fibrousness		Visual separation	
		2019	2020	2019	2020	2019	2020	2019	2020	2019	2020	2019	2020	2019	2019	2020	2019	2020
Breeders' rating	Flesh	1	1	0.96**	0.98**	0.97**	0.99**	-0.18	-0.49	-0.61	-0.85**	-0.16	-0.45	-0.74*	-0.58	-0.77**	-0.79**	-0.91**
	Skin	0.96**	0.98**	1	1	0.99**	0.99**	-0.17	-0.58	-0.59	-0.88**	-0.12	-0.54	-0.81**	-0.63	-0.75*	-0.85**	-0.92**
	Overall	0.97**	0.99**	0.99**	0.99**	1	1	-0.13	-0.54	-0.57	-0.85**	-0.09	-0.48	-0.79**	-0.60	-0.79**	-0.83**	-0.89**
7.62 cm cylinder	Work to rupture	0.50	0.33	0.54	0.26	0.57	0.34	0.69*	0.45	0.31	-0.01	0.72*	0.47	-0.12	0.10	-0.67*	-0.19	-0.02
	Total work	0.39	0.09	0.24	0.01	0.29	0.09	0.61	0.57	0.34	0.19	0.57	0.56	0.23	0.33	-0.47	0.11	0.20
	Elasticity	0.65*	0.79**	0.42	0.75*	0.47	0.79**	-0.04	-0.49	-0.28	-0.76*	-0.09	-0.53	-0.11	-0.08	-0.92**	-0.23	-0.68*
	Strain to rupture	0.30	ns	0.08	ns	0.11	ns	-0.62	ns	-0.58	ns	-0.63*	ns	-0.19	-0.22	ns	-0.24	ns
	Peak force	0.33	0.12	0.31	0.08	0.35	0.12	0.82**	0.59	0.50	0.12	0.82**	0.60	0.13	0.32	-0.35	0.05	0.10
	Rupture force	0.24	-0.34	0.14	-0.38	0.19	-0.34	0.79**	0.80**	0.53	0.59	0.77**	0.82**	0.32	0.45	0.08	0.21	0.55
Kramer shear cell	Cycle 1: work	0.26	-0.35	0.26	-0.44	0.30	-0.36	0.88**	0.86**	0.57	0.70*	0.89**	0.92**	0.25	0.47	0.05	0.21	0.64*
	Cycle 1: peak force	-0.08	ns	-0.07	ns	-0.05	ns	0.93**	ns	0.78**	ns	0.95**	ns	0.52	0.71*	ns	0.49	ns
2 mm cylinder	Work to rupture	-0.87**	-0.93**	-0.86**	-0.95**	-0.84**	-0.95**	0.59	0.62	0.89**	0.84**	0.56	0.57	0.87**	0.79**	0.81**	0.87**	0.83**
	Elasticity	-0.91**	-0.18	-0.97**	-0.10	-0.96**	-0.16	0.35	-0.6	0.73*	-0.33	0.28	-0.72*	0.92**	0.75*	0.19	0.94**	-0.17
	Rupture force	-0.70*	-0.89**	-0.64*	-0.93**	-0.63*	-0.91**	0.78**	0.78**	0.95**	0.92**	0.78**	0.76*	0.77**	0.78**	0.71*	0.76*	0.89**
	Skin work	-0.74*	-0.89**	-0.74*	-0.94**	-0.71*	-0.91**	0.70*	0.66*	0.90**	0.93**	0.69*	0.67*	0.87**	0.88**	0.81**	0.90**	0.89**
	Skin thickness	-0.13	ns	-0.11	ns	-0.08	ns	0.98**	ns	0.84**	ns	0.94**	ns	0.57	0.65*	ns	0.54	ns
	Skin peak force	-0.73*	-0.94**	-0.72*	-0.96**	-0.70*	-0.95**	0.72*	0.66*	0.91**	0.96**	0.72*	0.66*	0.85**	0.88**	0.76*	0.89**	0.96**
8 mm cylinder (flesh)	Peak force	0.72*	0.63*	0.85**	0.52	0.85**	0.62	-0.07	0.15	-0.42	-0.37	0.03	0.21	-0.83**	-0.59	-0.61	-0.82**	-0.44
	Total work	0.71*	0.73*	0.85**	0.66*	0.85**	0.73*	-0.05	0.00	-0.41	-0.50	0.04	0.07	-0.81**	-0.58	-0.70*	-0.81**	-0.55

[i]Detachability correlations in 2020 not shown due to lack of significant genotypic differences

[ii]ns indicates that there were no significant differences among genotypes for strain to rupture as measured by the 7.62 m cylinder, cycle 1 peak cycle force as measured by Kramer Shear Cell, and skin thickness as measured by a 2 mm probe in 2020

* and ** indicates significant pairwise Pearson correlations at $P \leq 0.05$ and $P \leq 0.01$

Table 4.7. Multiple linear regression models predicting descriptive sensory scores (Y) of seven muscadine genotypes and "Red Globe" with breeders' field ratings and instrumental measurements.

Trait	Adjusted r^2	*AIC*		Regression model	Model requirements
Awareness of skins	0.39	77.99	Y =	17 + -0.93(BR[i])	breeders' ratings
	0.84	56.52		2.46 + 1.20(RUP[ii])	2 mm cylinder
	0.85	56.18		5.42 - 0.48(ELAS[iii]) + 1.26(RUP)	2 mm cylinder
	0.83	58.48		2.06 + 1.22(RUP) + 0.04(BR)	2 mm cylinder + breeders' ratings
	0.85	57.40		8.69 - 0.67(ELAS) + 1.15(RUP) - 0.20(BR)	2 mm cylinder + breeders' ratings
	0.66	69.33		3.49 - 0.78(FLS[iv]) + 0.31(RUPW[v])	2 mm cylinder + 8 mm cylinder (Conner 2013)
Crispness	-0.02	61.41		6.76 - 0.14(BR)	breeders' ratings
	0.62	45.70		2.61 + 1.23*10^{-3}(KSC[vi])	Kramer shear cell
	0.80	35.96		1.26 + 8.55*10^{-4}(KSC) + 0.30(RUP)	Kramer shear cell + 2 mm cylinder
	0.61	46.74		3.17 + 1.20*10^{-3}(KSC) - 0.09(BR)	Kramer shear cell + breeders' scores
	0.90	25.07		-1.86 + 5.97*10^{-4}(KSC) + 0.56(RUP) + 0.32(BR)	Kramer shear cell + 2 mm cylinder + breeders' ratings
	0.44	52.62		0.13 + 1.82(FLS) + 0.13(RUPW)	2 mm cylinder + 8 mm cylinder (Conner 2013)
Hardness	0.02	49.36		7.13 - 0.13(BR)	breeders' ratings
	0.64	33.54		4.01 + 8.70*10^{-4}(KSC)	Kramer shear cell
	0.80	24.54		3.11 + 6.21*10^{-4}(KSC) + 0.20(RUP)	Kramer shear cell + 2 mm cylinder
	0.66	33.14		4.6 + 8.47*10^{-4}(KSC) - 0.10(BR)	Kramer shear cell + breeders' ratings
	0.82	23.75		1.93 + 5.24*10^{-4}(KSC) + 0.30(RUP) + 0.12(BR)	Kramer shear cell + 2 mm cylinder + breeders' ratings
	0.30	44.93		3.24 + 0.83(FLS) + 0.08(RUPW)	2 mm cylinder + 8 mm cylinder (Conner 2013)
Visual separation	0.70	69.52		17.92 - 1.31(BR)	breeders' ratings
	0.76	65.72		2.55 + 1.57(SKN[vii])	2 mm cylinder
	0.85	59.22		8.61 + 1.30(SKN) - 3.07(FLS)	2 mm cylinder + 8 mm cylinder
	0.83	61.47		9.01 + 1.00(SKN) - 0.64(BR)	2 mm cylinder + breeders' ratings
	0.84	60.63		9.56 + 1.15(SKN) - 2.32(FLS) - 0.24(BR)	2 mm cylinder + 8 mm cylinder + breeders' ratings
	0.71	69.59		10.25 - 3.40(FLS) + 0.24(RUPW)	2 mm cylinder + 8 mm cylinder (Conner 2013)
BR	0.84	46.75	BR =	4.04 + 3.55(FLS) - 0.50(RUP)	2 mm cylinder + 8 mm cylinder
	0.80	49.76		4.23 + 2.96(FLS) - 0.14(RUPW)	2 mm cylinder + 8 mm cylinder (Conner 2013)

[i]BR = breeders field ratings

[ii]RUP = rupture force (N) measured by penetration of intact grape and muscadine fruit with the 2 mm cylinder probe

[iii]ELAS = elasticity (mm) measured by penetration of intact grape and muscadine fruit with the 2 mm cylinder probe

[iv]FLS = maximum force (N) measured by the 8 mm cylinder probe after compressing exposed grape or muscadine flesh by 3 mm

[v]RUPW = work to rupture (mJ) measured by by penetration of intact grape and muscadine fruit with the 2 mm cylinder probe

[vi]KSC = total work (mJ) measured in cycle 1 of maceration with the Kramer shear cell

[vii]SKN = total work (mJ) measured by penetration of grape and muscadine skins using the 2 mm cylinder probe

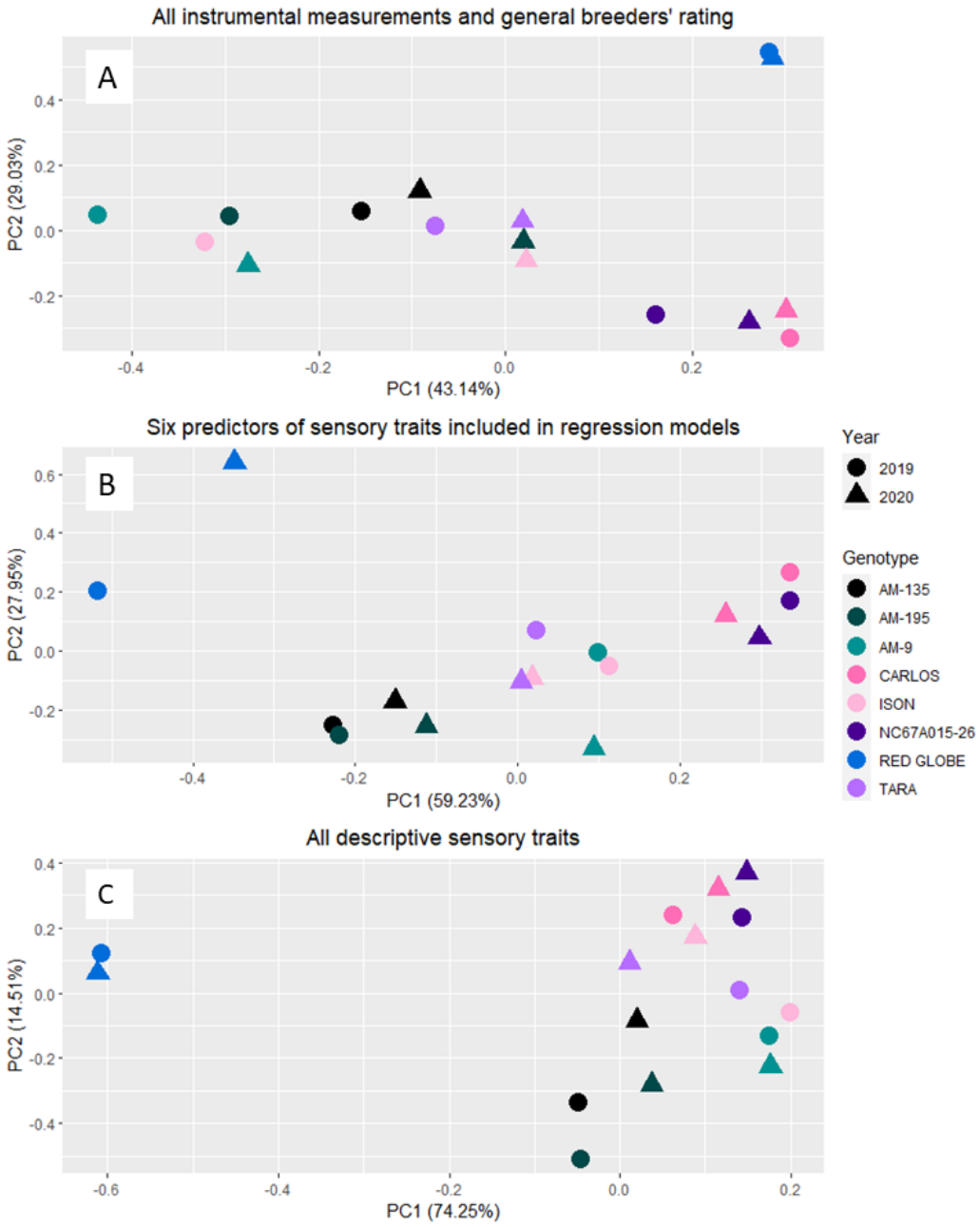

Figure 1. Principal component analysis (PCA) of seven muscadine genotypes and 'Red Globe' evaluated in 2019 and 2020 using all 19 instrumental measurements with genotypic differences in one or both years and a generalized breeders' rating of overall texture (A), all six instrumental measurements used as predictors in multiple regression analysis including berry rupture force (2 mm cylinder), berry elasticity (2 mm cylinder), KSC work, skin penetration work (2 mm cylinder), and flesh maximum force (8 mm cylinder) along with a generalized breeders' rating (B), and all six significant, texture-related descriptive sensory and visual muscadine traits including awareness of skins, crispness, detachability, fibrousness, hardness, and visual separation (C).

APPENDICES

Appendix A

Supplemental Table 1. Least square means of blackberry fruit length measurements in 2020 and 2021 using ShinyFruit image analysis and manual caliper methods.

Genotype	Fruit length - ShinyFruit				Fruit length - calipers			
	2020		2021		2020		2021	
A-2444T	30.73	b[iii]	30.96	ab	28.92	ab	29.44	ab
A-2453T	22.65	a	21.75	a	25.17	a	22.60	a
A-2454T	27.35	ab	28.59	ab	29.11	ab	26.71	ab
A-2491T	32.38	b	28.77	ab	33.25	ab	31.29	ab
Black Gem	28.18	ab	29.06	ab	29.70	ab	28.48	ab
Black Magic	28.64	ab	29.78	ab	27.63	ab	28.38	ab
SA[i] Caddo	31.21	b	29.99	ab	33.96	ab	29.41	ab
Natchez	33.98	b	39.18	b	36.93	b	37.04	b
Osage	24.59	ab	27.27	ab	25.17	a	23.96	a
Ouachita	26.00	ab	30.25	ab	27.41	ab	28.78	ab
PA[ii] Freedom	27.35	ab	35.36	b	28.48	ab	33.92	ab
PA Horizon	36.09	b	34.82	b	36.93	b	33.96	ab
PA Traveler	27.34	ab	32.11	b	30.97	ab	31.11	ab
SA Ponca	25.61	ab	25.89	ab	26.73	a	26.32	ab
P value	<0.001		<0.001		0.004		0.012	

[i]Sweet-Ark®

Appendix B

Supplemental Figure 1. The four steps of graphical determination of the true *K*(*) value as reported following Evanno et al. (2005). (A) Mean *L*(*K*) over three runs for each *K* value. (B) Rate of change in the likelihood distribution calculated as *L*'(*K*) = *L*(*K*) – *L*(*K*-1). (C) Absolute values of the second order rate of change in likelihood distribution calculated according to the formula: |*L* ''(*K*)| = |*L* '(*K* + 1) – *L* '(*K*)|. (D) ΔK calculated as *ΔK* = m |*L* ''(*K*)| / s[*L*(*K*)]. The modal value of this distribution is the true *K*(*).

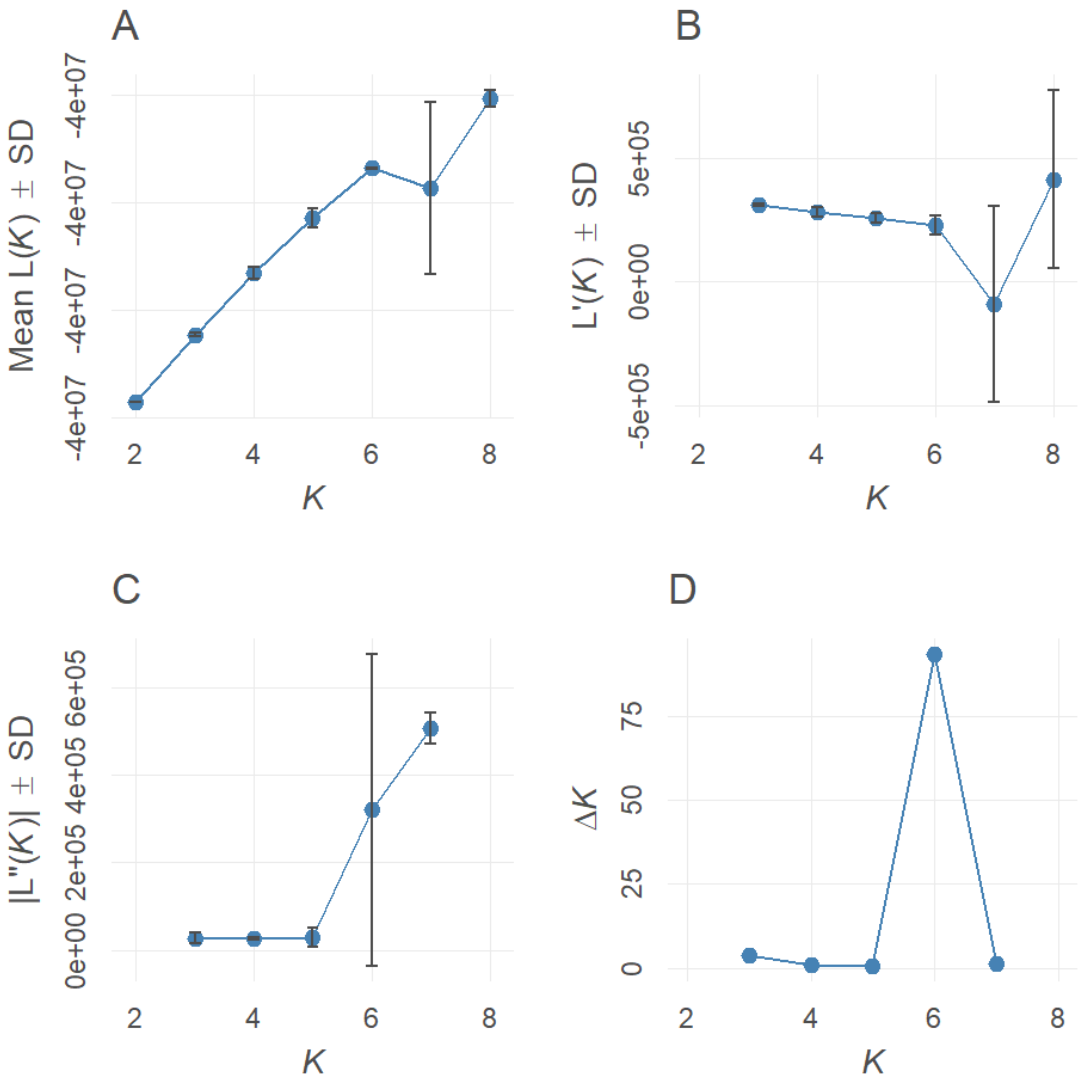

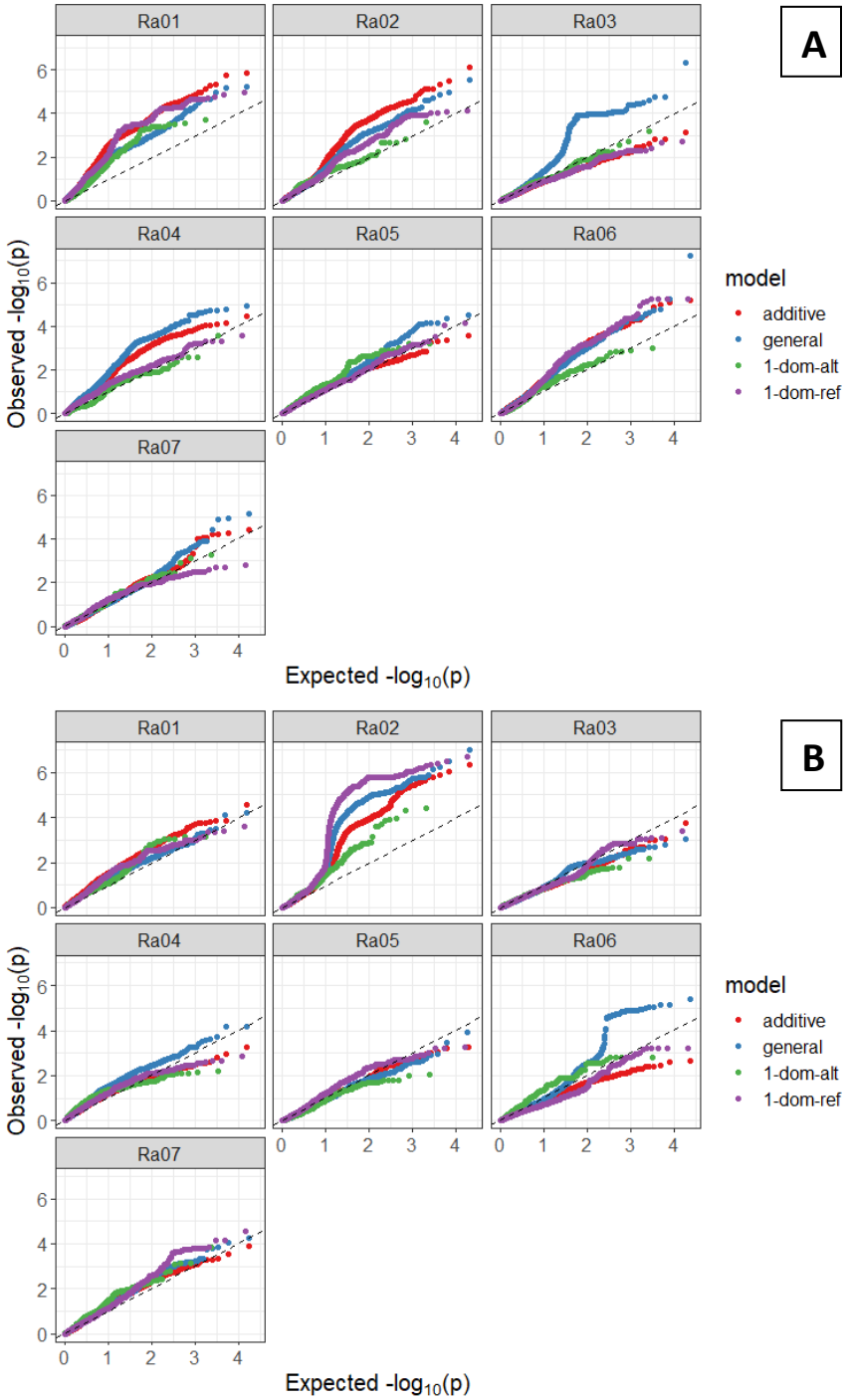

Supplemental Figure 2. QQ-plots of (A) fruit firmness and (B) red drupelet reversion

Supplemental Figure 3. Heatmap of absolute values of Lewontin's D' estimated between 220 SNPs significantly associated with red drupelet reversion on Ra02. Nonsynonymous variants of texture-related homologs are marked in blue.

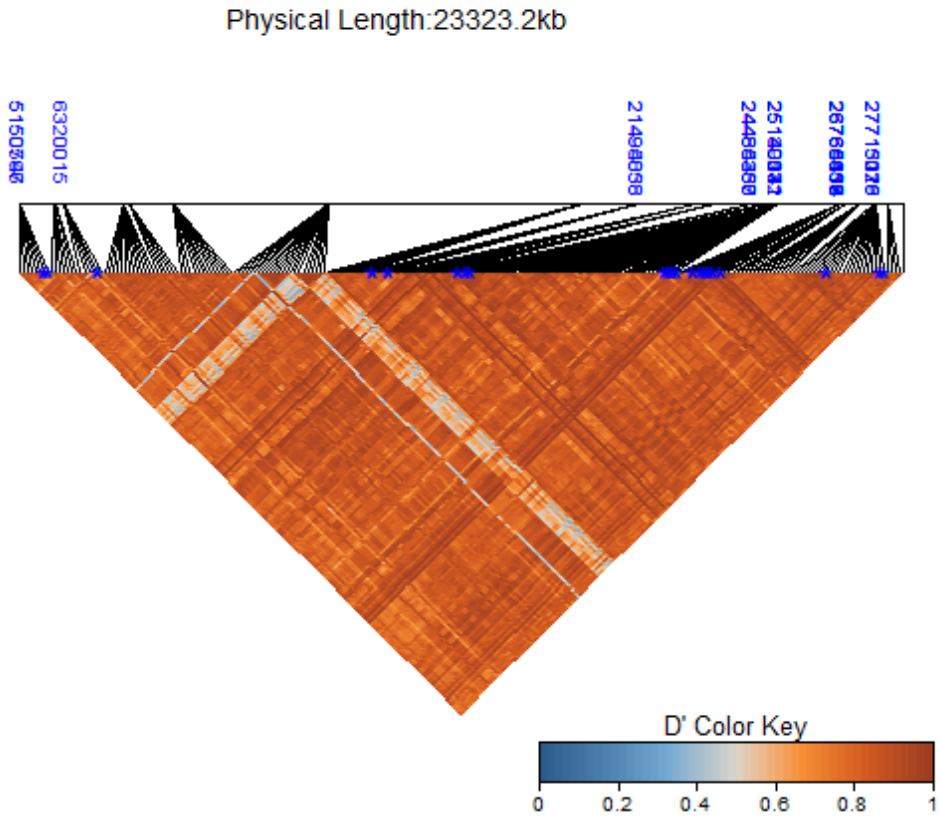

Appendix C

Supplemental Table 1. TA.XT texture analyzer probes and protocols.

Part #	Probe description	Type of test	Test speed ($mm.s^{-1}$)	Target distance	Trigger force (N)	Tare height
TA-52	2 mm cylindrical	penetration	1.0	9 mm	0.07	35 mm
TA-52	2 mm cylindrical	skin thickness	0.2	100% strain	0.07	35 mm
TA-58	8 mm cylindrical	flesh compression	0.5	3 mm	0.07	35 mm
TA-30	7.62 cm cylindrical	compression	1.0	50% strain	0.07	35 mm
TA-42	45° chisel	compression	1.0	50% strain	0.07	35 mm
TA-91	Kramer shear cell	maceration	1.0	35 mm	2.00	above the cell